AN EXPERIMENTAL STUDY OF FORCED VENTILATION GLOVEBOX FIRES

by

Michelle J. Peatross

Thesis submitted to the Faculty of the

Virginia Polytechnic Institute and State University

in partial fulfillment of the requirements for the degree of

MASTER OF SCIENCE

in

Mechanical Engineering

APPROVED:

R. J. Roby, Chairman

L. A. Roe

C. L. Beyler

August, 1992

Blacksburg, VA

c.2

An Experimental Study of Forced Ventilation Glovebox Fires

by
Michelle J. Peatross
Committee Chairman: Dr. Richard J. Roby
Mechanical Engineering

(ABSTRACT)

An experimental study was performed to investigate the integrity of gloveboxes when subjected to lathe drip pan fires. These fires are potentially dangerous since glovebox failure may allow hazardous gases to escape containment. A full scale mockup of a glovebox and corresponding air flow system was constructed. Careful consideration was given to the two components expected to cause glovebox failure: the gloves and windows. In addition to normal tests, tests which introduced added ventilation openings (i.e. missing gloves, missing window) were also performed.

The glovebox ventilation system places these fires in the category of overhead forced ventilation compartment fires. Since little data has been obtained previously for this type of fire, further experiments were conducted to determine the effect of fuel surface area on fire behavior. In the past, these fires have been successfully modelled as well-stirred reactors.

Results showed that overall containment was achieved under normal glovebox conditions. Added ventilation opening tests, however, showed that these scenarios would lead to a loss of containment. Nevertheless, under no conditions did a catastrophic glovebox failure occur. Furthermore, experiments with reduced fuel surface areas showed that the fires became less hazardous as the pan diameter decreased. Exhaust gas concentrations, temperature data, burn rates, smoke generation, and heat releases were

the criteria used to form this conclusion. Neither a well-stirred or two-layer environment was observed.

Acknowledgments

First, I would like to thank my advisor Dr. Richard Roby for his guidance throughout the last year and a half. I found his constant support and encouragement to be uplifting. In addition to Dr. Roby, I would like to express my appreciation to Dr. Craig Beyler who provided me with the opportunity to work on this project. He has been extremely insightful and I am honored that he was willing to serve as an off-campus member of my committee.

Next, I would express my gratitude to Dan Gottuk for the immeasurable amount of help he has given me. He "came to the rescue" on more than one occasion and helped me through some tight spots.

I was fortunate enough to have two undergraduate assistants, Alison Gebauer and Brian West, to help with my project. They both assisted me enormously with a seemingly endless amount of drilling. Many thanks go to them for their hard work.

Furthermore, I cannot neglect Ms. Willie Hylton for all of her help ordering my equipment. Also, I want to thank the guys in the instrumentation shop for their assistance. In particular, I want to express my gratitude to Ben Poe for the countless number of computer ailments he repaired.

In addition, I want to thank my officemates Jim Hunderup, Linda Blevins, Dan Gottuk, James Reaney and Doug Wirth for all of their advice, both academic and non-academic. I wish all of them great success in their careers.

I would like to express my appreciation to EG&G Rocky Flats (Bruce Campbell) and the National Institute of Standards and Technology for funding this project.

Most importantly, I would like to thank my parents and brother for always encouraging me to pursue my goals and supporting my decisions.

TABLE OF CONTENTS

LIST OF FIGURES

LIST OF TABLES

1. INTRODUCTION

1.1 Background

Gloveboxes are often employed for handling hazardous materials. A glovebox is typically constructed of steel and has windows in the sides and ceiling so that one can see inside. Gloves are also attached on the sides so that workers may manipulate toxic substances without being exposed to them. In some applications, lathes are placed inside the boxes and used to machine the material. Machining is aided by a mixture of oil and solvent which serves to cleanse and cool the specimen. This mixture is sprayed on the material and collected in a lathe drip pan located on the glovebox floor. Periodically, the mixture is emptied from the pan but can reach a depth of several centimeters before that time.

Currently, the solvent used is carbon tetrachloride, a nonflammable chlorinated hydrocarbon solvent. Due to growing pollution concerns, a non-chlorinated hydrocarbon solvent is being considered as a substitute. This change raises the issue of fire safety since this class of solvents is more combustible than the chlorinated class.

In some cases, the machined material is plutonium, a pyrophoric metal. In dense quantities, plutonium will not burn efficiently. However, shavings and small particles will ignite more easily thereby introducing an ignition source for the oil/solvent mixture [1]. Consequently, it is important to investigate this fire potential and determine if the glovebox can contain the combustion products. Because of the possible release of radioactive gases, a fire in one of these structures would be devastating if glovebox integrity were lost. If indeed glovebox failure is observed in experiments, modifications must be made to the box construction or working environment to prevent the occurrence

of such a disaster. This thesis describes the research that was conducted to evaluate this problem.

Due to the ventilation configuration in these gloveboxes, a second purpose for these experiments was introduced. A closed air system is used to provide a vacuum within the gloveboxes, preventing leakage of radioactive products. Air is introduced through an inlet in the glovebox ceiling, thus classifying these fires as overhead forced ventilation compartment fires. Understanding the effect of this type of ventilation on fire behavior is valuable from a modelling standpoint because it is a common scenario for buildings with air conditioning systems vented in the ceiling. Despite the need for predicting overhead forced ventilation fire behavior, little research has been documented in this area. Therefore, in addition to evaluating glovebox fire safety, this thesis will provide more insight on compartment fires with forced overhead ventilation.

1.2 Expected Glovebox Failure Modes

Two glovebox components have the greatest potential of causing loss of glovebox integrity. One component, lead-lined neoprene gloves, are likely to burn out in the event of a fire. Glove burnout is hazardous because it creates a new ventilation source, allowing an additional oxygen source to stoke the fire and an escape route for toxic gases. The other component is the windows which are in danger of breaking in response to thermal stresses induced by a rapid temperature rise. As with glove burnout, window breakage would add a new ventilation opening and allow the fire to flourish. Most glovebox windows have a larger area than the glove holes thereby presenting more of a containment hazard.

Glass breakage has been investigated both experimentally and theoretically since it is an important consideration for modelling fires [2-6]. A valuable result of this work is that window breakage occurs under different thermal conditions and in different manners depending on the edge characteristics. One type of window is edge-protected; that is, the edge is shielded from fire. The other type of window is edge-unprotected where the entire pane is exposed to the same thermal environment. When comparing the edge temperature to the temperature at the pane center, edge-protected windows crack at temperatures differentials on the order of 110C less than edge-unprotected windows do. Furthermore, when edge-protected windows crack, they usually break eventually whereas edge-unprotected ones remain intact after cracking [5].

Skelly found experimentally that an average temperature gradient of 90C produced glass cracking [5]. His results were similar to theoretical predictions of 70C by Keski-Rahkonen and 58C by Pagni [2,4]. Differences in Skelly's results were attributed to radiation effects on the glass thermocouples which caused the temperature readings to be elevated.

1.3 Earlier Glovebox Testing

Historically, glovebox fires have occurred in a number of the large hazardous material processing facilities. For example, a fire occurred at Rocky Flats in 1969 causing an estimated 45 million dollars worth of damage. Four hours elapsed before the fire was brought under control while isolated areas still burned for another 12 hours. Glovebox failure occurred when windows broke and provided a means for plutonium oxide to flow into the atmosphere. Fortunately, contamination was contained within plant boundaries [7].

As a result of fires of this type, research efforts have concentrated on preventing future fires [8-12]. Emphasis was placed on the following areas: a) thermal behavior of construction materials, b) improved design of filtration and ventilation systems, and c) improved methods for heat detection [8].

Modifications that resulted from these studies and that are relevant to this study include the design of glove hole covers and metal keepers for the windows. Glove hole covers are metal plates which hang in front of the glove holes allowing access to the gloves by lifting them. Their purpose is to block air flow in the event of glove burnout. Presumably, at any given time, only one pair of gloves will be utilized so that all glove covers except these two will be covering the holes. Metal keepers or window guards are sheet metal covers which shield the gasket on the glovebox interior. Since most gaskets are neoprene, thermal decomposition is likely, posing the danger of windows falling out. These guards protect the gaskets from direct flame impingement and will catch the glass if it should fall out [8].

1.4 Background of Compartment Fire Behavior

Two models are commonly used to describe compartment fire behavior: the two-zone system and the well stirred reactor. In the two-zone system, traditionally observed in naturally ventilated compartment fires (i.e. open window, vent), an upper layer consisting of hot exhaust gases and a lower layer consisting of cooler ambient air are present. As the fire develops, the upper layer will become deeper until a ventilation opening is encountered for gas outflow. The interface between these layers is evident when vertical temperature profiles are examined as there will be a gradient change at the interface. Since exhaust gases in a two layer system are only present in the upper layer, exhaust species concentrations must be sampled at this location [13].

On the other hand, the well-stirred reactor model assumes that there is a homogeneous mixture of gases throughout the compartment. Unburned gases and exhaust gases mix immediately to create this type of environment [14]. Consequently, gas concentrations are independent of the sampling location and vertical temperature profiles display a uniform temperature gradient. Previously, overhead forced ventilation compartment fires or fires with no ventilation have been modelled using this concept [15].

In addition to examining the vertical temperature profiles, the principle of the Limiting Oxygen Index (LOI) can be used to categorize fire environments as well-stirred or two-layer. The LOI refers to the minimum oxygen concentration required to sustain a flame. LOI's span a wide range and are sensitive to temperature and pressure. Typical LOI's for hydrocarbons range between 8 and 14% while Flame-Retardant Fibers such as wool and cotton have LOI's of 32% [16-18].

With this concept in mind, oxygen concentrations measured in the exhaust should not be below the LOI if the system is well-stirred since no flame could exist. Conversely, in a two-layer system, oxygen concentrations in the exhaust which are below the LOI are not unreasonable.

1.5 Previous Forced Ventilation Fire Studies

As stated earlier, little research has been documented on forced ventilation fires, especially those with overhead forced ventilation. For modelling purposes, it is valuable to predict temperature profiles with this type of configuration in hopes of understanding the fire growth patterns and assessing flashover potential.

Beginning in 1981, Foote et al. conducted a series of forced ventilation tests at Lawrence Livermore National Laboratories [19-21]. Experiments were conducted to determine the effects of ventilation configuration, ventilation rate, plenum presence, and fire elevation on fire behavior. Their test compartment was 4 m by 6 m by 4.5 m high and a methane burner was used so that the heat release rate could be controlled.

Ventilation configuration was tested by supplying air at floor level, ceiling level, and by supplying no air. In the case where ventilation was provided from the floor, a two-layer system resulted if the ventilation rate was 2-3 times the stoichiometric amount. On the other hand, they found that fires with overhead ventilation did not yield a two layer system no matter what the ventilation rate was. These observations were based on plots of the temperature profiles which were linear when the fire was not well-ventilated. When the ventilation was supplied at a high level, the ceiling temperatures were approximately the same as with low level ventilation. Therefore, it was suggested that the vertical mixing created from the inflowing air allowed the lower gases to be warmed and the upper gases to be cooled. For the case of fires with no ventilation supplied, the fires self-extinguished when the oxygen supply was depleted. In addition to these results, they found that elevated fires developed hotter layers as the elevation increased. In the same manner, the lower the plenum, the hotter the layer [21].

Six different models were used to predict results for Foote et al.'s first set of test results which used floor level ventilation. These models were from Harvard (Mitler and Emmons, 1981; Mitler, 1982), LANL (Krause, 1982), LLNL (Creighton, 1982), Cal Tech II (Zukowski, 1980), PNL (Orzawski, 1982), and Cal Tech I (Zukowski, 1982). With the exception of the last model, these were two-layer zone models. Eight risk indicating parameters were chosen to measure each model's effectiveness. These

parameters included: 1) upper layer gas temperature, 2) fire strength, 3) total heat loss to walls, 4) oxygen concentration, 5) lower layer height, 6) inlet ventilation, 7) wall temperature, and 8) lower layer gas temperature. No model was consistent in predicting these values accurately. In fact, fire strength was the only quantity which was calculated consistently within 5% by any of the models [19]. These results reinforce the need for a better understanding of forced ventilation fires.

Beyler performed an analysis of Foote's data for overhead ventilation fires and no ventilation fires using correlations developed by Deal and Beyler [22]. In this analysis, he successfully predicted the temperature rise and extinction time. The correlation for the temperature rise was developed using a quasi-steady simplified energy equation with simple wall heat loss. The values predicted using this model and those actually measured by Foote agree quite well except after long periods of time. This limitation is due to the failure of the heat loss model. Extinction time was predicted successfully using a well-stirred reactor model and the concept of limiting oxygen index as a basis. Agreement of these results suggests that the LOI may be used to predict the maximum heat release [15].

Several important characteristics have been discovered in the work discussed. The primary result is that enclosure fires with overhead forced ventilation exhibit well-stirred characteristics regardless of the ventilation rate. Compartment temperatures and extinction times have been successfully predicted using Beyler and Deal's model. Unfortunately, an insufficient amount of testing has been conducted in this area to properly validate this theory and allow it to be implemented in fire models.

1.6 Experimental Goals

This thesis has two focuses: evaluating the danger of glovebox fires and investigating the behavior of overhead forced ventilation enclosure fires. A realistic

mockup of the glovebox setup was constructed and tested so that glovebox integrity could be evaluated. This experimentation was directed toward preventing catastrophic glovebox fires in which toxic gases are expelled into the atmosphere. Important conclusions include determining if and how a glovebox fails to contain a fire.

Since these fires fall into the category of compartment fires with overhead forced ventilation, additional data was taken in hopes of better understanding this class of fires. Data was collected by instrumenting the glovebox system and varying the fuel surface areas burned. An important difference between this work and Foote's experiments is that one variable is eliminated in these tests: the ventilation rate.

In order to accomplish these goals, three sets of experiments were performed. These tests included preliminary open burn tests, full scale pan glovebox experiments and reduced pan diameter glovebox experiments. The design of the glove and window assemblies were intended to closely imitate those actually used. Measurements which were monitored throughout the glovebox tests include temperature, fuel weight, exhaust flow rate, smoke obscuration, and exhaust gas species.

2. EXPERIMENTAL SETUP

2.1 Introduction

This chapter describes the construction of the mock glovebox system and how it was instrumented. When building the glovebox, careful consideration was given to the design of the gloves and windows since they were the expected sources of failure. In addition, the air flow system was duplicated as closely as possible since this is another critical parameter. Furthermore, a fuel pan with dimensions similar to an actual lathe drip pan was constructed along with three smaller pans. With these features in mind, the glovebox system was constructed to be as realistic as possible.

Supporting instrumentation was installed to measure temperatures, fuel weight, heat flux, exhaust gas concentrations and exhaust flow rates. A detailed explanation of these instruments and their configuration is also provided below.

2.2 Glovebox Construction

An isometric view of the test glovebox is shown in Figure 2.1. The glovebox consisted of a 31.75 mm angle iron frame with steel panels attached to it. Overall dimensions of the glovebox were 3.66 m wide x 1.22 m deep x 1.22 m high. The panels were 3.18 mm thick steel with the exception of the front panels which were 6.35 mm thick steel and were either bolted or tack welded to the frame. The front panels were required to be thicker because of the gaskets which were supplied for the front window assembly. The box panels were divided into quarters with one window per panel in the ceiling and one per panel in the front. All other panels were solid. Shop drawings of the ceiling and front panels are located in Appendix A.

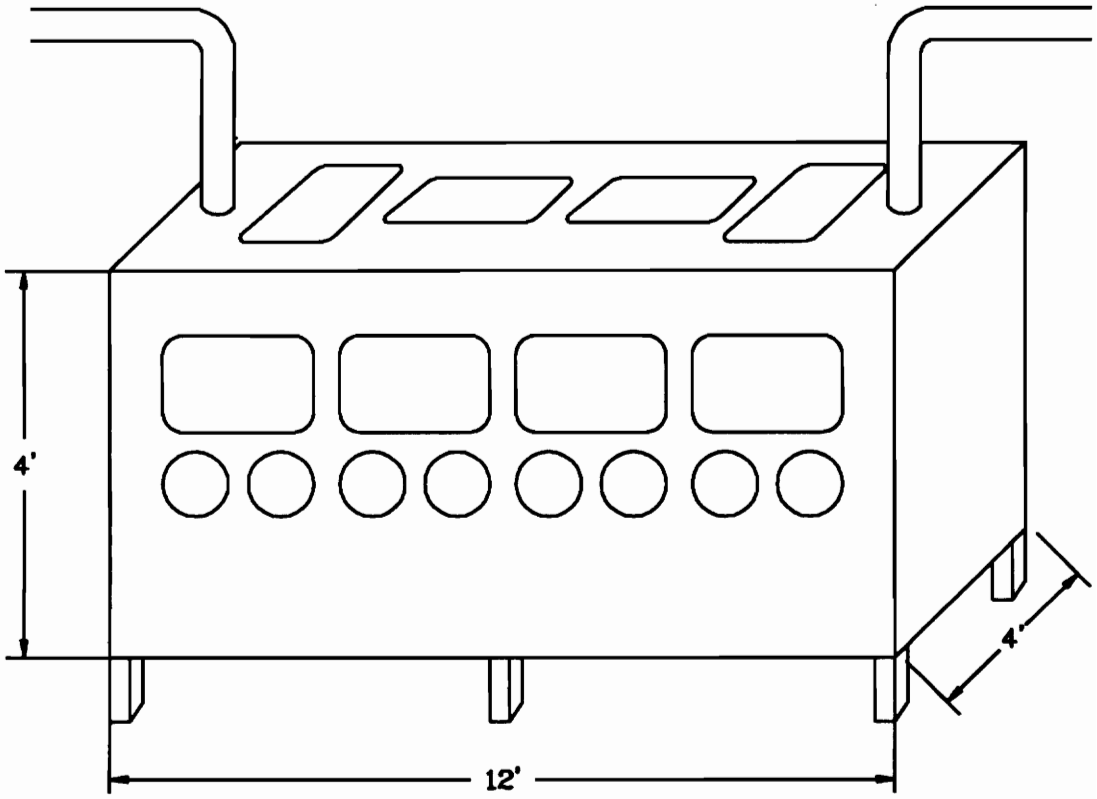

Figure 2.1: Sketch of Mock Glovebox

Each front panel had two glove holes below the window with neoprene gloves attached. The gloves, purchased from VWR Scientific, were 0.76 mm thick and extended to ones shoulder with a 20.3 cm opening. Collars, constructed of stove pipe exhaust duct, were bolted onto the front panels and the gloves were placed around them using hose clamps for security. The windows in these panels had overall dimensions of 24.4 cm x 62.5 cm x 12.7 mm thick and consisted of a composite structure manufactured by Schott America. Following the specifications from Rocky Flats, the windows were constructed of a 7.9 lead glass core with 3 mm float glass laminated on either side (Figure 2.2). Neoprene gaskets supplied by Rocky Flats were used to hold the windows in the panels. Drawings detailing these gaskets are provided in Appendix B.

In the ceiling panels, fire-rated wire glass with dimensions of 24.1 cm x 62.2 cm x 6.35 mm thick was used for the windows. As with the front lead glass windows, these windows were secured in the panels with neoprene gaskets from Rocky Flats (Appendix B). In addition to housing a window, the outer ceiling panels each had a 15.2 cm diameter hole cut in it, one for the air inlet and the other for the air exhaust.

Window guards and glove hole covers, as mentioned in Section 1.3, were installed. The window guards were constructed from four steel strips which were bent on either side. The strips were then riveted together to make one structure which was bolted onto the glovebox panel so that the gasket was covered. Also, glove hole covers, consisting of a steel disc, were bolted onto the glovebox in front of each glove opening.

Experiments were conducted at the Fire Research Lab at the Price's Fork Research Facility. A schematic of the lab is provided in Figure 2.3. Prior to this experimentation, a test building, fire wall, measurement trailer, and small storage shed (not shown) were present. The gas analyzers, computer, and most instrumentation were located in the

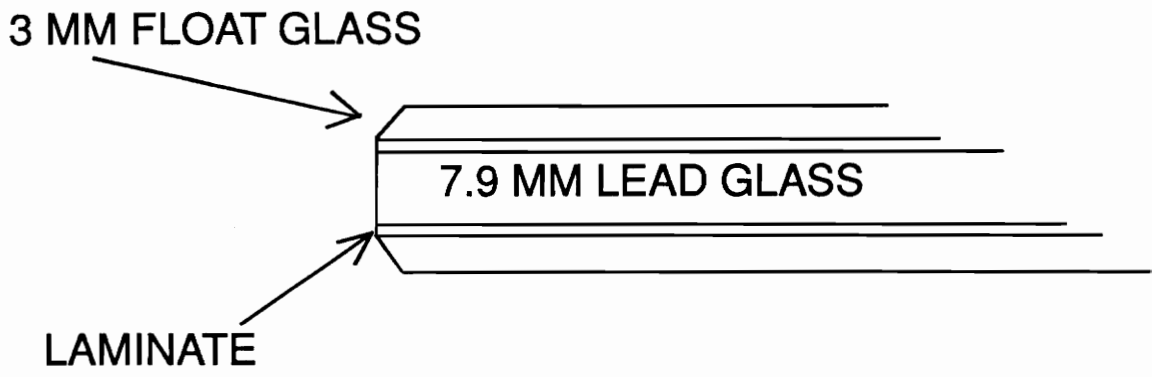

Figure 2.2: Specifications for Lead Glass Window Composition

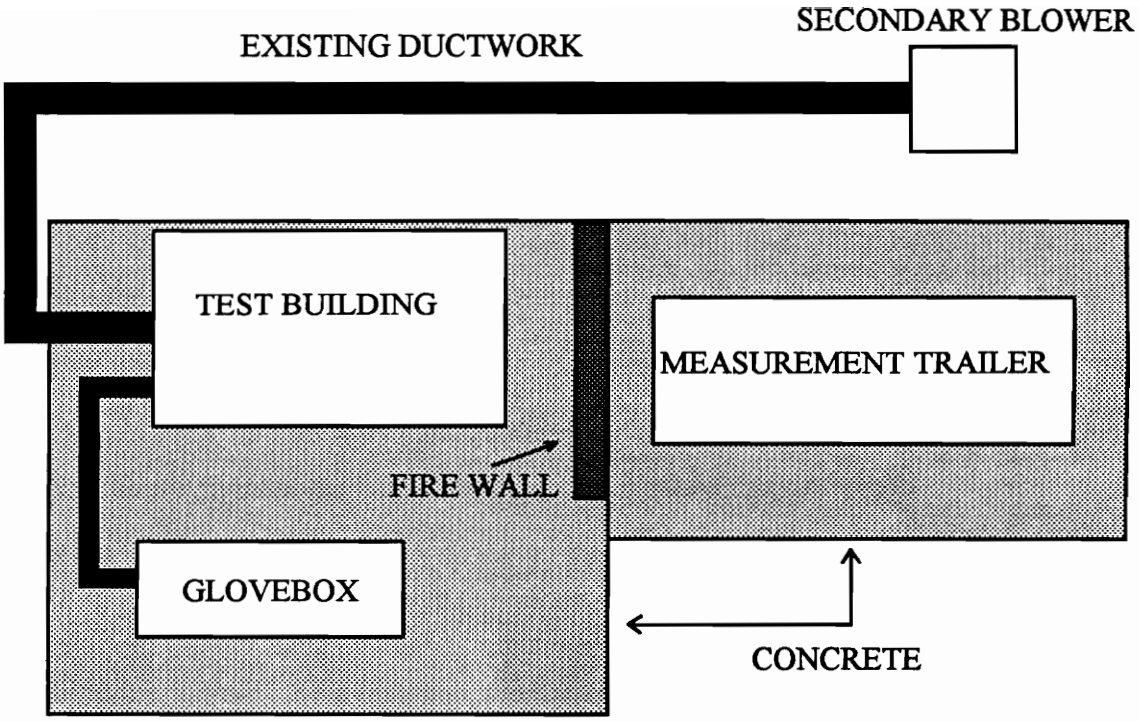

Figure 2.3: Layout of Price's Fork Fire Research Lab

measurement trailer. Following construction, the glovebox was moved out to the lab where it was positioned on the concrete. The existing ductwork and blower, used to vent the exhaust from the test building, were used in the secondary air flow system.

2.3 Air Flow System

The air flow system was designed to provide an exhaust flow from the box between 0.071 - 0.094 m^3/sec (150 - 200 cfm) with a negative pressure of 1.4 torr (3/5 inch of water) present inside of the box. A Dayton High-Pressure, Direct-Drive Blower was used to maintain this exhaust flow. The performance curve supplied with the blower is provided in Appendix C.

A schematic of the ductwork system is shown in Figure 2.4. All ductwork was 15.24 cm diameter stove pipe exhaust duct. Since the performance curve for the blower specified a flow rate far in excess of 200 cfm to operate at the desired pressure, a bypass duct was installed downstream of the box. A flapper type valve was installed in the box inlet and bypass duct so that the flows could be adjusted. This mixture of glovebox exhaust air and bypass air was drawn through the "primary blower" and flowed into an exhaust hood in the test compartment building. The "secondary blower" then pulled the diluted mixture through the duct.

In order to determine the exhaust flow from the glovebox, an orifice meter was installed according to ASME Standards [23]. This meter had a diameter of 7.6 cm corresponding to a beta ratio of 0.5. Pressure taps corresponding to D and 1/2 D specifications were used. A Datametrics Model 590 Barocel Pressure Sensor and Model 1450 Electronic Manometer measured the pressure drop across the plate which was then used to calculate the exhaust flow rate.

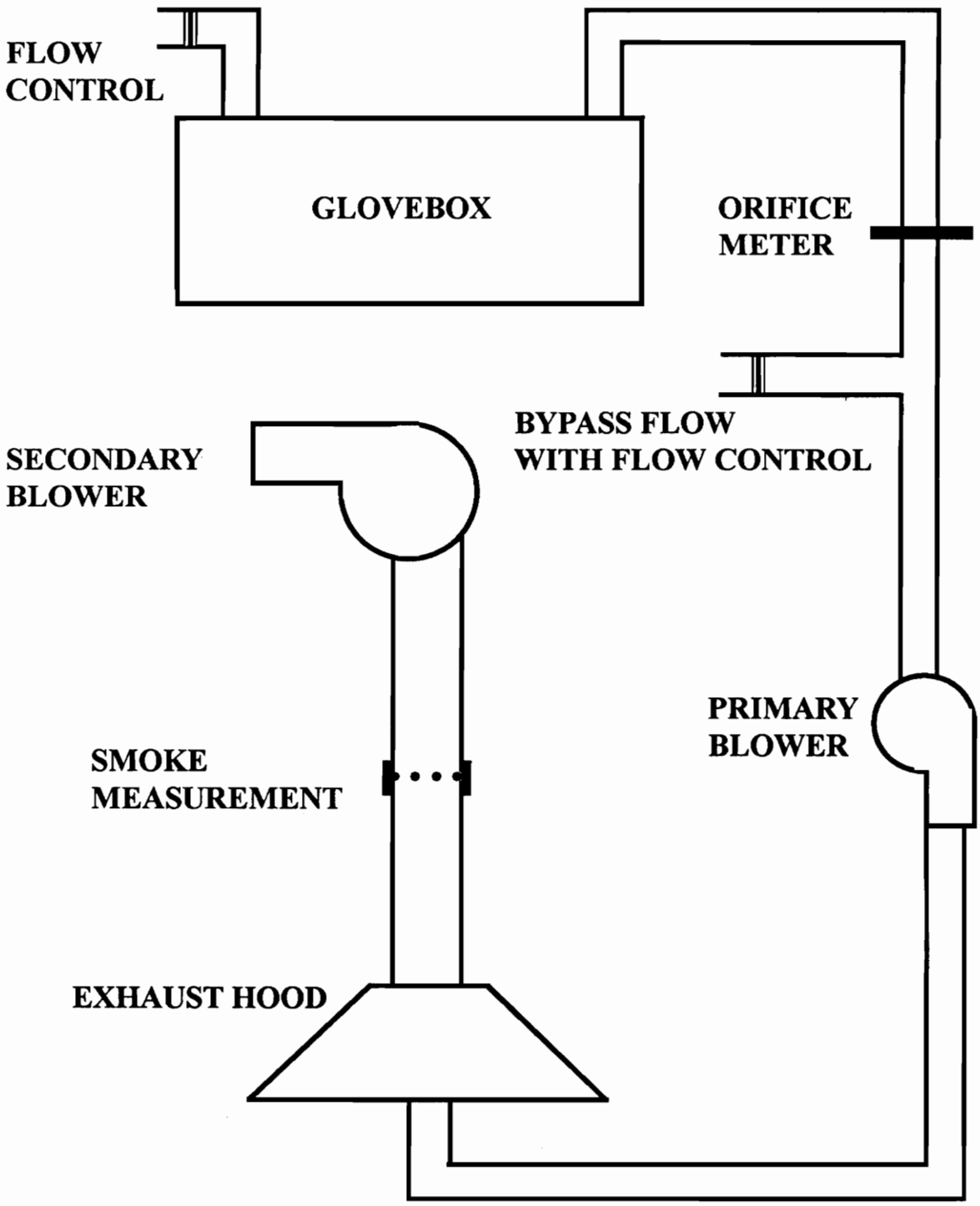

Figure 2.4: Schematic of Glovebox Air Flow System

2.4 Fuel Pan and Fuel Description

A fuel pan, referred to as the full scale pan, was designed to duplicate the size of actual lathe drip pans. It was constructed of 3.18 mm steel and was 91.4 cm x 91.4 cm x 12.7 mm deep. The pan was welded to an angle iron table to minimize warpage. During the tests, the table legs were placed through holes in the glovebox floor so that the pan was centered around the second front window from the air inlet.

For the reduced fuel surface area tests, two circular pans were constructed, also of 3.18 mm thick steel. They had diameters of 62.2 cm and 83.8 cm corresponding to fuel surface areas of 0.304 and 0.552 m^2, respectively. A third pan of diameter 27.9 cm and area 0.061 m^2 was machined from a piece of aluminum stock. During the glovebox tests, these pans were placed in the full size pan instead of being welded to a table such as the full size pan.

In each of the tests, Regal Oil R&O 32, a turbine oil manufactured by Texaco, and 140 Solvent-66, an aliphatic hydrocarbon manufactured by Ashland Chemical, were used as fuel. Table 2.1 lists some important characteristics of these liquids. In tests where the mixture had not been preheated by a previous fire, a paper rag was placed in the pool to serve as a wick for ignition.

2.5 Gas Sampling System

A gas sampling system already existed at the test facility requiring that only a 3.96 m extension tube be connected to accommodate a sampling point 3.58 m from the glovebox air outlet. The existing system was constructed of 6.4 mm inner diameter stainless steel tubing which covered the length of the test building and led to the measurement trailer. Particulates greater than 0.1 microns were trapped in a Balston

Table 2.1 Oil and Solvent Properties

	OIL	SOLVENT
Density (kg/m^3)	866.4	783.7
Heat of Vaporization (kJ/kg)	248.9	279.1
Heat of Combustion (kJ/kg)	45292	46360
Flashpoint (C)	168	61
H:C Ratio	2.3	2.1
$(Fuel/Air)_{stoichiometric}$	15.2	14.9

filter and a trap placed in a Fisher cold bath collected water from the sample. Water removal was necessary for the carbon monoxide, carbon dioxide, and oxygen analyzers. However, the total hydrocarbon analyzer required that water remain in the sample so that higher molecular weight hydrocarbons would not drop out. Therefore, the sample to the hydrocarbon analyzer bypassed the cold trap and Thermolyne/Briskheat* Heating Tape was coiled around the entire length of sampling line so that water would remain in the gas phase. This heating tape was coated with Fibrox* fibrous glass insulation which made it suitable for metal contact and was rated for 482 C. A Variac (variable voltage source) was used to provide current to the heating tape. A schematic of the sampling system is shown in Figure 2.5. Further description of this system can be found in reference [24].

Carbon monoxide and carbon dioxide concentrations were measured with Beckman Model 880 NDIR analyzers. A range of 0 - 10 % was used for carbon monoxide while a range of 0 - 20 % was used for carbon dioxide. The analyzers were calibrated with nitrogen as a zero gas and a 9.03% carbon monoxide/17.98% carbon dioxide span gas.

A Siemens Paramagnetic OxyMat 5 analyzer was used to determine the exhaust oxygen concentrations. This analyzer was configured for a range of 0 - 22 %. As with the Beckman analyzers, it was calibrated with a nitrogen zero gas and a span gas with an oxygen concentration of 4.74%.

A Flame Ionization Detector (FID) was used to measure unburned hydrocarbons (UHC's). A schematic of this system is shown in Figure 2.6. Calibration was performed using 4.71% ethylene gas and a nitrogen zero gas. Following each test, all analyzers were checked to determine if they were still calibrated properly.

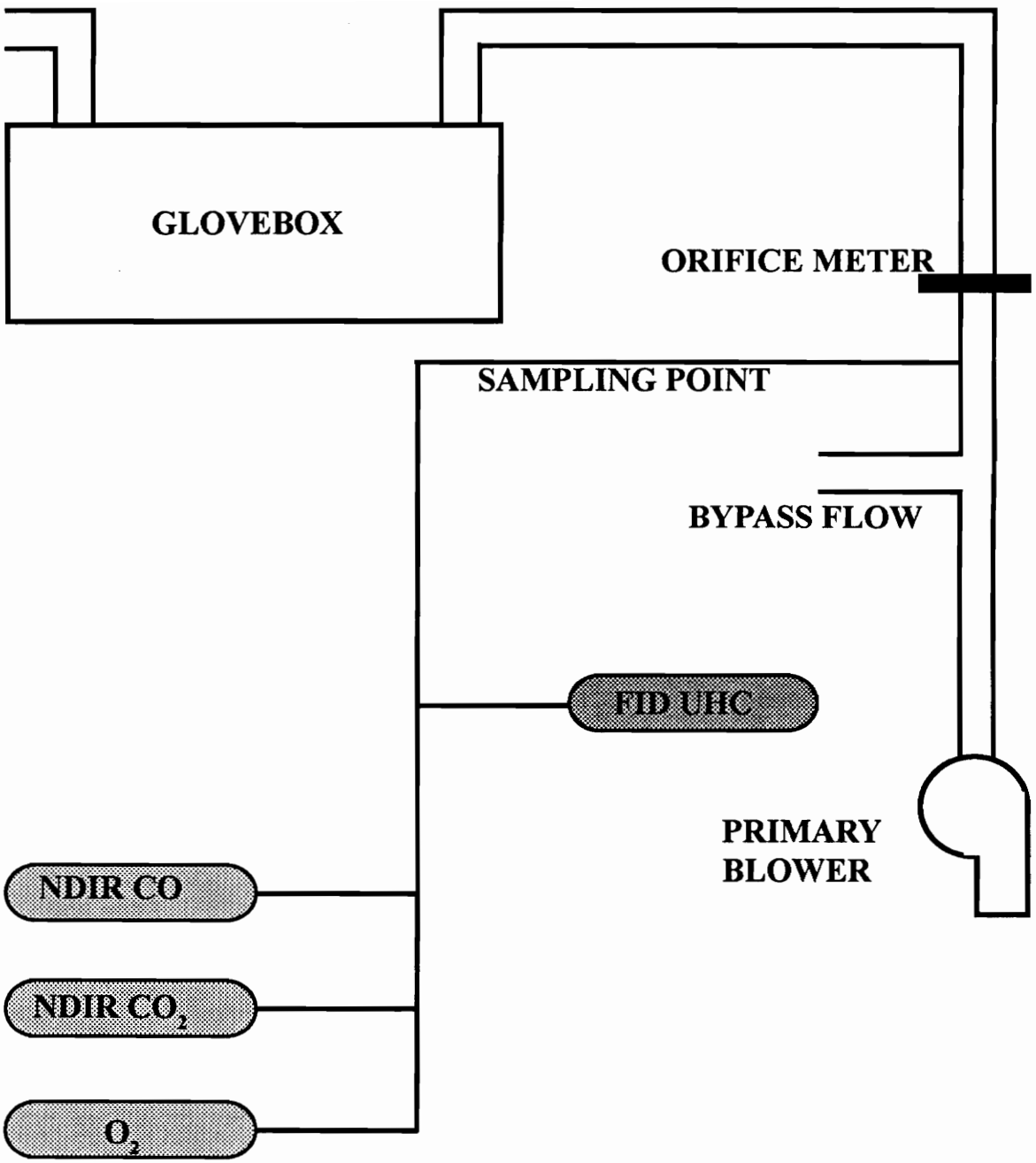

Figure 2.5: Schematic of Gas Sampling System

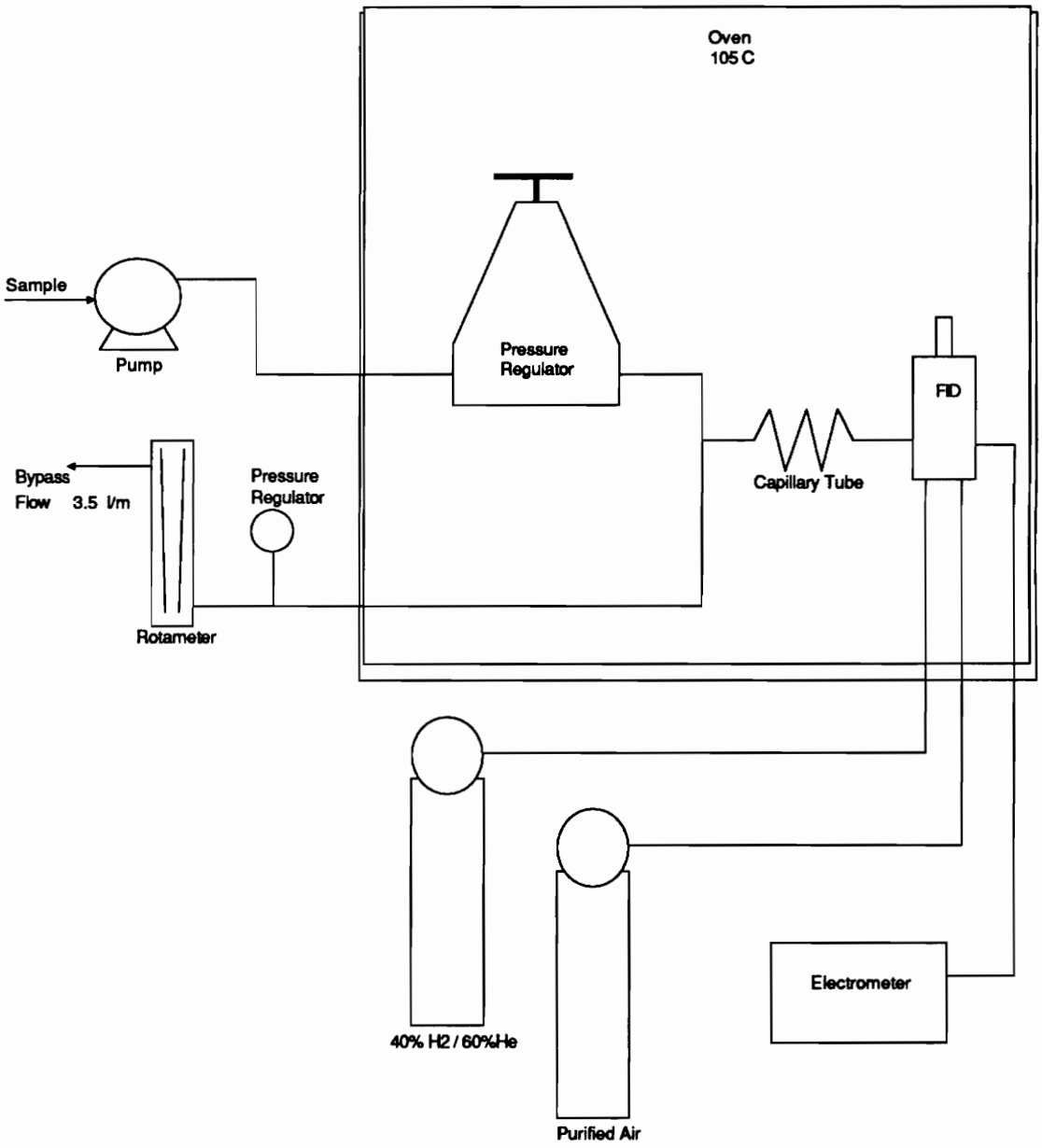

Figure 2.6: Schematic of Total Hydrocarbon Analyzer System

2.6 Supporting Instrumentation

The glovebox was instrumented with thermocouples to measure both gas temperatures in the box and window glass temperatures. Furthermore, the fuel weight and heat flux inside the glove box were recorded. A laser system in the exhaust duct was used to determine smoke obscuration.

2.6.1 Temperature Measurements

An aspirated thermocouple tree with 8 branches spaced 12 cm apart monitored the temperature profile within the glovebox. The rake was positioned 38 cm away from the air inlet end of the box with the highest branch 15 cm away from the ceiling and the lowest branch 23 cm away from the floor. Figure 2.7 shows the location of these branches in relation to the ceiling. Type K, 30 gage thermocouples were used.

In order to aspirate the tree, a 249 W (1/3 hp) pump was attached so that it drew air past each thermocouple bead at a velocity of 3 m/sec [25]. An ice/water trap was placed between the tree and pump to allow water and particulates to condense out of the air being drawn through the pump. By aspirating the thermocouple beads, radiation effects should be eliminated.

Two thermocouples were also placed at the exhaust end of the box to determine if there was any temperature change between there and the thermocouple rake. These thermocouples were located in the horizontal center of the end panel and 21 and 100 cm from the ceiling (Figure 2.7). Figure 2.8 shows the location of these thermocouples and the rake as viewed from the glovebox ceiling.

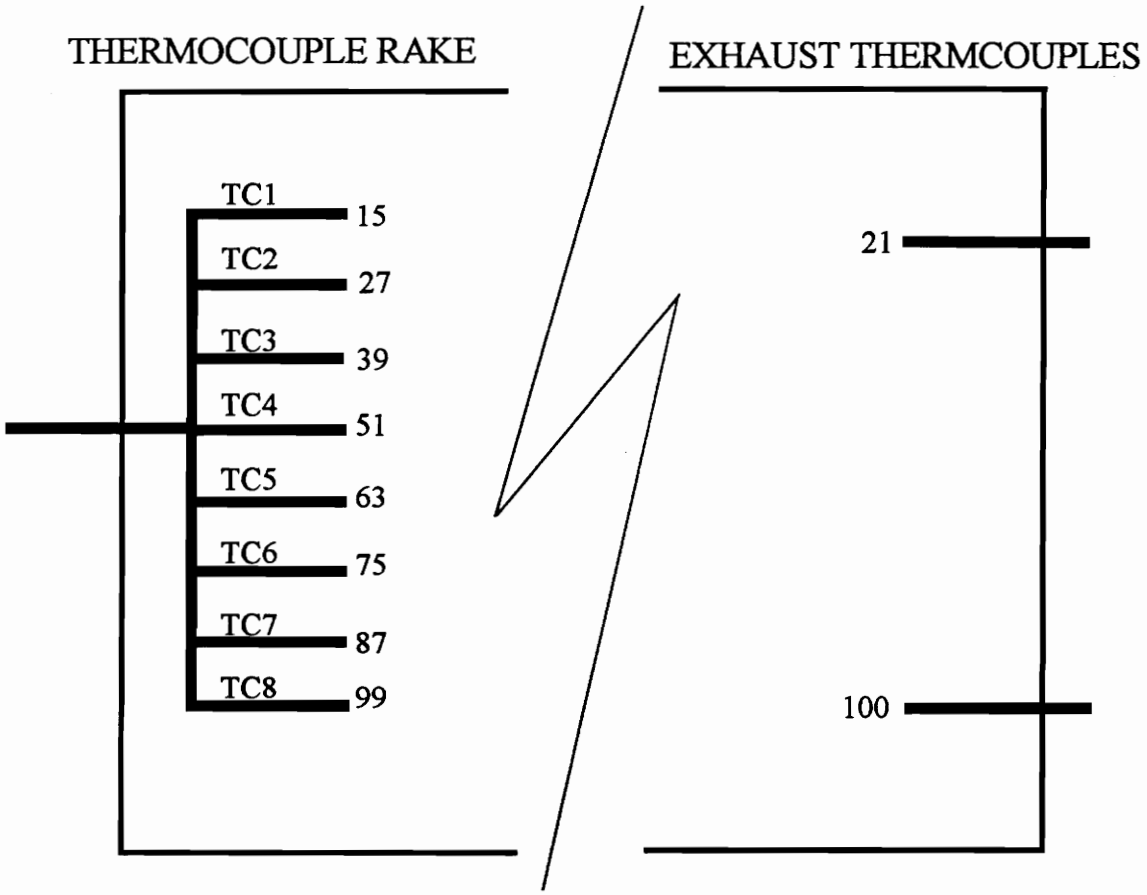

Figure 2.7: Vertical Location of Rake and Exhaust Thermocouples

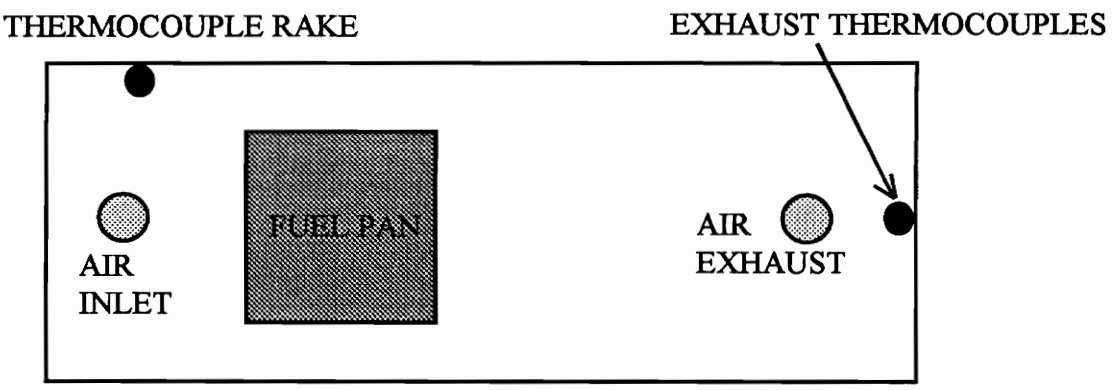

Figure 2.8: Location of Rake and Exhaust Thermocouples as Viewed From Glovebox Ceiling

Chromel-Alumel (Type K) "Cement-on" butt-welded thermocouples from Omega were placed on the glove box side of each window in the center and at the edge underneath the gasket so that the temperature differential could be measured and correlated with failure. Durabond 950, a high temperature cement manufactured by Cotronics Corporation, was used to attach the thermocouple to the glass. Specifications for this metal-based cement approve it for use up to 510 C (950 F).

2.6.2 Fuel Weight Measurements

Fuel weight was monitored using an A & D Weighing Division FV/FW Series 150 kg capacity load cell. It was calibrated using a collection of weights which totaled 131.5 kilograms. The load cell was placed underneath the glovebox. Four holes were drilled in the box floor to allow the legs of the pan/table structure to pass through and rest on the load cell.

2.6.3 Heat Flux Measurements

Heat flux measurements were obtained using total heat flux transducers manufactured by Medtherm Corporation. These transducers were calibrated for a maximum heat flux of 200 kW/m^2. A typical calibration curve corresponding to a transducer is shown in Appendix D. Since water cooling was required for this heat flux range, a garden hose with proper fittings was hooked up to the gages to allow a continuous supply of cool water to circulate. Two of the transducers were located in the center of the box, one on the ceiling and one on the floor. The third was located on the wall opposite the fuel pan.

2.6.4 Smoke Measurements

Smoke yields and smoke generation rates were calculated based on smoke obscuration measurements taken in the secondary exhaust duct. A photodiode was used to measure attenuation of the 670 nm laser in the duct. Calculations of the smoke generation rate and yield assumed a Rayleigh scattering regime [26].

2.7 Data Acquisition

Four Data Translation boards were used with a 286 Zenith Data Systems computer to acquire the data for these experiments. Two of the boards were model DT2801-A and the other two were DT2805 all of which are capable of gains of 1, 2, 4, and 8. One of the DT2801-A boards was connected to a DT707 panel and the other to a DT756-Y panel, which provides temperature compensation and signal conditioning. Both DT2805 boards were hooked up to DT707-T screw terminal panels which are equipped with temperature compensation. The three screw terminal panels, which were capable of temperature compensation, could also gain the small voltages corresponding to the thermocouples so that they could be monitored more accurately.

The gains for these boards were adjusted automatically by the computer as measurements were taken in order to take advantage of the full range. Each board was configured for differential measurements except the DT2801-A board which was connected to the DT756-Y panel. One of the unique features of this panel is that it allows thermocouples to be measured in a single-ended mode resulting in twice as many channels. Further configuration included bipolar setup for all boards except the DT2801-A board which was attached to the DT707 panel. It should be noted that thermocouple measurements require a bipolar configuration.

A data acquisition program was written using PCLAB. Each channel was sampled at 2 second intervals, a time period sufficient to monitor system changes. The number of measurements collected varied with each test so that several acquisition programs were utilized. A typical program listing can be found in Appendix E.

In addition to collecting data with a computer, each test was videotaped from at least two locations: from the roof of the test building and from the ground approximately 10 feet from the front of the glovebox. These tapes were used to correlate the times of window cracking and other significant occurrences to the measurements taken with the computer. Furthermore, visual observations made from the tape enabled comparison of the fires' behaviors.

3. TEST PROCEDURES

3.1 Introduction

This chapter explains the experimental procedures used for the three sets of experiments: open burn tests, full scale pan tests, and reduced fuel surface area tests. The purpose of the open burn tests was to provide a baseline for the burning rates corresponding to each pan size. Following this evaluation, full scale pan experiments were conducted to observe the response of the glovebox to pan fires. Then, pan surface area was varied to determine if the fires became more or less intense. A summary of these experiments is provided in Table 3.1.

3.2 Open Burn Tests

For the open burn test set, the fuel pan was placed outside the glovebox on the load cell where there would be an unlimited supply of oxygen and no radiation feedback from the enclosure. During the burns, fuel mass loss was recorded using the data acquisition system. Six tests were performed; three in the full scale pan and one in each of the smaller pans. The fuel depth was 5.1 cm for the full scale pan tests, 2.5 cm for the 83.8 cm diameter and 62.2 cm diameter pans, and 3.8 cm for the 27.9 cm diameter pan test.

Full scale pan tests were conducted with three mixture compositions which were determined on a volume basis. The compositions were varied because the actual composition in the lathe drip pan is variable. It begins as pure oil and becomes 50% oil and 50% solvent by the time the pan is emptied. Consequently, it was necessary to determine if mixture composition affected the burning rate. Mixture compositions which were used include 50% oil and 50% solvent, 75% oil and 25% solvent, and 90% oil and 10% solvent. No burns were conducted with 100% oil due to the difficulty associated with igniting it.

Table 3.1: Description of Tests Conducted

TEST NO.	PAN SIZE (CM)	TEST CONDITIONS
1	91.4 X 91.4	OPEN BURN, 50/50 OIL & SOLVENT
2	91.4 X 91.4	OPEN BURN, 75/25 OIL & SOLVENT
3	91.4 X 91.4	OPEN BURN, 90/10 OIL & SOLVENT
4	83.8 dia	OPEN BURN
5	62.2 dia	OPEN BURN
6	27.9 dia	OPEN BURN
7	91.4 X 91.4	NORMAL
8	91.4 X 91.4	NORMAL
9	91.4 X 91.4	NORMAL
10	91.4 X 91.4	#3 GLOVE HOLE OPEN
11	91.4 X 91.4	#3&4 GLOVE HOLES OPEN
12	91.4 X 91.4	#3&4 GLOVE HOLES OPEN
13	91.4 X 91.4	#2-4 GLOVE HOLES OPEN
14	91.4 X 91.4	#1-4 GLOVE HOLES OPEN
15	91.4 X 91.4	#4 GLOVE HOLE OPEN
16	91.4 X 91.4	#4 GLOVE HOLE OPEN
17	91.4 X 91.4	#3&4 GLOVE HOLES OPEN
18	91.4 X 91.4	#3&4 GLOVE HOLES OPEN
19	91.4 X 91.4	#2 WINDOW REMOVED
20	83.8 dia	NORMAL
21	62.2 dia	NORMAL
22	27.9 dia	NORMAL

In addition to the full scale pan tests, one test was conducted with each of the smaller fuel pans. The fuel was prepared as a 50 % oil and 50% solvent mixture since it was determined that the mixture composition does not significantly affect the burning characteristics. For all remaining experiments, this composition was used.

3.3 Full Scale Pan Tests

Three experiments were full scale mockups of a glovebox fire (referred to as "normal" conditions). In order to achieve the proper vacuum (1.4 mm Hg), panel seams and glove collars were sealed with Permatex high temperature sealant to prevent air leakage. Also, an exhaust flow of 0.085 m^3/sec was established. For the purpose of imitating typical working conditions, the gloves in the second panel by the fuel pan were left inside the box with the glove hole covers raised while the other gloves were pulled out and the covers were down.

Next, scenarios with additional ventilation openings were tested to determine what effect they would have on the fire dynamics. Ventilation openings were created by removing gloves or by removing a window. These tests were intended to simulate cases where gloves were already missing or a window was already broken. First, one at a time, gloves were removed and glove hole covers raised to simulate the loss of gloves. This practice was done until 4 glove holes (as ordered in Figure 3.1) were open. Then, tests with either one or two glove holes open were repeated to determine the reproducibility of the results. Next, a test was performed after removing the front window (#2) overlooking the fuel pan. The glove holes were covered in this scenario.

As the gloves endured more fires, they began to pyrolyze and, in some cases, had holes in them. Eventually, the gloves were removed and the glove holes were covered

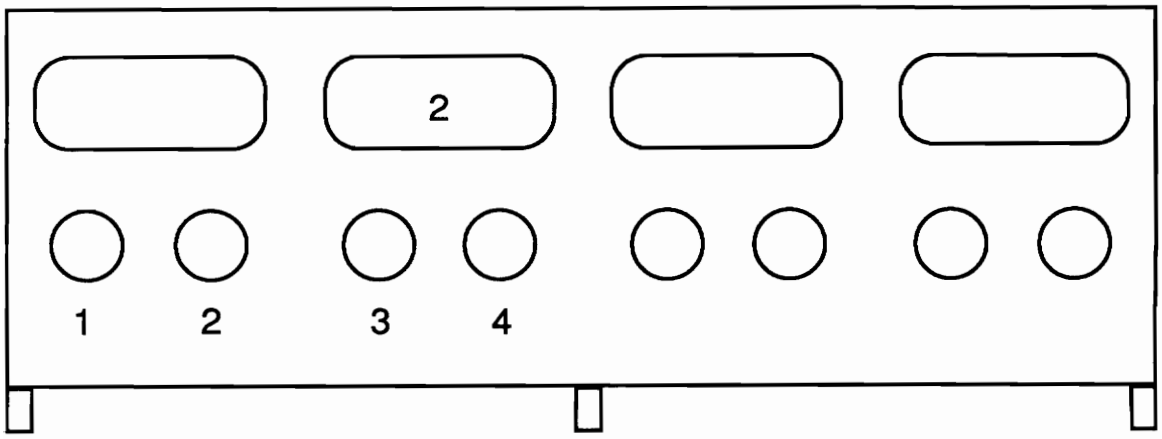

Figure 3.1: Numbering System for Glove Holes and Window

with steel plates and sealed with the sealant. Likewise, window gaskets were replaced as they burned to the point where substantial air leakage was possible. When new gaskets were no longer available, the windows were removed and the resulting holes were covered in the same manner as the glove holes.

3.4 Reduced Fuel Surface Area Tests

After performing experiments with the full scale fuel pan, the three circular pans were tested. The two largest pans were filled with approximately 1.3 cm of liquid. The smallest pan was filled with 5.1 cm of fuel so that load cell fluctuations would not correspond to such a large percentage of the total fuel weight. The exhaust flow rate remained the same as in the full scale pan tests.

4. RESULTS

4.1 Introduction

This chapter presents the data, both qualitative and quantitative, obtained from open burn experiments and glovebox experiments. First, open burn rates will be presented and discussed. Next, results from full scale pan experiments will be addressed, followed by the reduced surface area pan experiments. A comparison and discussion of burning rates, equivalence ratios, heat release rates, exhaust gas concentrations, temperature-time histories, and vertical temperature profiles will be provided in situations where enough data was available.

4.2 Data Reduction and Presentation

Raw voltage readings were manipulated to represent dry gas concentrations, burning rates, air flow rates, and temperatures. Further calculations were performed to obtain wet gas concentrations, equivalence ratios, and heat release rates. As an aid in this process, several FORTRAN programs, found in Appendix F, were written to reduce this data. A further description of these calculations is provided below.

Burn rates were calculated by dividing the fuel loss during a specified time period by the number of seconds in the time period in order to reduce the amount of noise in the results. Although larger time periods smooth data further, important characteristics can be lost. Careful attention was paid to this point so that time periods were kept as short as possible. Average values for burn rates throughout each fire were determined by averaging the values during a time period which was considered to be representative of a "steady-state" burning. It should be noted that this was an subjective interpretation and

in some cases, there was no definite steady-state period. The standard deviation of the values during this interval was also calculated and is reported with the average values.

Two equivalence ratios were calculated: the plume equivalence ratio and the exhaust gas equivalence ratio. The equivalence ratio, also referred to as phi, is the ratio of the measured fuel/air ratio to the stoichiometric fuel/air ratio:

$$\phi = (fuel/air)_{measured} / (fuel/air)_{stoichiometric}$$

Table 2.1 listed stoichiometric fuel/air ratios of 15.2 and 14.9 for the oil and solvent, respectively. Therefore, by averaging these values, an overall stoichiometric fuel/air ratio of 15.0 was assumed. Since the exact molecular composition of the fuel was not known, a carbon-to-hydrogen ratio sensitivity analysis was performed. Results showed that the stoichiometric fuel/air ratio does not change significantly for the range of carbon-to-hydrogen ratios typical of these types of liquids. In order to calculate the plume equivalence ratio, the burn rate (kg/sec) as determined from load cell measurements was divided by the exhaust air rate (kg/sec) constituting $(fuel/air)_{measured}$. Then, this value was multiplied by 15.0.

A different concept was utilized in calculating the exhaust gas equivalence ratio. With this method, a system of equations was formed by performing atomic balances on each element. In the tests where this method was used, carbon monoxide, carbon dioxide, oxygen, and hydrocarbon concentrations were known; therefore, there was enough information to solve the system and determine the exhaust equivalence ratio.

Uncertainties associated with the plume equivalence ratio involve the accuracy of the load cell, the validity of the orifice meter, and the assumption of the stoichiometric

air-to-fuel fraction. The load cell used for these tests had an accuracy of ± 20 grams, which proved to be significant with the smallest pan since the burn rate was very small. Also, as will be discussed in more detail later in this chapter, the load cell readings drifted in some tests. In addition, exhaust air rates are subject to several sources of error resulting from pressure and temperature measurements at the orifice meter and the estimation of a discharge coefficient. On the other hand, the equivalence ratio calculated from the exhaust gas concentrations depends on the accuracy of the gas analyzers and the assumptions made for the hydrogen concentration and molecular composition of the unburned hydrocarbons. Post test calibration checks on the analyzers did not show significant drifts with the exception of the carbon dioxide analyzer which, in some tests, drifted by values as high as 1.5%.

Fire heat release rates were calculated by employing three methods, depending on the data available. One method calculated the mass loss heat release rate which involved multiplying the burn rate and the heat of combustion as shown in the following equation:

$$\dot{Q}_{mass\ loss}\ (kW) = \Delta H_c\ (kJ/kg) * burn\ rate\ (kg/sec)$$

where ΔH_c was approximated as 46000 kJ/kg

There are some important assumptions associated with this expression that should not be overlooked. First, it assumes that all fuel is reacting completely, i.e. all carbon is converted to carbon dioxide. Also, it assumes that all mass that is lost is taking part in the combustion process so that the burn rate and the fuel mass loss rate are equivalent. Both of these assumptions are idealistic, but there is value in this calculation since it should represent the maximum heat release rate.

Another method of calculating the heat release rate was based on oxygen depletion. The basis for this method is that the mass fraction of oxygen consumed in the combustion process multiplied by an experimentally determined heat of reaction for oxygen ($\Delta H_{c,oxygen}$) results in the heat release rate. Oxygen heat of reactions may range from 11 to 14 MJ/kg depending on the fuel [13]. In this analysis, $\Delta H_{c,oxygen}$ = 13 MJ/kg was assumed. In order to develop an expression for the mass fraction of oxygen consumed, conservation of mass was applied. Since the burn rate and exhaust mass flow rate were both measured, the inlet air flow rate was assumed to be the difference between these quantities. The oxygen mass fraction into the compartment results by multiplying this quantity by the mass fraction of oxygen in air (0.23). Likewise, the oxygen mass fraction out was simply the exhaust mass flow rate multiplied by the exhaust oxygen concentration. These equations result from this derivation:

$$Q_{oxygen\ depletion} = (O_2\ m.f._{in} - O_2\ m.f._{out}) * \Delta\ H_{c,oxygen}$$

where

$$O_2\ m.f._{in} = 0.23*(air_{exhaust} - burn\ rate)\ (kg/sec) \text{ and}$$

$$O_2\ m.f.\ out = x_{O2,exhaust} * air_{exhaust}\ (kg/sec)$$

A third method for calculating heat release rate involves the equivalence ratio which was calculated from the exhaust gas concentrations as mentioned above. Since the stoichiometric fuel/air ratio and the air rate were known, the mass loss rate was calculated. This value was then multiplied by the heat of combustion as in the mass loss method described.

When considering the parameters which introduce uncertainty into these methods, each one is affected by the accuracy of the exhaust air rate measurement. Furthermore,

both the mass loss and oxygen depletion heat release rate utilize burn rate calculations thereby introducing the error from the load cell. In addition to these two sources, the oxygen depletion method relies on measurements from the oxygen analyzer. On the other hand, besides the exhaust rate measurement, the exhaust equivalence ratio only depends on the reliability of the gas analyzers.

Since water was removed from the exhaust sample prior to carbon monoxide, carbon dioxide and oxygen analysis, these measurements had to be corrected so that water was included as an exhaust product. This correction was performed by assuming that the ratio of carbon dioxide-to-water formation remains constant, regardless of the equivalence ratio. Therefore, by using the carbon dioxide-to-water ratio at stoichiometric conditions, the wet concentrations were estimated.

Temperature-time histories were plotted for every other branch on the thermocouple rake beginning with TC1. This sampling was used since plotting every branch crowded the graph so that it was unreadable. In several cases, one of these measurements was bad and another thermocouple was substituted.

Plots displaying vertical temperature profiles include the temperatures at each rake branch several times throughout the fire. Curves or lines are fit through the profiles at each particular time. Points, represented by solid symbols, also appear on these plots to represent the thermocouples located by the glovebox exhaust at the same times as the rake temperatures. These points are valuable in assessing the horizontal homogeneity of the glovebox.

Smoke obscuration measurements were used to determine smoke yield (g smoke produced/g fuel burned) and smoke generation rate (kg/m^2*sec). First, the extinction

coefficient was determined based on Beer's Law:

$$K = (1/L) * ln(I/Io)$$

where I and I_O represent the attenuated laser beam measurement and the reference beam measurement, respectively; and L is the path length, or, in this case, the diameter of the secondary exhaust duct. Further calculations were based on the Rayleigh scattering regime which applies to soot particles which are an order of magnitude less than the incident wavelength. Since the laser used in these experiments had a wavelength of 670 nm, this theory assumes that the soot particles are less than 67 nm in diameter. Soot particles may range between a few nanometers to tens of microns so the validity of this assumption is questionable [27]. Tewarson defines a smoke yield (grams of smoke produced per grams of fuel burned) based on the mass concentration of smoke (C_S), volumetric flow rate through the sampling volume (V_T), generation rate of fuel vapors per fuel surface area (G_f), and the fuel surface area (A), resulting in the following equation:

$$Y_S\,(g/g) = C_S * V_T / (G_f * A)$$

The mass concentration of smoke is based on the specific extinction coefficient, which must be assumed, and the optical density per unit length. Similarly, the mass generation rate, G_S (kg/m^2*sec) can also be calculated [28]:

$$G_S = C_S * V_T / (A)$$

Problems involving point discretization and physically unreasonable readings were encountered with the heat flux transducer measurements. Therefore, this data will not presented in this chapter. However, plots of each transducer output as a function of time for a normal full scale pan test and for the full scale pan test with a window removed (Tests #8 and #19) are included in Appendix G to demonstrate these problems.

In addition to these calculations, visual data from the videotapes was tabulated for the flame extinction times. As will be discussed later, some fires self-extinguished while others burned until all fuel had been consumed. These results are provided in Table 4.1 where the symbol "*" denotes tests where the fires were stable enough to burn until all fuel was depleted. Usually, there was no definite means of determining when this extinction occurred thus these times were estimated.

4.3 Open Burn Tests

The burn rate as a function of time is plotted in Figure 4.1 for the full scale pan open burn using a fuel mixture of 50/50 mixture of oil and solvent. An initial rise to 30 g/sec is followed by a steady decline throughout the fire with an average burn rate of 27 ± 3.2 g/sec between 330 and 600 seconds. This behavior would suggest that the molecular mixture composition is changing throughout the fire since a steady burning condition is never achieved. It is possible that the lighter hydrocarbons are burning first leaving the higher molecular weight components thus accounting for the decreasing burning rate. The results of the second open burn, also in the full scale fuel pan, are shown in Figure 4.2. The mixture composition consisted of 75/25 oil and solvent. In contrast to the 50/50 oil and solvent experiment and for an unknown reason, the burn rate increased slightly throughout the fire and had an average burn rate of 24 ± 1.9 g/sec.

Table 4.1: Estimated Flame Extinction Times (* denotes fires where all fuel was depleted)

TEST NO.	BURN TIME (MINUTES)
1	23*
2	22*
3	17*
4	16*
5	18*
6	45
7	2.5
8	135*
9	10
10	7.6
11	1.7
12	2.5
13	0.9
14	5.4
15	0.7
16	1.5
17	1
18	1
19	44*
20	33*
21	30*
22	30*

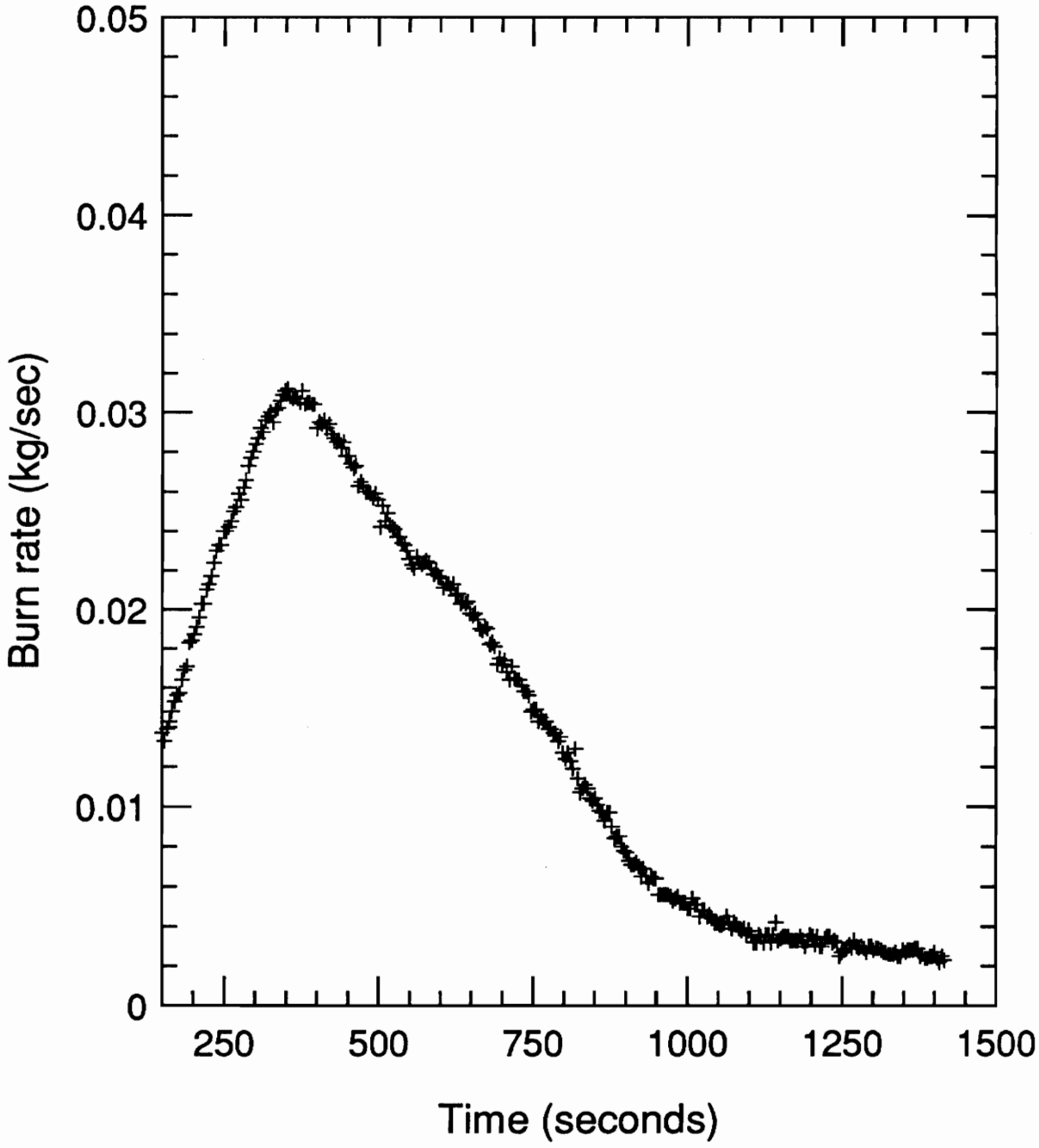

Figure 4.1: Open Burn Rate-Time History for Test #1: Full Scale Pan, 50/50 Oil and Solvent Mixture

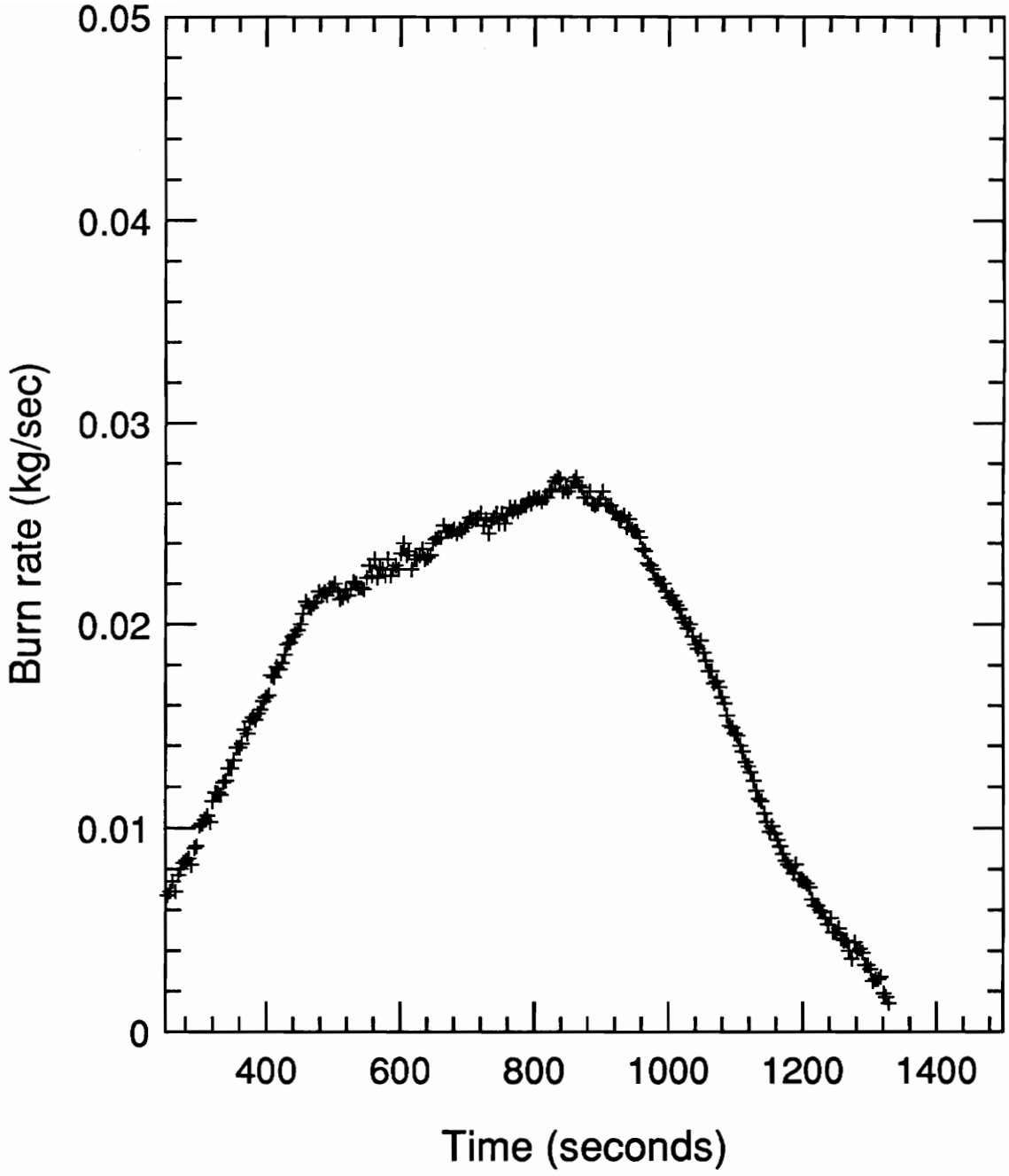

Figure 4.2: Open Burn Rate-Time History for Test #2: Full Scale Pan, 75/25 Oil and Solvent Mixture

Likewise, in the last full scale pan open burn with 90/10 oil and solvent mixture, this same trend is observed (Figure 4.3). Again, the burning rate increases throughout the fire. An average burn rate of 26 ± 1.5 g/sec was determined.

A time history of the burn rate corresponding to the 83.8 cm diameter pan is displayed in Figure 4.4. From this plot, a nearly steady burning rate is seen with an average of 17 ± 0.4 g/sec. In addition, the open burn rate for the 62.2 cm diameter pan is shown in Figure 4.5. This pan area resulted in an average burn rate of 6 ± 0.3 g/sec.

Figure 4.6 shows the burn rate for the last open burn experiment with the 27.9 cm diameter fuel pan. As can be seen in this plot, point discretization emphasizes poor load cell resolution. An overall increase in burn rate is noticed in this test with an average value of 0.9 ± 0.1 g/sec.

As a means of examining the dependence of pan diameter on burn rate, the open burn rate divided by the fuel surface area is plotted as a function of pan diameter in Figure 4.7. Since the full scale pan was square, an effective diameter of 1.03 m was calculated and the average burn rate for the 50/50 test was plotted to remain consistent with the smaller pan tests. A larger burn rate per surface area results with increasing pan diameters. This trend can be compared with Drysdale's description of open pool fire behavior. He defines three regimes for these fires with the first characteristic of pan diameters less than 0.03 m. Flames are laminar in this regime and the burn rate increases as the pan diameter decreases. At pan diameters greater than 1 m, the flame is turbulent and will be unaffected by pan diameter. In the transition zone, 0.03 m - 1 m, the burn rate increases to reach the value where it levels off when a turbulent flame is achieved [13].

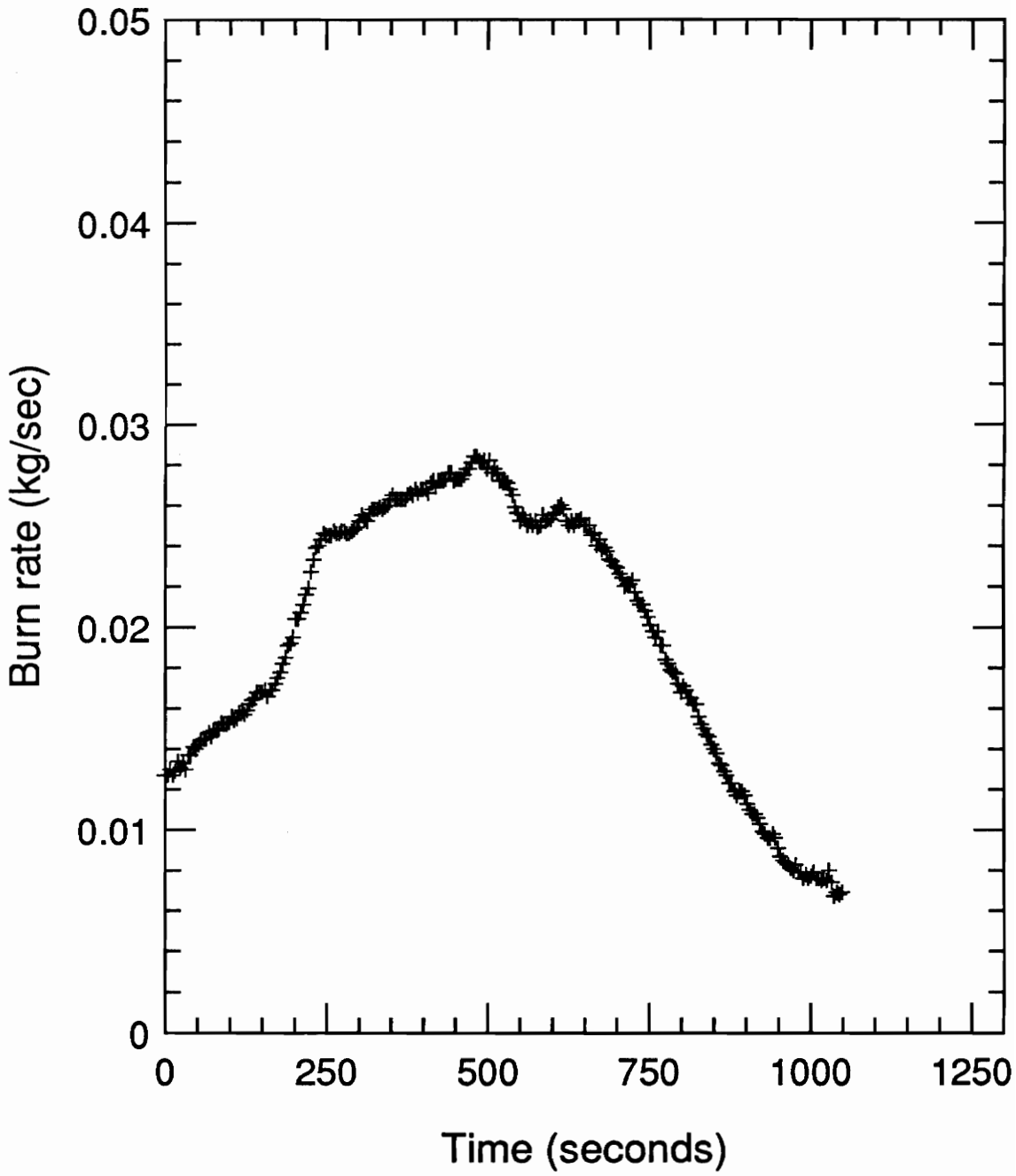

Figure 4.3: Open Burn Rate-Time History for Test #3: Full Scale Pan, 90/10 Oil and Solvent Mixture

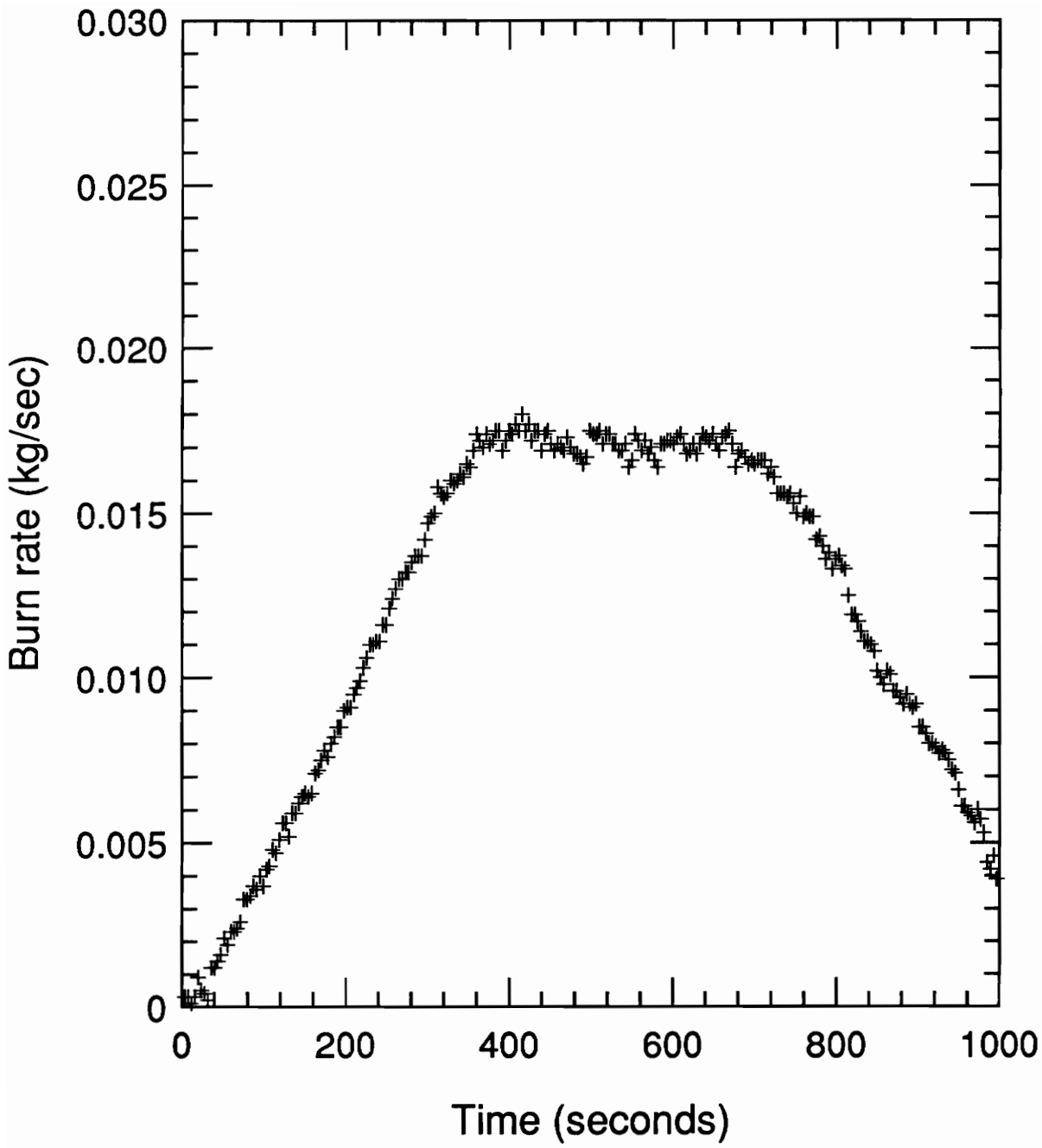

Figure 4.4: Open Burn Rate-Time History for Test #4: 83.8 cm diameter Pan

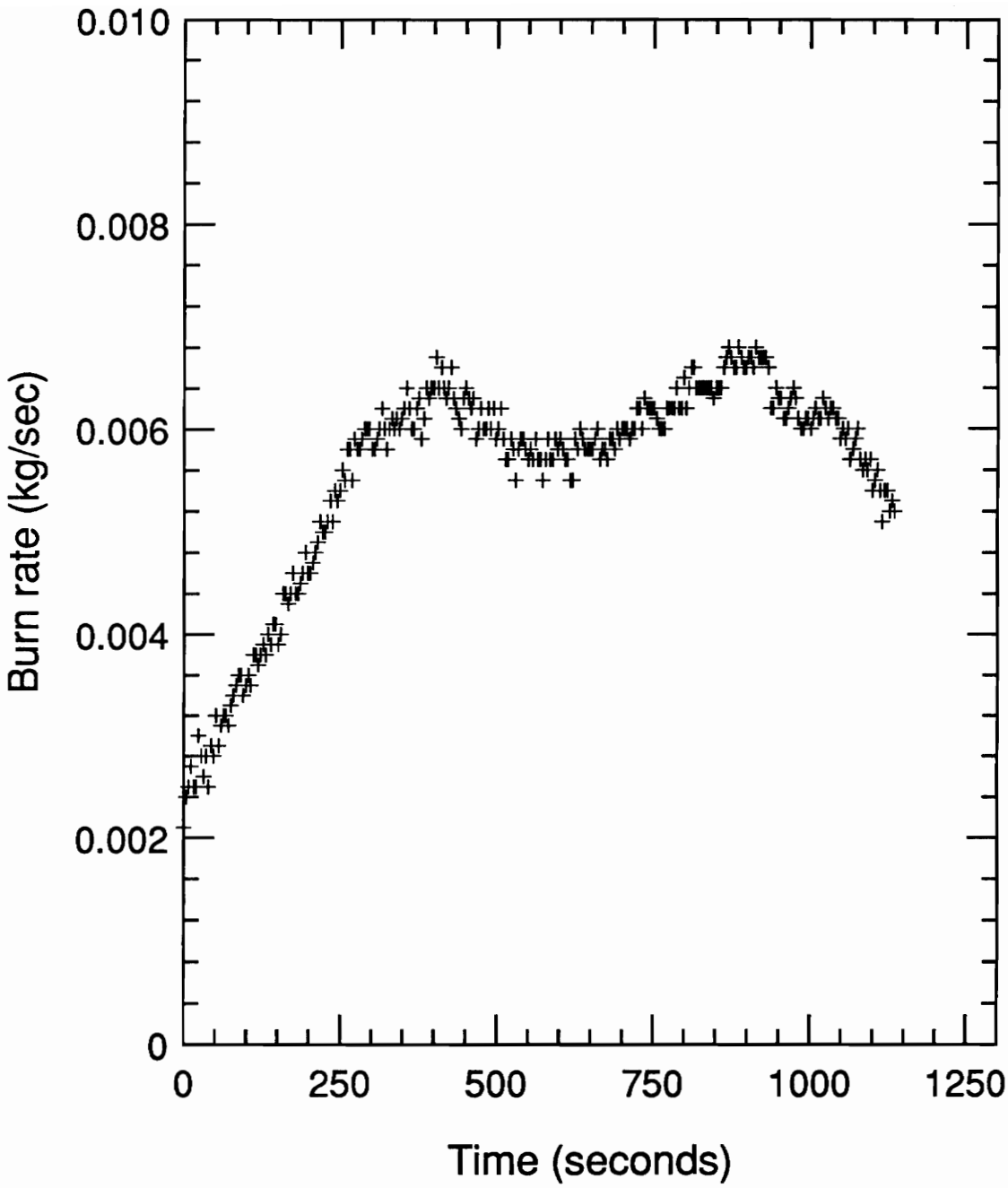

Figure 4.5: Open Burn Rate-Time History for Test #5: 62.2 cm diameter Pan

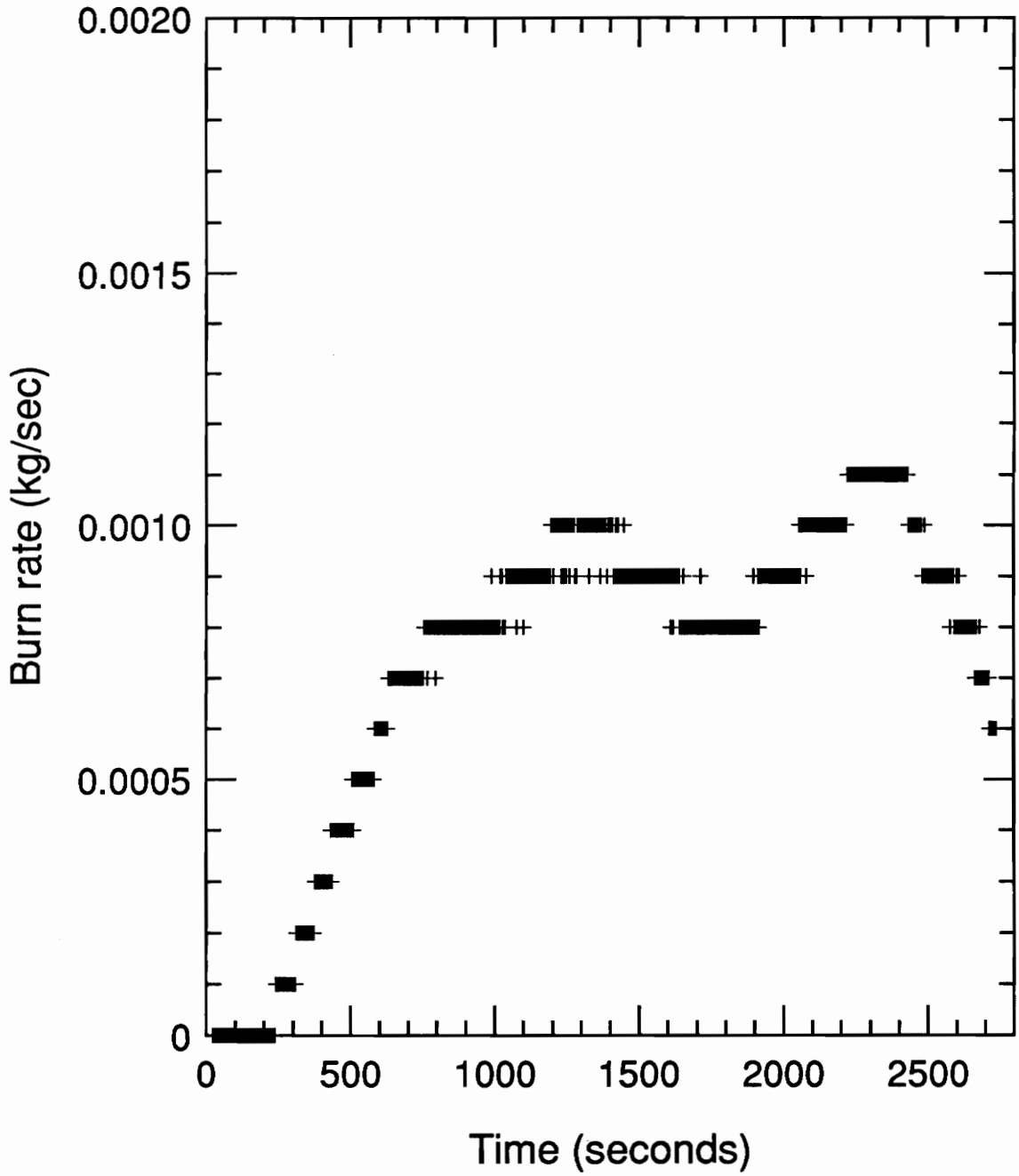

Figure 4.6: Open Burn Rate-Time History for Test #6: 27.9 cm diameter Pan

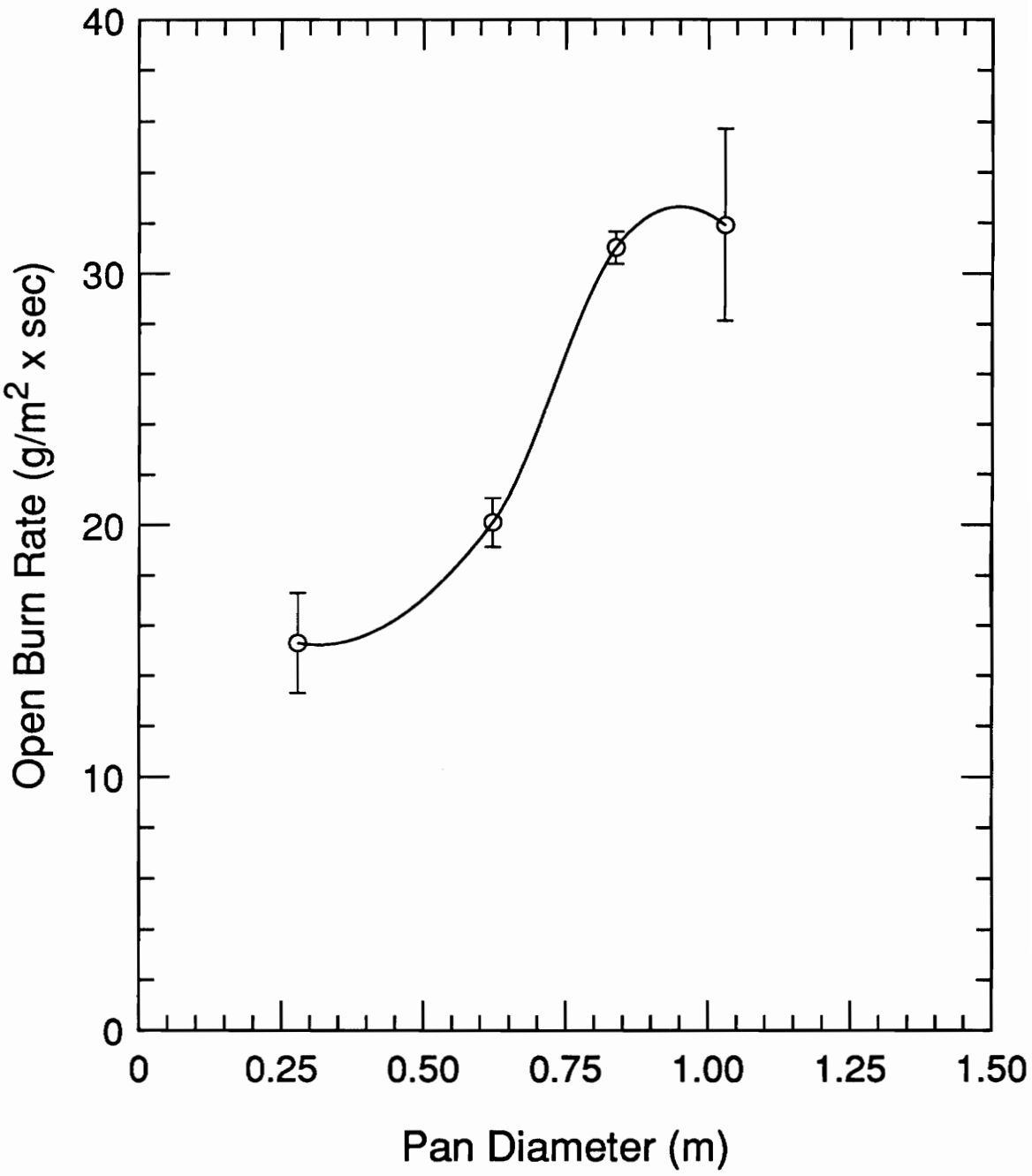

Figure 4.7: Average Open Burn Rate Per Fuel Surface Area vs. Pan Diameter

For these tests, the three smallest pans fall into the transition region and fit the trend that Drysdale explained. The largest pan, corresponding to the end of the transition zone, shows a leveling off behavior as Drysdale predicted. Although there are not enough points to properly verify the three regimes, the data obtained in these tests suggests agreement with the open burn rate characteristics that Drysdale describes.

In comparing the burn rates resulting from different mixture compositions, it was concluded that the burn rate does not change significantly with mixture composition (Figures 1-3). This result is as expected based on the similar heats of vaporization for these two liquids. Mixtures consisting of 50% oil and 50% solvent were used in the remaining experiments because it is the most realistic lathe drip pan composition.

No consistent trends were observed in burning rate behavior as a function of time. Three out of the six tests have burning rates which increased with time but the other three tests provide dissimilar behavior. Therefore, no conclusion may be drawn in this area.

4.4 Full Scale Pan Experiments

In this section, visual results from the sealed glovebox experiments will be explained followed by the presentation of numerical data. Then, results are provided from the tests with added ventilation openings.

4.4.1 Normal Glovebox Experiments

The first test performed (Test #7) self-extinguished approximately 2 minutes after full pan ignition because of insufficient oxygen. Due to electrical problems, numerical data was not collected; however, some important visual observations were made. Most importantly, in this test, the glovebox contained the exhaust gases. All windows cracked

but did not break and only the gloves which were left in the box were destroyed, allowing an insignificant amount of leakage to occur.

An interesting phenomenon of puffing was witnessed during this fire. One could visually observe the fire "breathe"; that is, it would draw in air, consume it, and expel smoke and combustion gases. The pressure in the box oscillated between negative and positive to such an extent that the gloves were pulled in and pushed back out. This puffing occurred with a frequency on the order of 0.25 Hz. The flame "danced" around the fuel surface, often disappearing from view. This behavior was a problem in many tests as it was difficult to determine when the fire was completely out. Furthermore, this problem was complicated by the heavy layer of soot which blocked vision through the windows. When the flame could be observed, it tended to lean toward the air inlet, waiting for the fresh oxygen supply. Eventually, the flame extinguished when it could no longer obtain enough oxygen.

On the second occasion that this scenario was tested (Test #8), the flame did not self-extinguish, but rather burned until all fuel was consumed, about 2 hours 15 minutes. New ceiling windows were installed as well as a new lead glass window in the front #2 position. As in the first test, the windows cracked but did not break and no glass temperature data was obtained. The laminate used in the lead glass windows melted but the separated pieces did not fall out of the gasket. At approximately 45 minutes into the burn, the pressure built up within the box so that the ceiling window closest to the inlet duct was pushed out of the gasket. It remained in a position which blocked all but a small amount of exhaust gases. Following this phenomenon, the gasket burned until only charred remnants remained. However, the window guard prevented the window from falling into the box.

As in the first test, the third sealed glovebox experiment (Test #9) self-extinguished after 10 minutes. Again, a puffing behavior was observed and no significant containment losses were noticed. The reason why extinction did not occur in Test #8 as it did in Tests #7 and #9 is unknown.

Burn rates as a function of time are shown in Figures 4.8 and 4.9 for Tests #8 & 9, respectively. In Figure 4.8, the burn rate is very unsteady and points are discretized. Prior to smoothing the data points, the burn rate was reported as negative at a time close to 2000 seconds. This behavior is physically impossible as it implies that mass is being created during the combustion process. This trend was observed in later tests and was attributed to the load cell's temperature compensation. Although the load cell was equipped with temperature compensation, a rapid temperature change can cause a temporary shift in the readings before the compensation catches up. This assumption was supported by the fact that the fuel weight shifted back to reasonable values before the fire was over. Furthermore, calculation of the burn rate from the exhaust gas concentrations indicated that the burn rate was fairly steady throughout the fire and did not experience spikes as seen in Figure 4.8. From Figure 4.8, an average burn rate of 4 ± 1.1 g/sec was obtained while a lower burn rate of 2.0 ± 0.2 g/sec was obtained for the self-extinguishing test (Figure 4.9).

Heat release rates are shown in Figures 4.10 and 4.11 for these tests. As seen in Figure 4.10, the unsteadiness in the load cell measurements is apparent in the mass loss heat release rate. Also, for heat release rates based on oxygen consumption, an oxygen concentration of 2% was assumed for most of the fire due to a malfunction in the data acquisition system. This concentration was observed on the analyzer's LED readout for

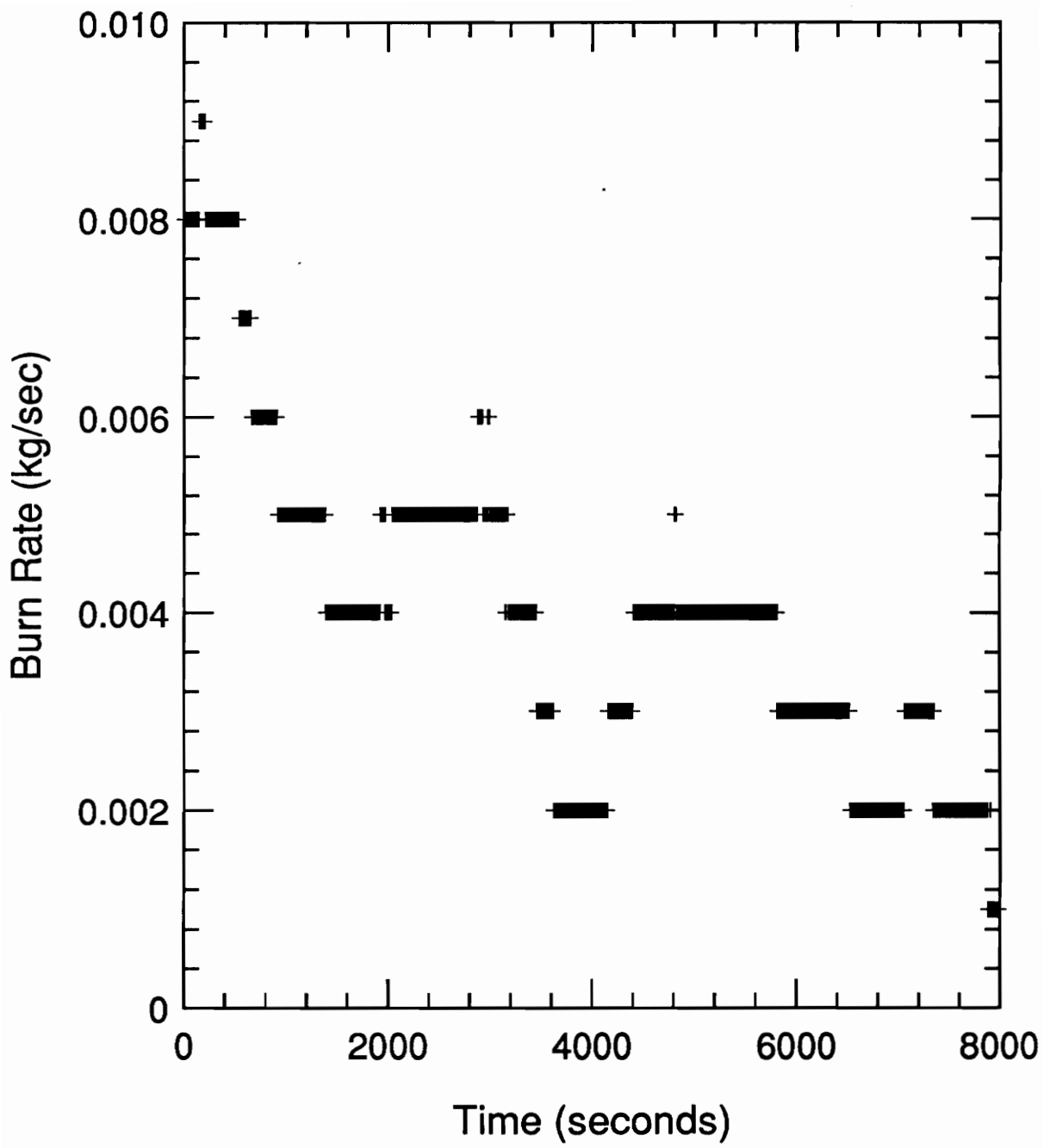

Figure 4.8: Burn Rate-Time History for Test #8: Full Scale Pan

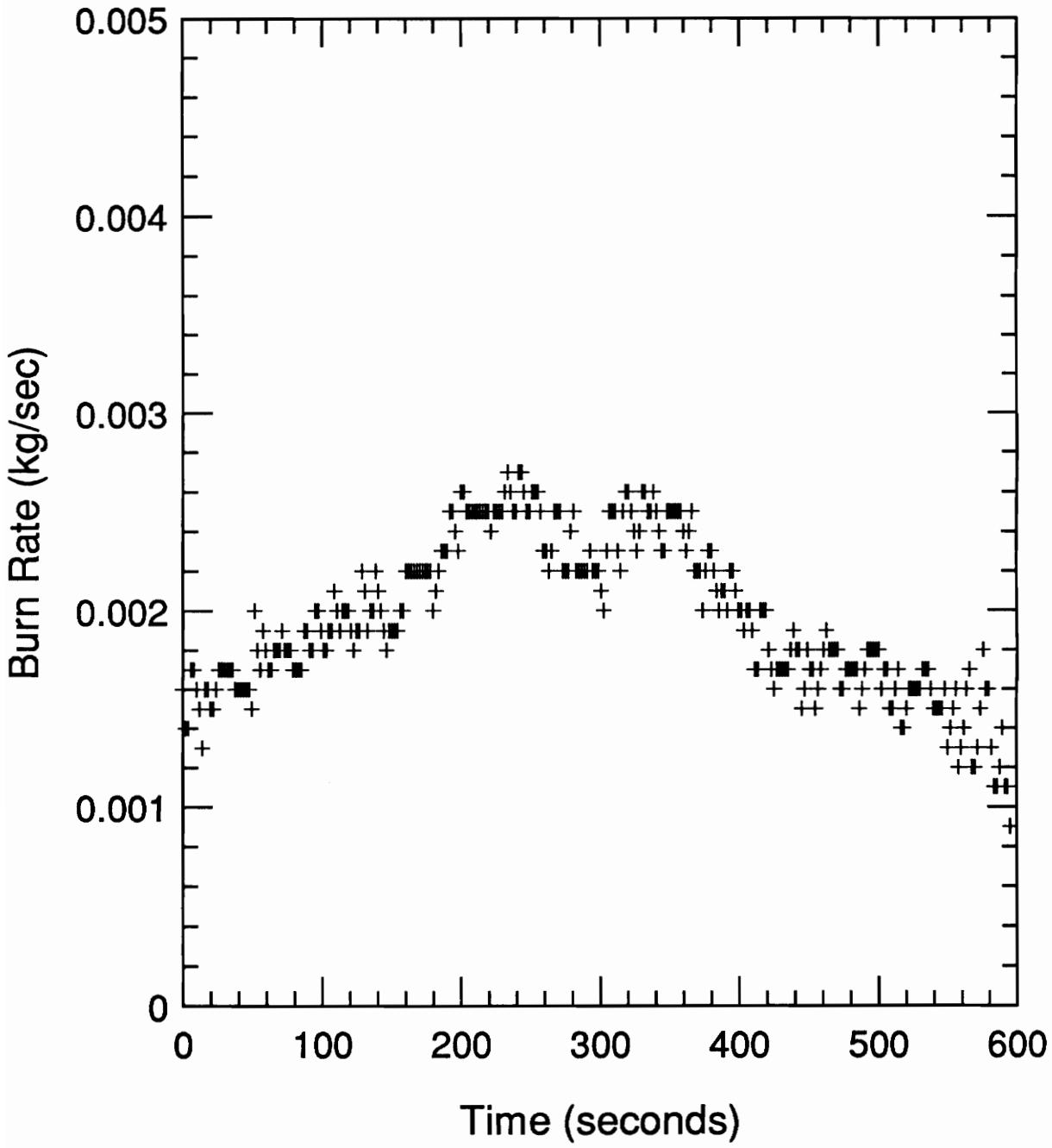

Figure 4.9: Burn Rate-Time History for Test #9: Full Scale Pan

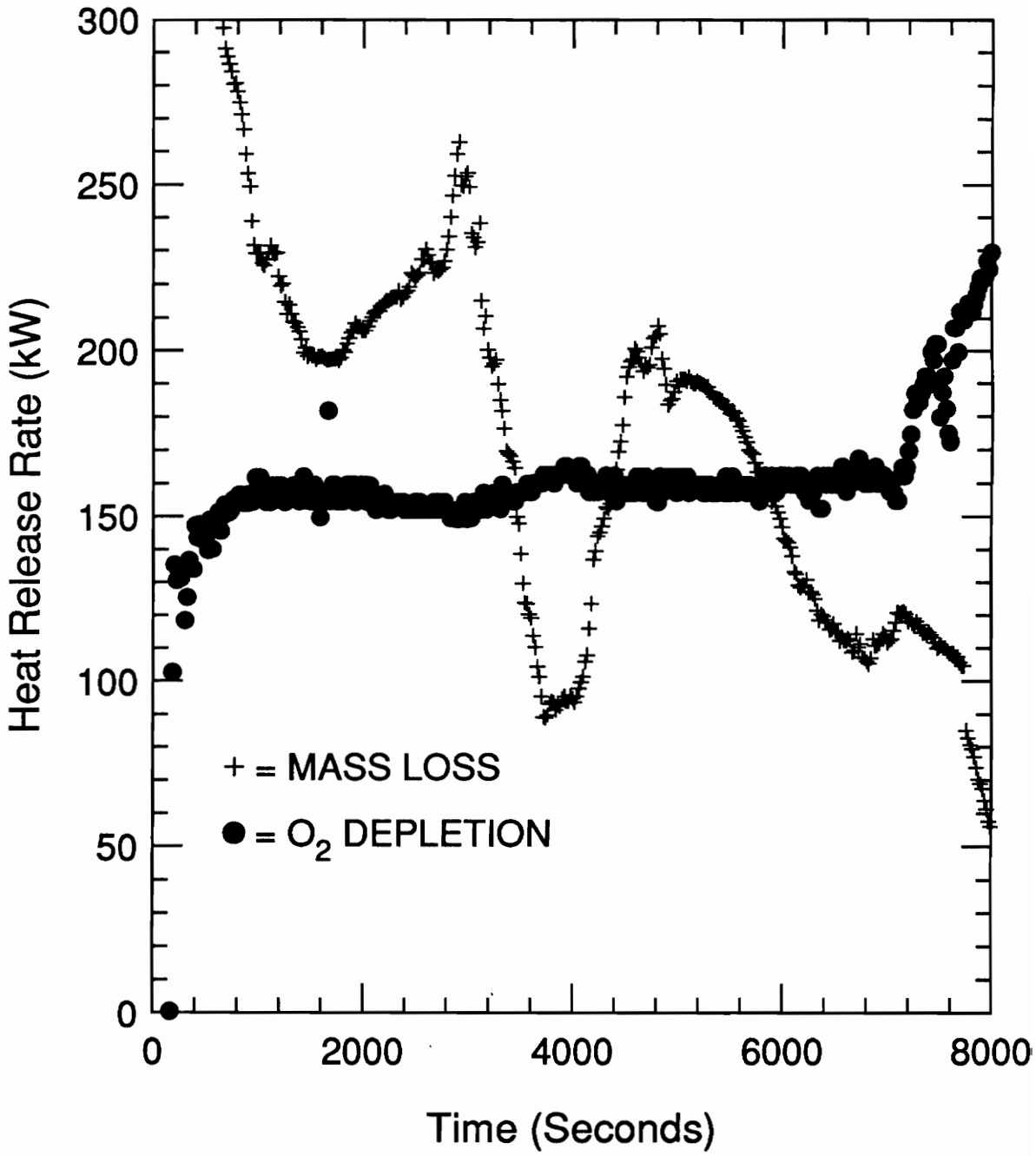

Figure 4.10: Heat Release Rate-Time History for Test #8: Full Scale Pan

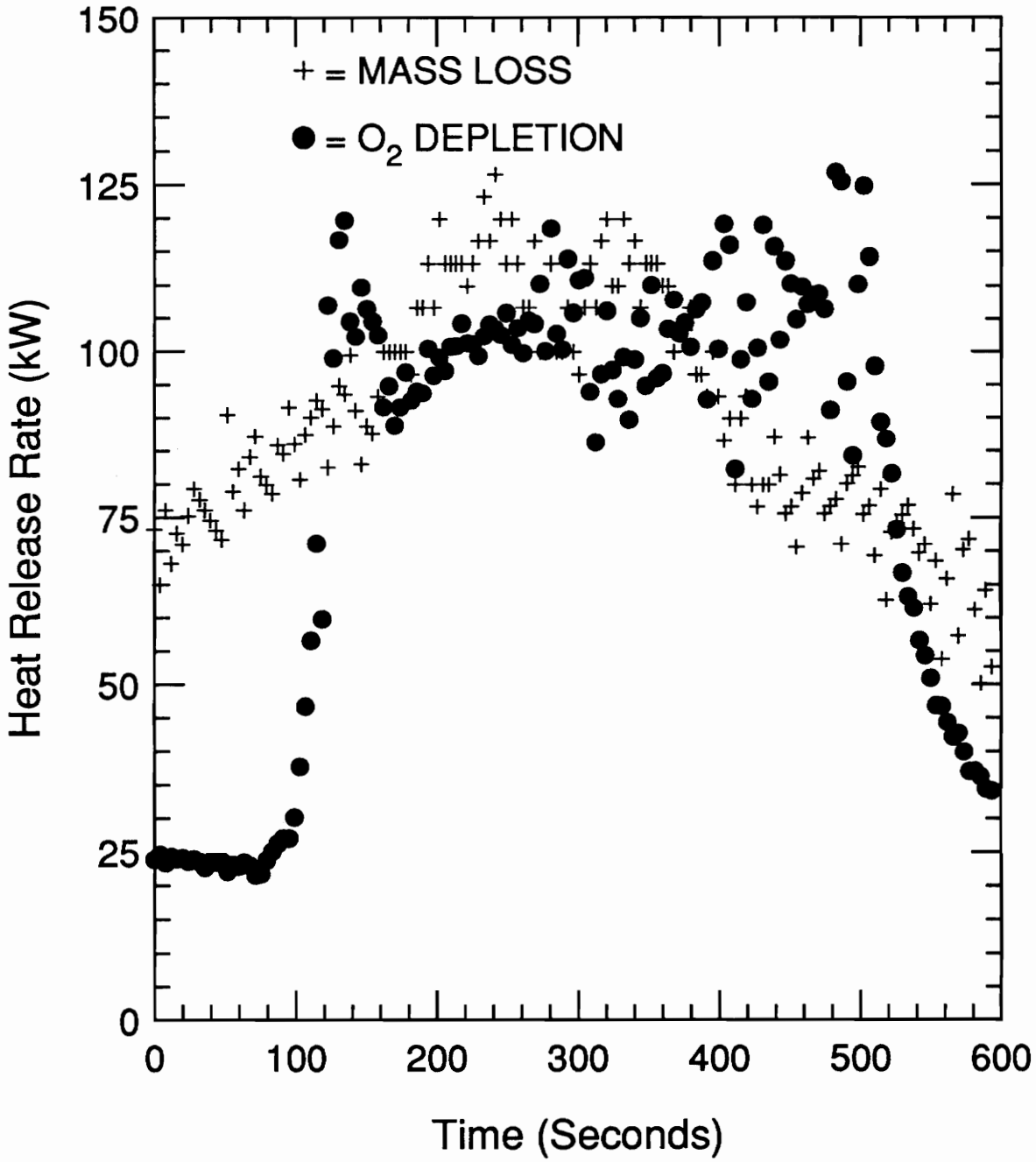

Figure 4.11: Heat Release Rate-Time History for Test #9: Full Scale Pan

most of the test. Figure 4.11 shows good agreement between the two methods and reports a fire less intense than in Test #8.

Figures 4.12 and 4.13 plot the exhaust gas concentrations for these two fires as a function of time. In the first of these plots, the carbon monoxide rises to a dangerous 4% 1700 seconds into the test and then experiences an overall decrease for the duration of the fire. A dashed line is plotted at 2% for the oxygen concentration which, as mentioned above, abruptly dropped to 0% after 1600 seconds according to the data acquisition system. In addition to visually observing nonzero concentrations throughout the fire, this measurement was considered invalid since it did not fluctuate at all; a behavior which is highly unusual for this type of instrument. Furthermore, a post test calibration of the analyzer indicated that it had maintained its calibration throughout the test. Unburned hydrocarbon data was not available for this test. In the second plot, corresponding to Test #9, no significant concentrations of carbon monoxide and unburned hydrocarbons were measured. The lack of carbon monoxide production is curious as carbon monoxide is a product of incomplete combustion. In addition, oxygen concentrations are higher and carbon dioxide concentrations are lower than in the previous test. The fact that the same fuel was able to burn until the supply was depleted in an environment with 2% oxygen in the exhaust and extinguished in a 7% oxygen environment suggests that conditions were very unstable.

The thermal environments presented in these two experiments are shown in Figures 4.14a and 4.15. Thermocouple 1 reports average temperatures of 600C and 400C, for the two tests, respectively. Since these tests had vastly different extinction times, the temperature history for Test #8 is also plotted for the first 600 seconds to allow for an easier comparison of the initial temperature growth (Figure 4.14b). Comparison

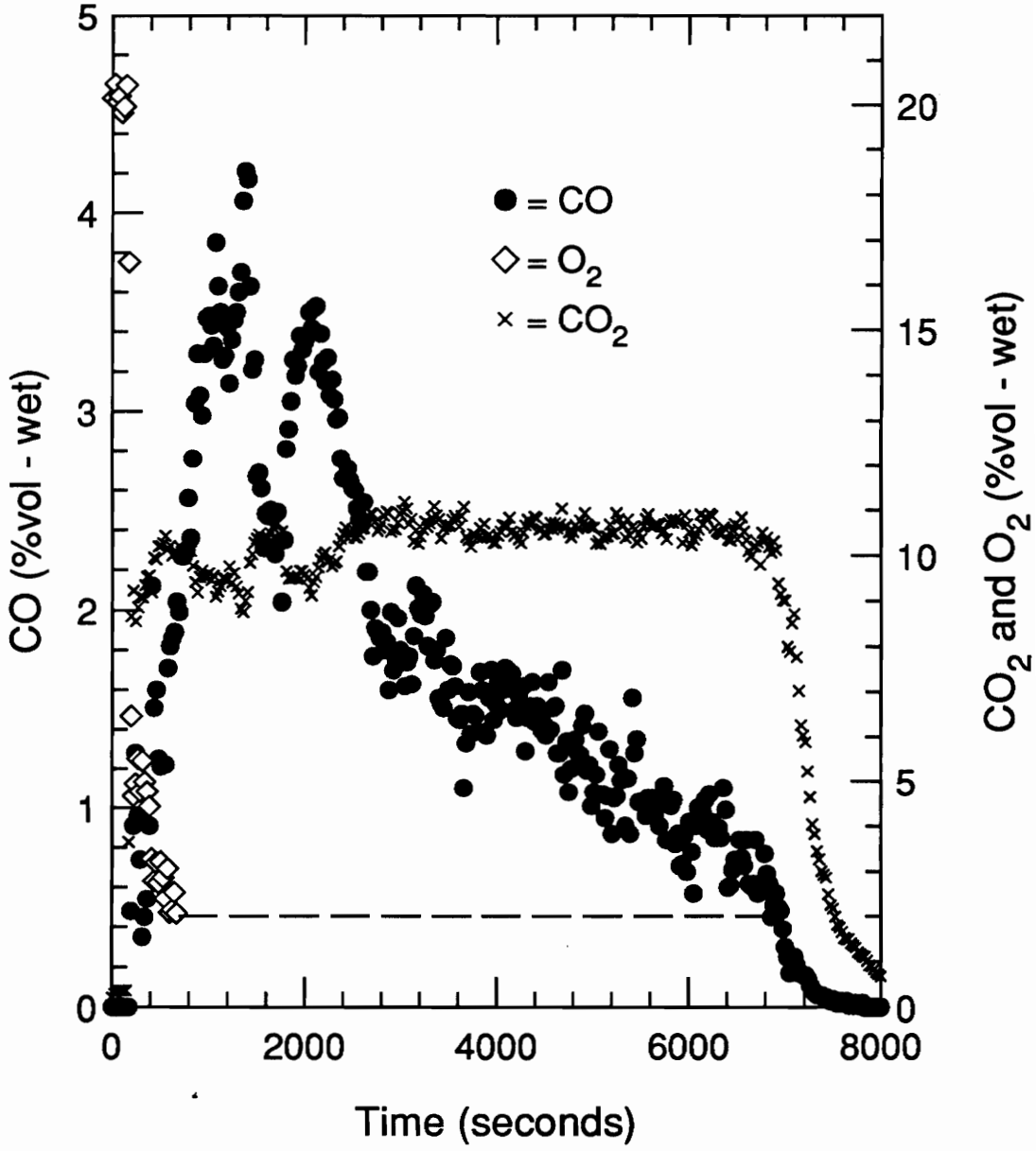

Figure 4.12: Carbon Monoxide, Carbon Dioxide, and Oxygen Concentration-Time Histories for Test #8: Full Scale Pan

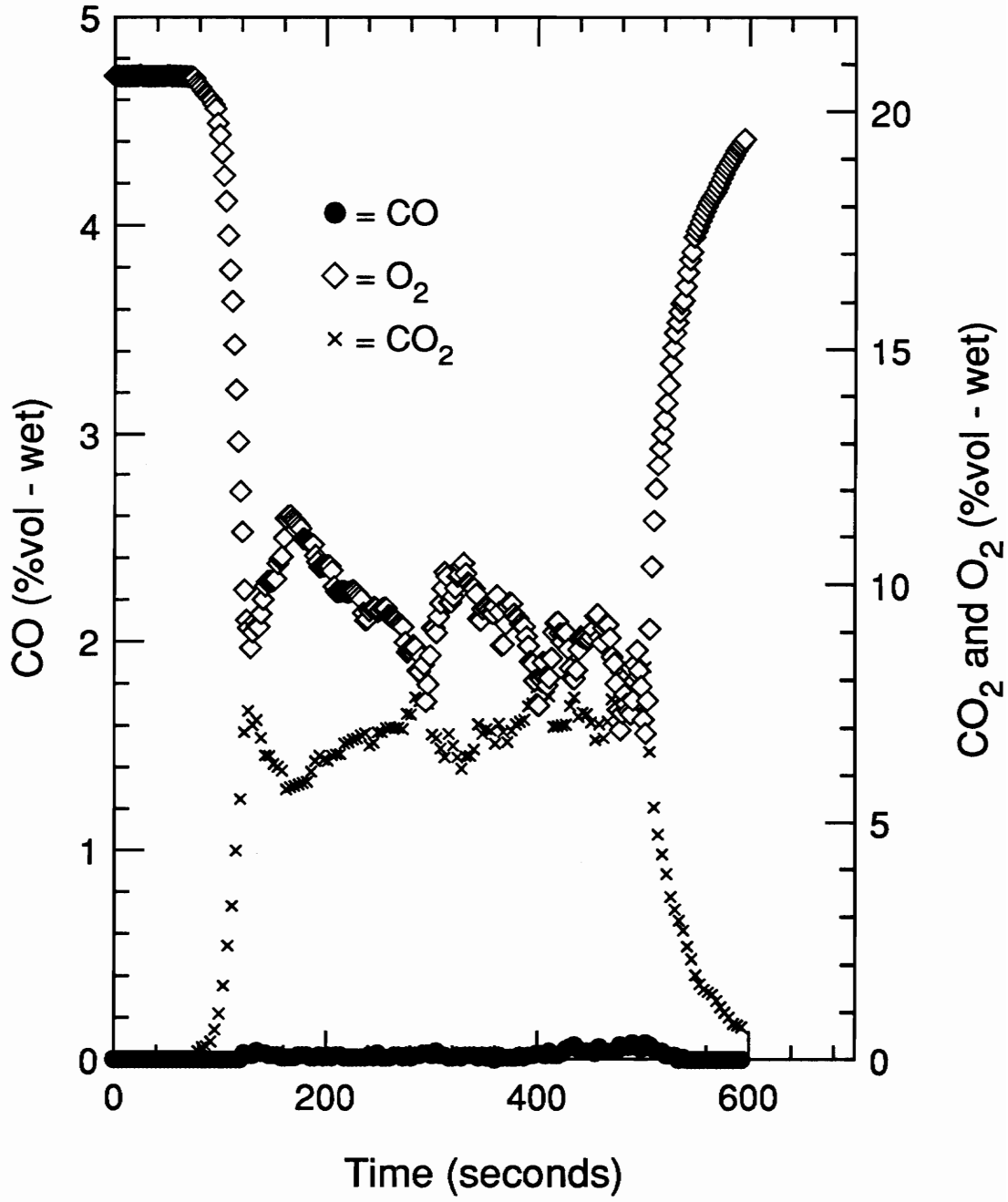

Figure 4.13: Carbon Monoxide, Carbon Dioxide and Oxygen Concentration-Time Histories for Test #9: Full Scale Pan

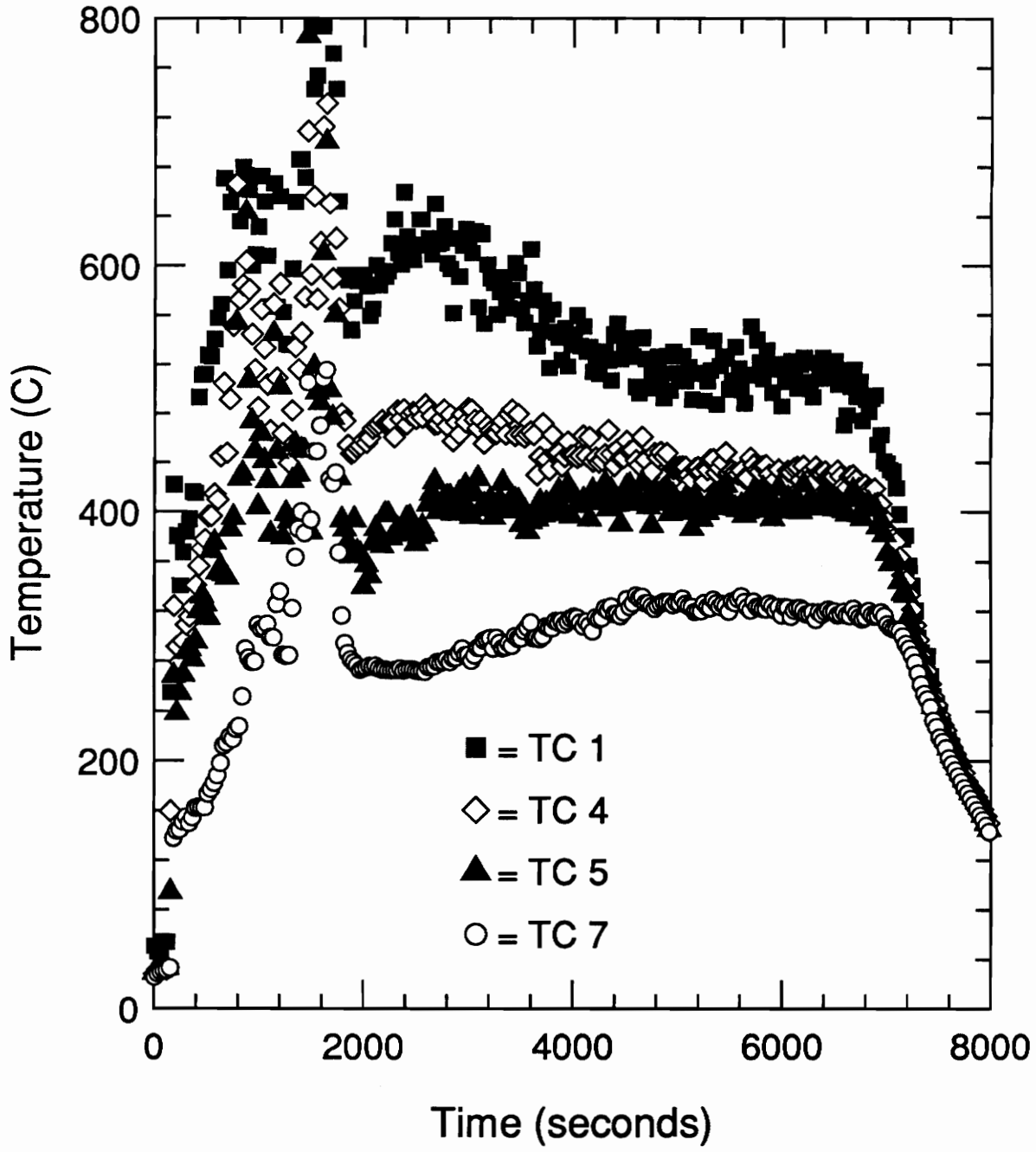

Figure 4.14a: Thermocouple Rake Temperature-Time History for Test #8: Full Scale Pan

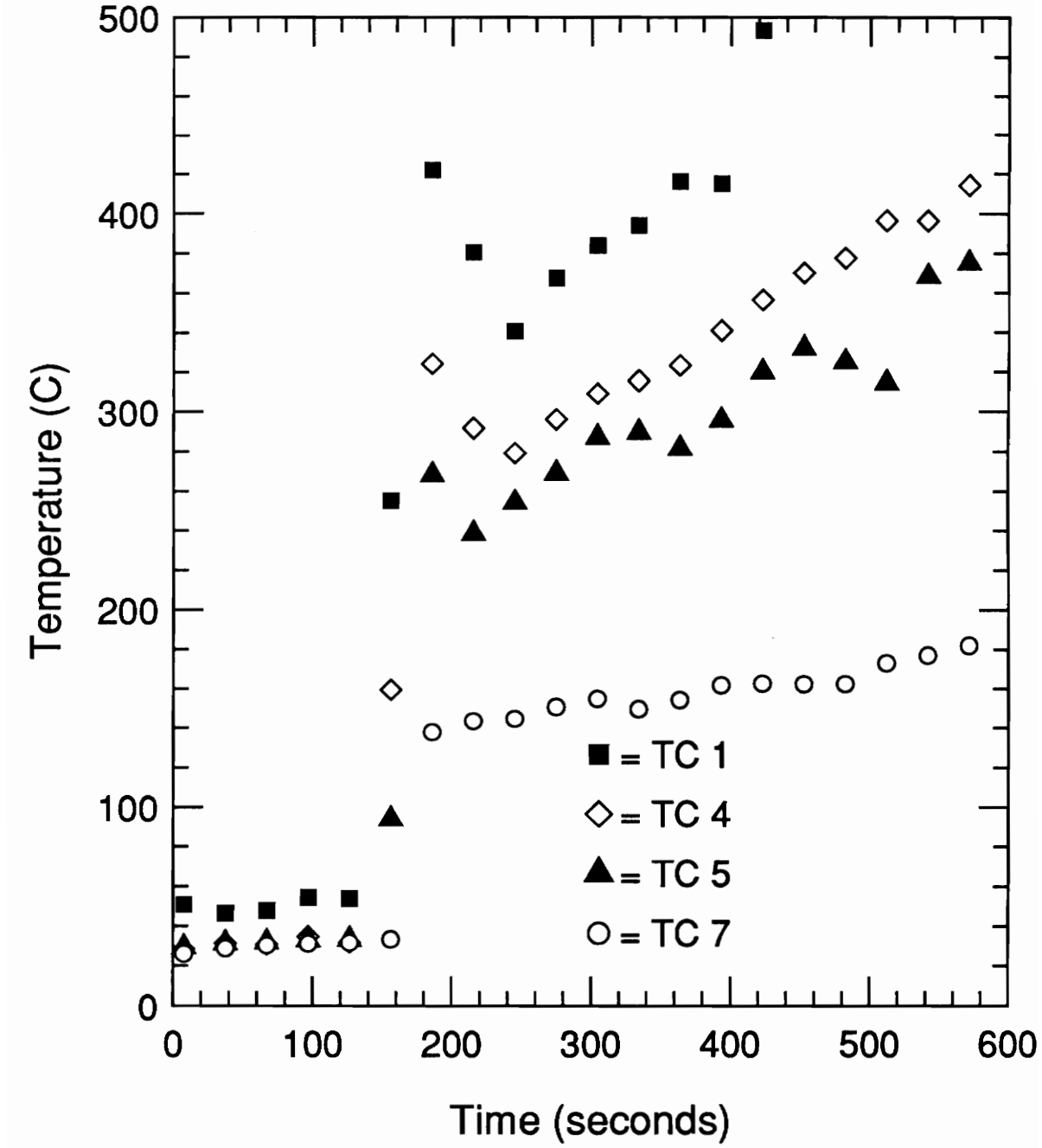

Figure 4.14b: Thermocouple Rake Temperature-Time History for Test #8: Full Scale Pan (Shortened Time Scale)

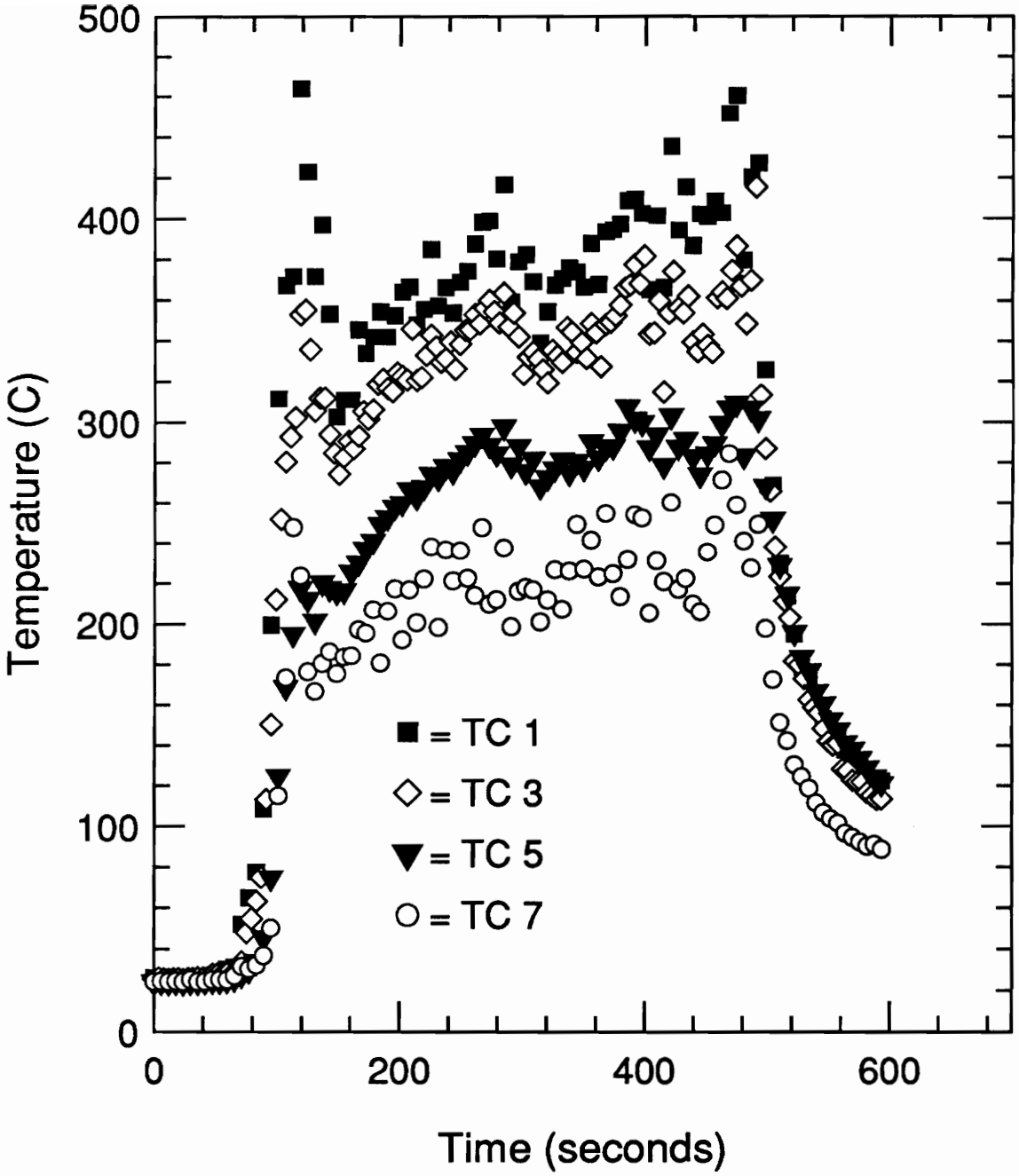

Figure 4.15: Thermocouple Rake Temperature-Time History for Test #9: Full Scale Pan

of this graph with Figure 4.15 shows that the temperatures are rising at the same rate in this time period with the exception that the thermocouple closest to the floor shows that the temperature near the floor is rising more slowly in Test #8.

Vertical temperature profiles for these two tests both indicate that a uniform system exists vertically (Figures 4.16 and 17). Furthermore, temperatures at the exhaust box end, indicated by solid symbols, are cooler than those observed at the rake. This shift is especially noticeable with the higher thermocouple. The vertical temperature gradient is smaller by the exhaust duct than at the thermocouple rake. This indicates that heat was transferred to the walls so that the air was cooled before leaving the compartment and a more uniform temperature environment was created.

4.4.2 Added Ventilation Opening Glovebox Experiments

All tests conducted with gloves removed self-extinguished at random times (Table 4.1). In agreement with the tests where the box was sealed, a puffing behavior was observed. For these conditions, containment was lost when the puffs were expelled from the glovebox. Puffing became stronger as more glove holes were opened, indicating greater pressure fluctuations and a larger containment loss.

Important results from these tests are wet gas concentrations. Due to the short duration of these tests, fuel weight measurements were too noisy to be instrumental in calculating burn rates and heat release rates. Gas concentration data was not available for Tests 10-14, so graphical representations are only provided for two of the tests with one glove removed (Tests 15&16) and two of the tests with two gloves removed (Tests 17&18). Hydrocarbon measurements were not obtained for any of these tests.

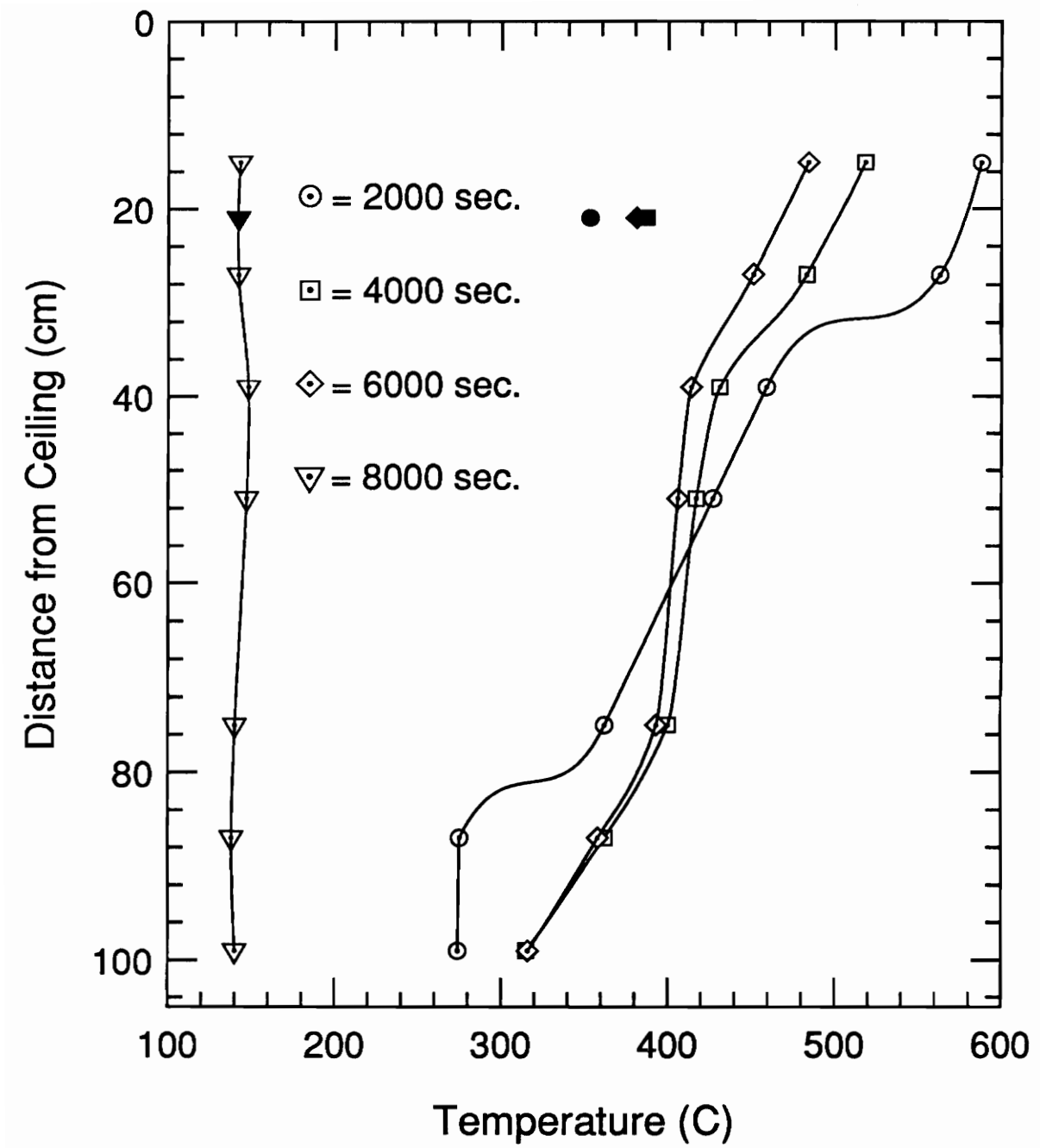

Figure 4.16: Vertical Temperature Profiles for Test #8: Full Scale Pan

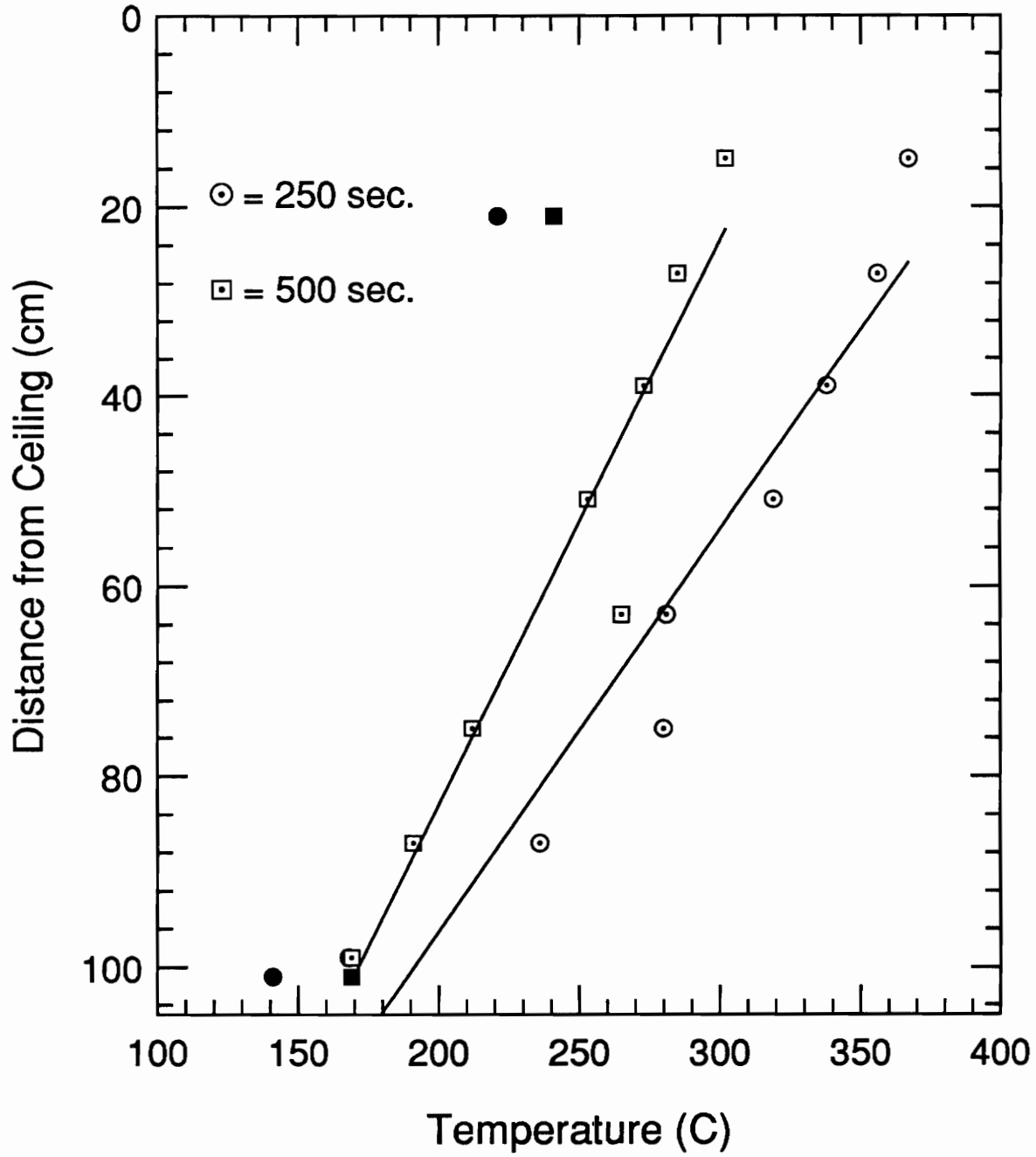

Figure 4.17: Vertical Temperature Profiles for Test #9: Full Scale Pan

Figures 4.18 - 4.21 present the exhaust gas concentrations as a function of time for these four tests, the first pair corresponding to tests with one glove missing and the last pair to tests with two gloves missing. Similar trends are seen in these plots which are characterized by a sharp decrease in oxygen concentration which correlates well with sharp increases in carbon dioxide production. Similar to Test #8, the oxygen concentration in Test #16, as reported by the computer, dropped suddenly to zero and is not plotted. In the latter three plots, at a time about 20 seconds after the rise in carbon dioxide occurs, the carbon monoxide concentrations also rises reaching values of near 2%. This trend is an indication of incomplete combustion and, in these tests, is predicting when extinction occurs.

The remaining test performed with an added ventilation opening was the test with the second front window removed (Test #19). This fire burned until all fuel was depleted, indicating that the loss of a window allows sufficient ventilation to sustain a flame. A steady flow of exhaust gases escaped through the window and the exiting gas volume was larger than that occurring in any of the tests with gloves removed.

Figure 4.22 shows the fuel burn rate as a function of time. This plot is somewhat noisy and discretized with several spikes occurring. An average burn rate of 2.4 ± 1.3 g/sec was determined. This value falls in between the burn rates seen in Tests #8 and #9. Due to the excessive noise in the burn rate, mass loss heat release rates were not calculated. Furthermore, since the mass flow rate of combustion products out the window was not measured, heats release rates based on oxygen depletion could not be calculated.

Observation of the exhaust gas concentrations in Figure 4.23 yields low carbon monoxide concentrations of 0.6% and oxygen concentrations reaching 2 % at several

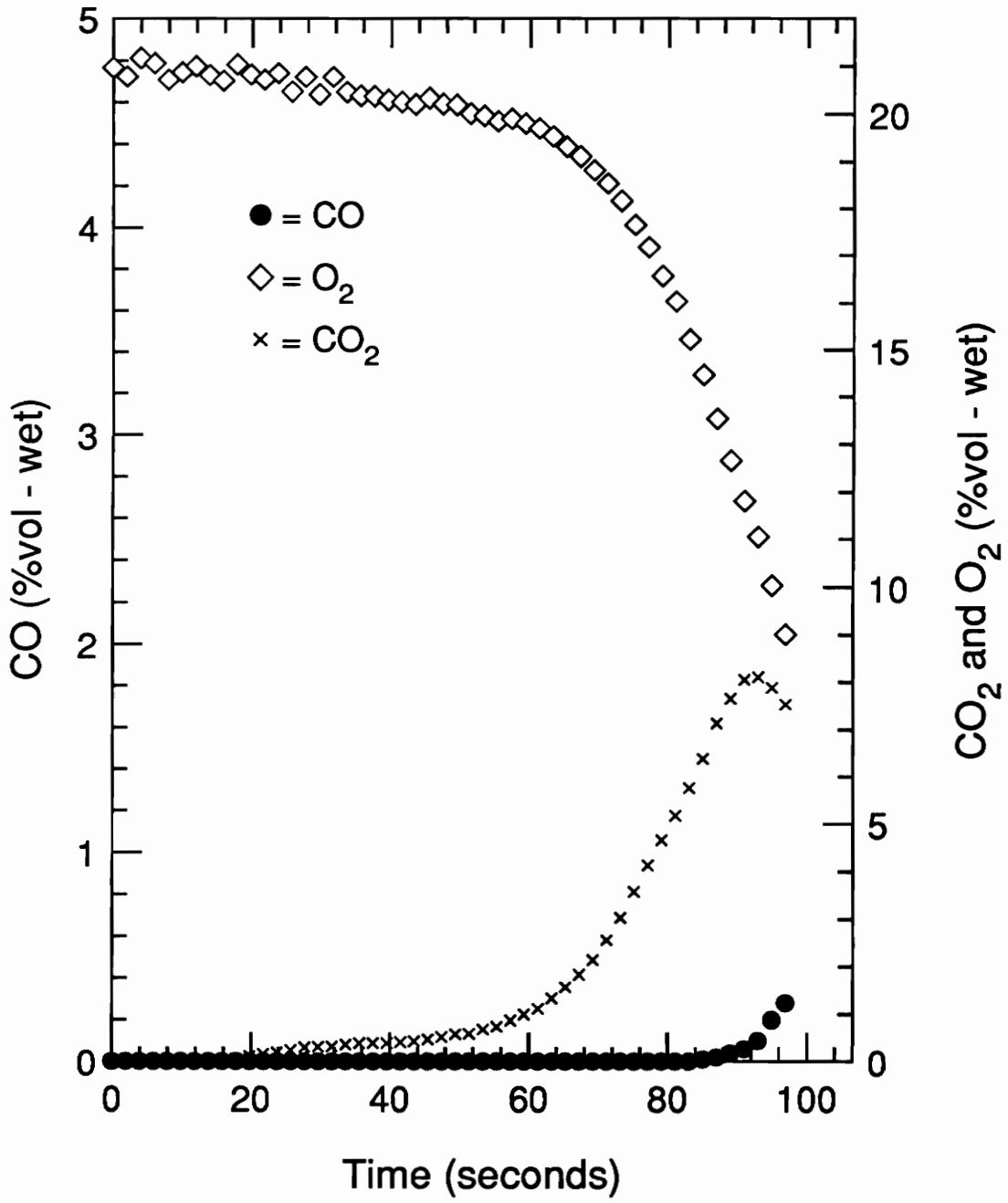

Figure 4.18: Carbon Monoxide, Carbon Dioxide and Oxygen Concentration-Time Histories for Test #15: Full Scale Pan, One Glove Missing

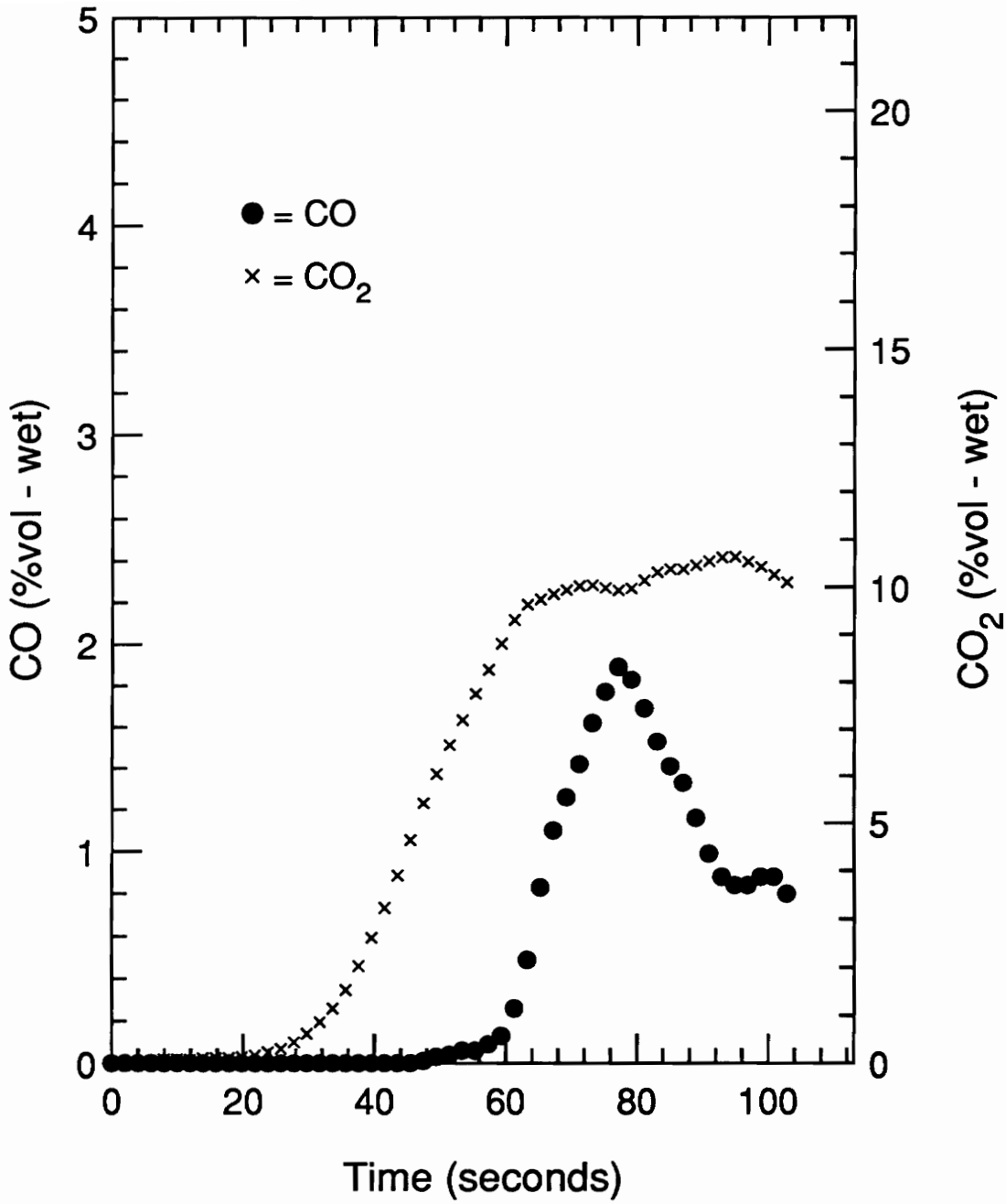

Figure 4.19: Carbon Monoxide and Carbon Dioxide Concentration-Time Histories for Test #16: Full Scale Pan, One Glove Missing

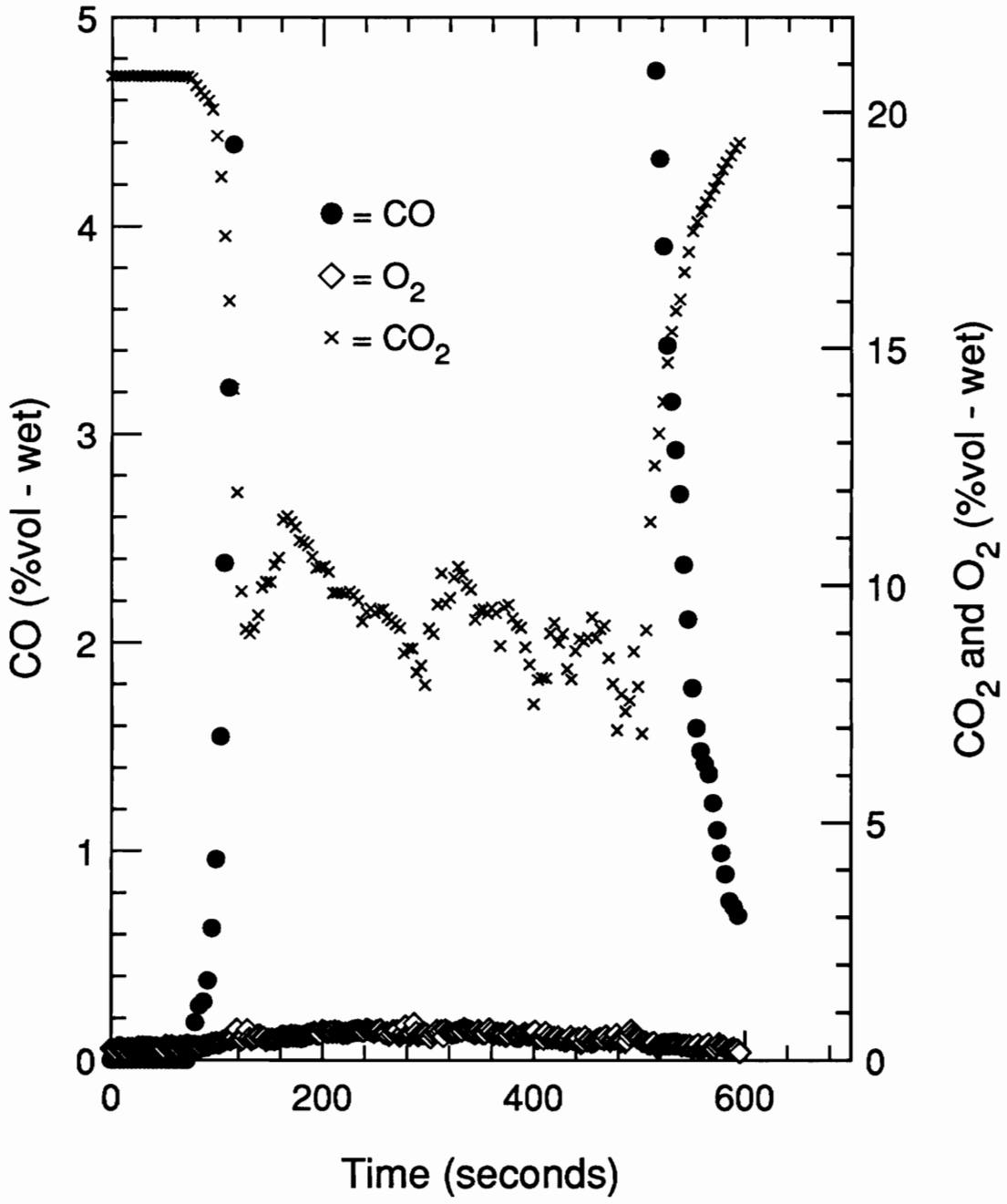

Figure 4.20: Carbon Monoxide, Carbon Dioxide and Oxygen Concentration-Time Histories for Test #17: Full Scale Pan, Two Gloves Missing

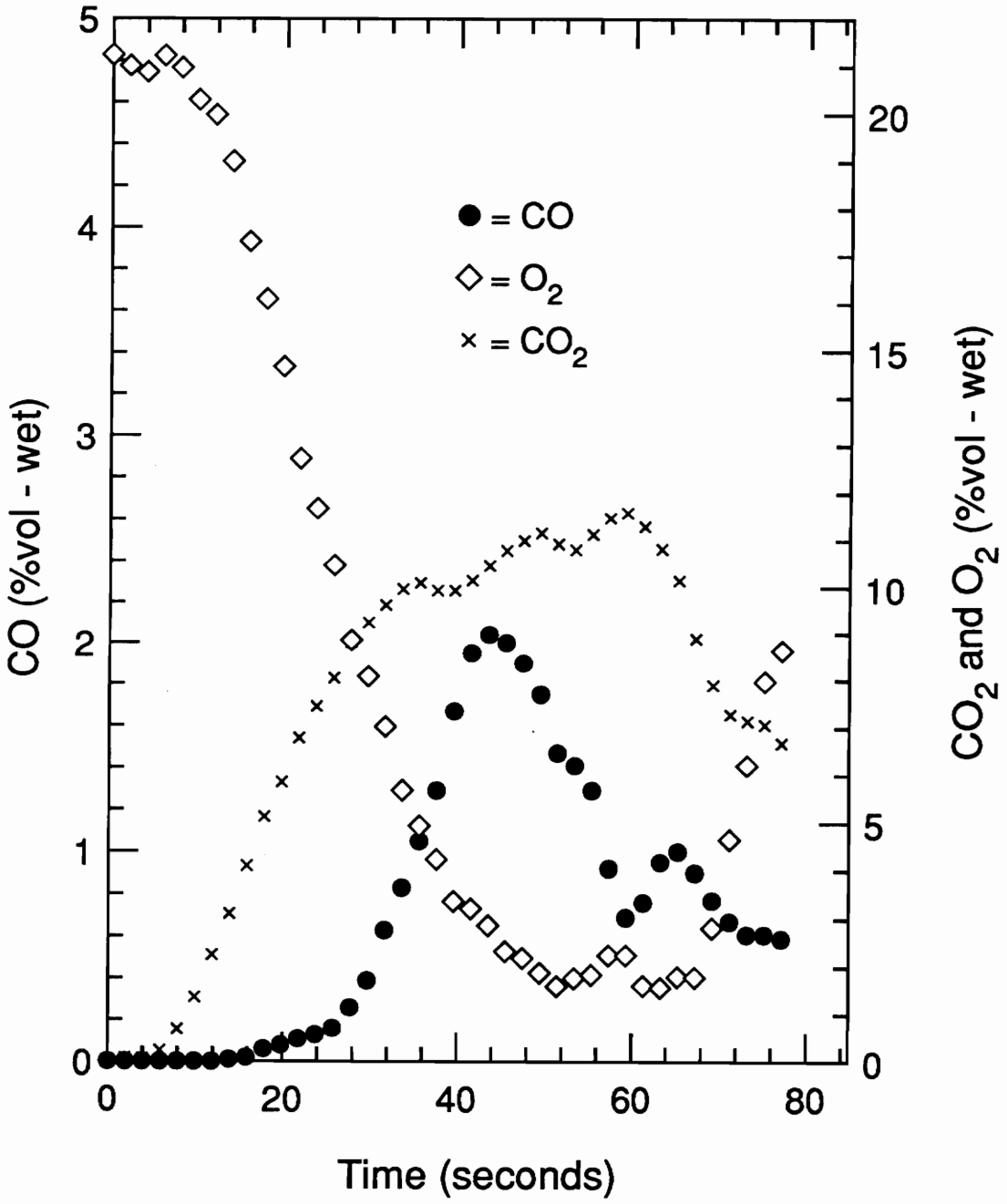

Figure 4.21: Carbon Monoxide, Carbon Dioxide and Oxygen Concentration Time Histories for Test #18: Full Scale Pan, Two Gloves Missing

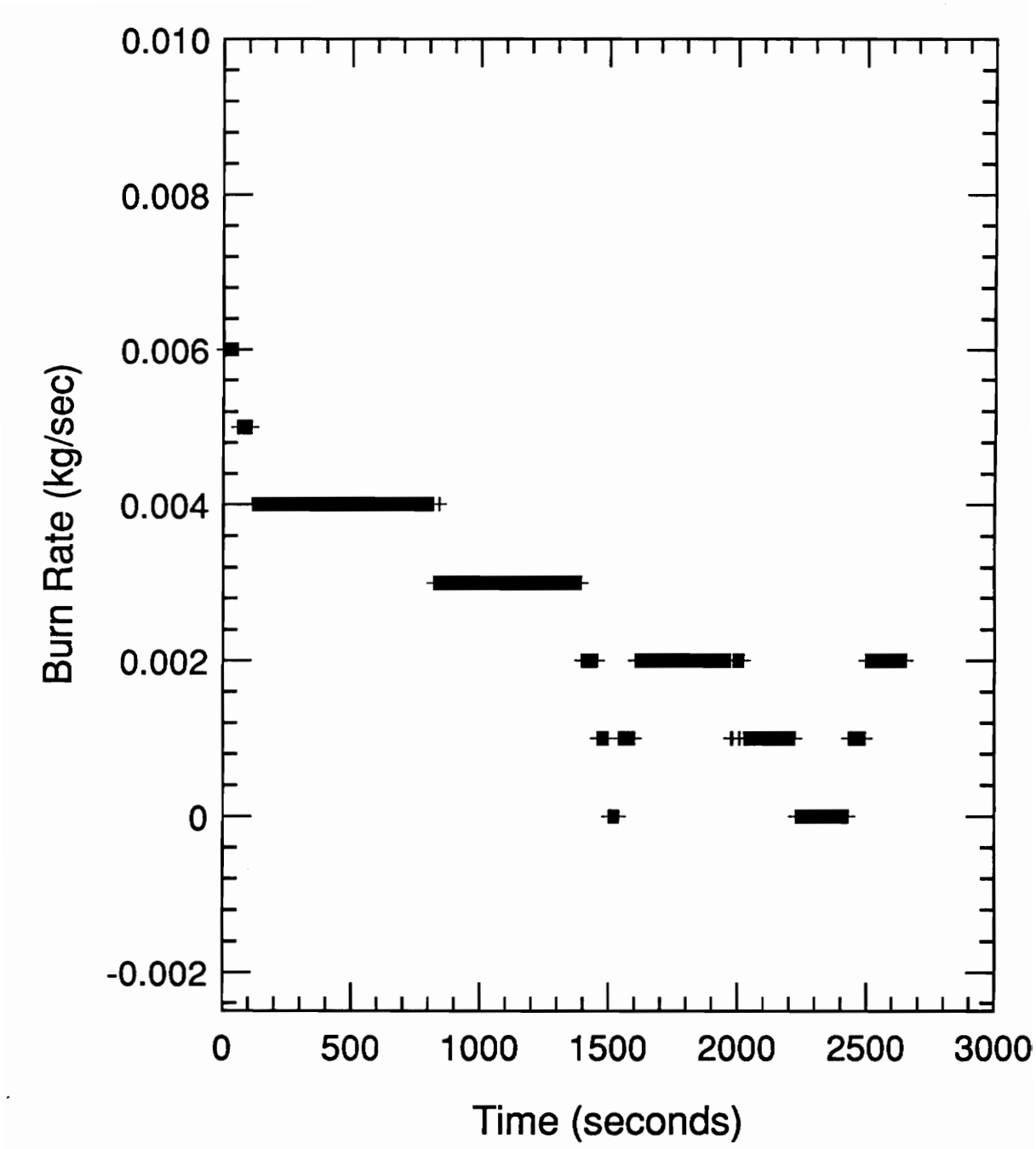

Figure 4.22: Burn Rate-Time History for Test #19: Full Scale Pan, Window Removed

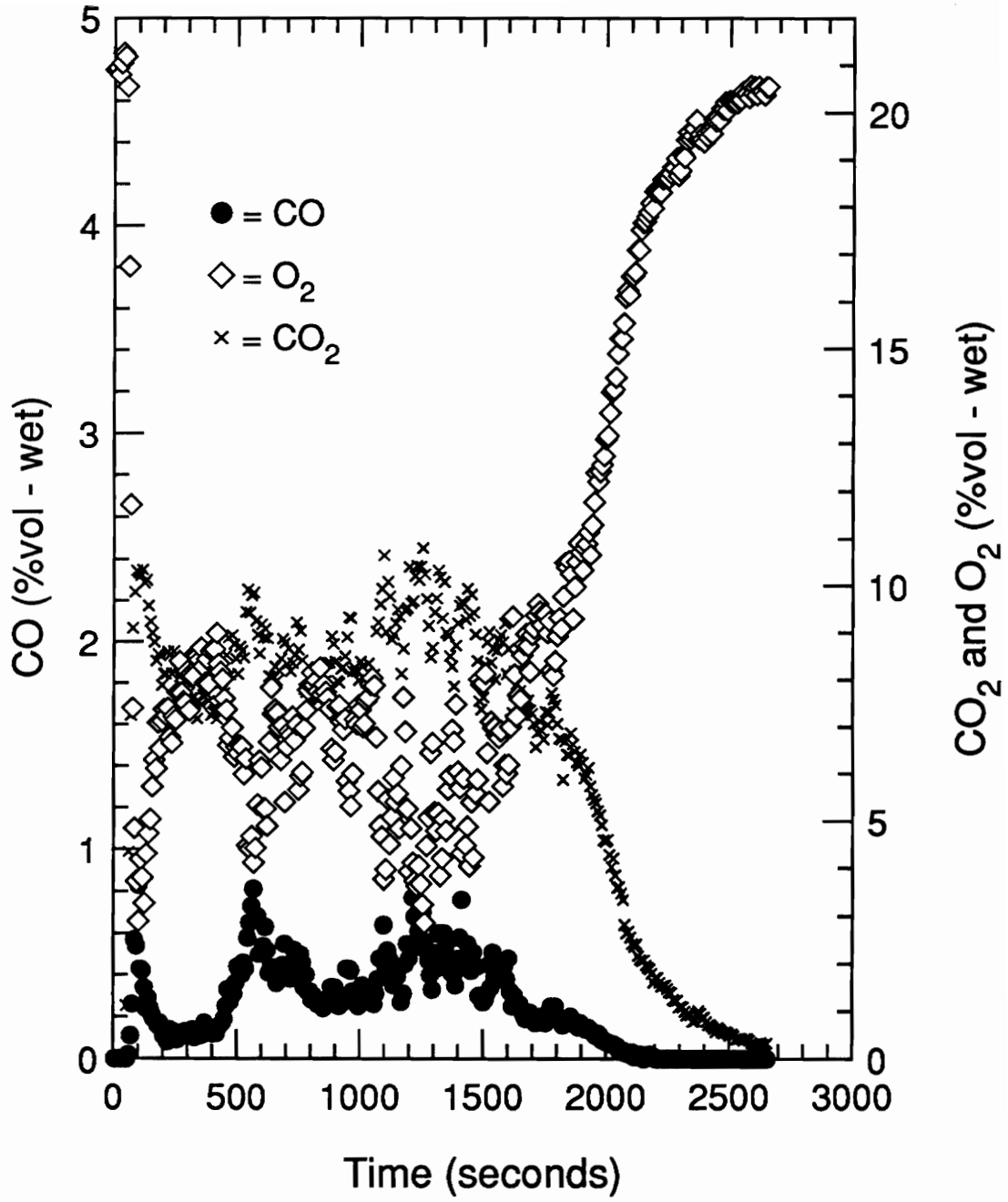

Figure 4.23: Carbon Monoxide, Carbon Dioxide, and Oxygen Concentration-Time Histories for Test #19: Full Scale Pan, Window Removed

times. These measurements indicate that the fire was underventilated and complete combustion did not occur.

Temperature data for this fire scenario reveals temperatures ranging from 500C near the ceiling to 220C near the floor (Figure 4.24), corresponding to an environment slightly warmer than in Test #9 and cooler than in Test #8. A small increase in temperature is seen throughout the fire until a sudden decrease at 1800 seconds. Temperature profiles are uniform with a comparable slope at all times except at 2000 seconds where the temperature varies only by 60C from the glovebox ceiling to floor (Figure 4.25).

4.5 Reduced Fuel Surface Area Experiments

The following section compares the burn rates, equivalence ratios, heat release rates, exhaust gas concentrations, temperature-time histories and vertical temperature profiles which resulted from the reduced fuel surface area tests. To facilitate a comprehensive comparison, results from the second full scale pan test will be compared with the following results to investigate the effect of pan diameter on these quantities.

Each of these tests had flames which were steady enough to allow the fuel supply to be depleted before extinguishment. However, due to the small burn rate occurring with the 27.9 cm pan (Test #22), the test was terminated after 33 minutes. Burn rates as a function of time are shown for each of the reduced pan diameter tests (Tests #20-22) in Figures 4.26 - 4.28. In the first of these graphs, representing the 83.8 cm diameter fuel pan, a sharp rise followed by a sharp decline into negative burn rates occurs at 1000 seconds. This behavior was seen in previous sections and again, is labeled as an artifact of scale measurement due to poor temperature compensation. A dashed line is filled in to

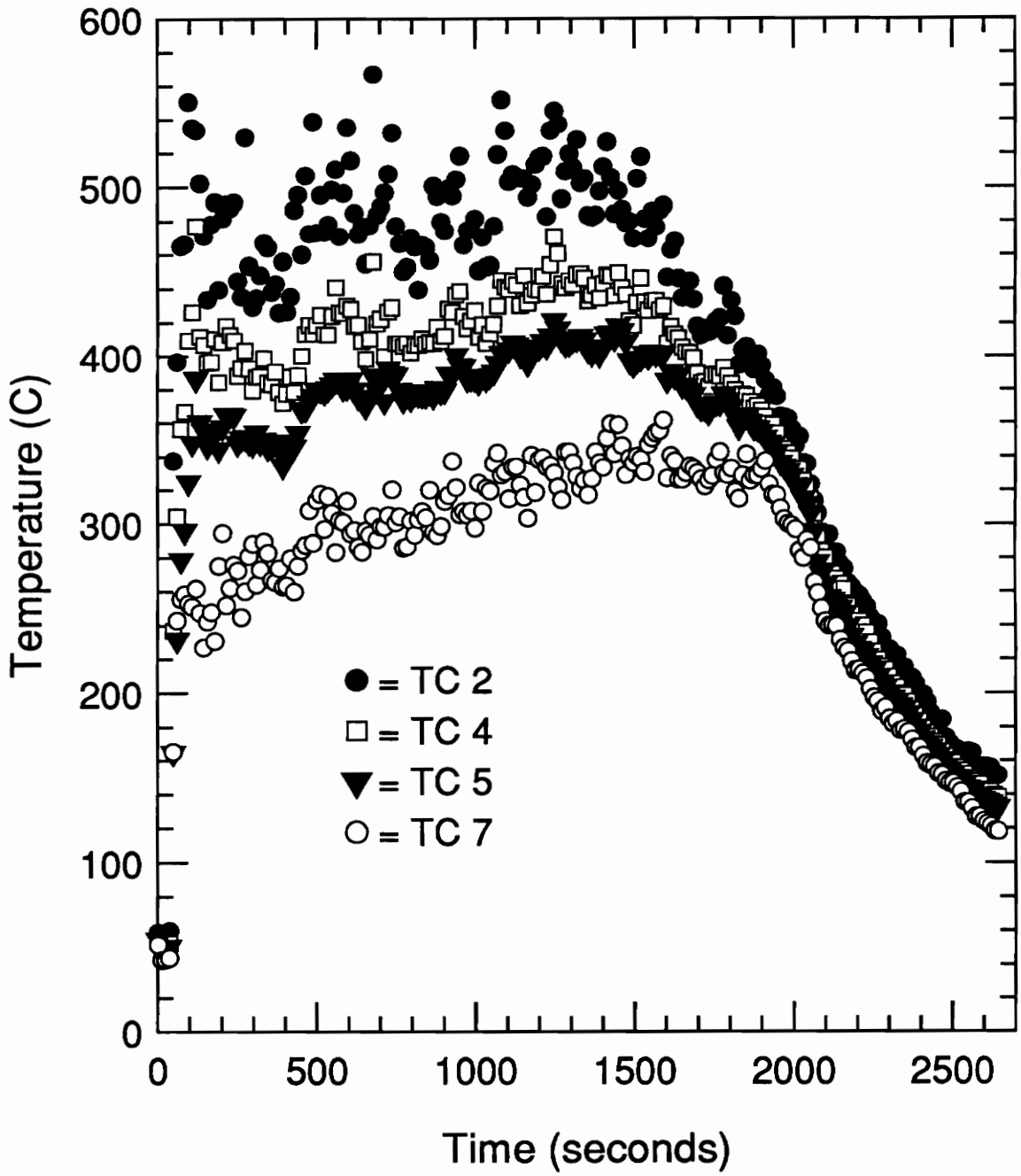

Figure 4.24: Thermocouple Rake Temperature-Time History for Test #19: Full Scale Pan, Window Removed

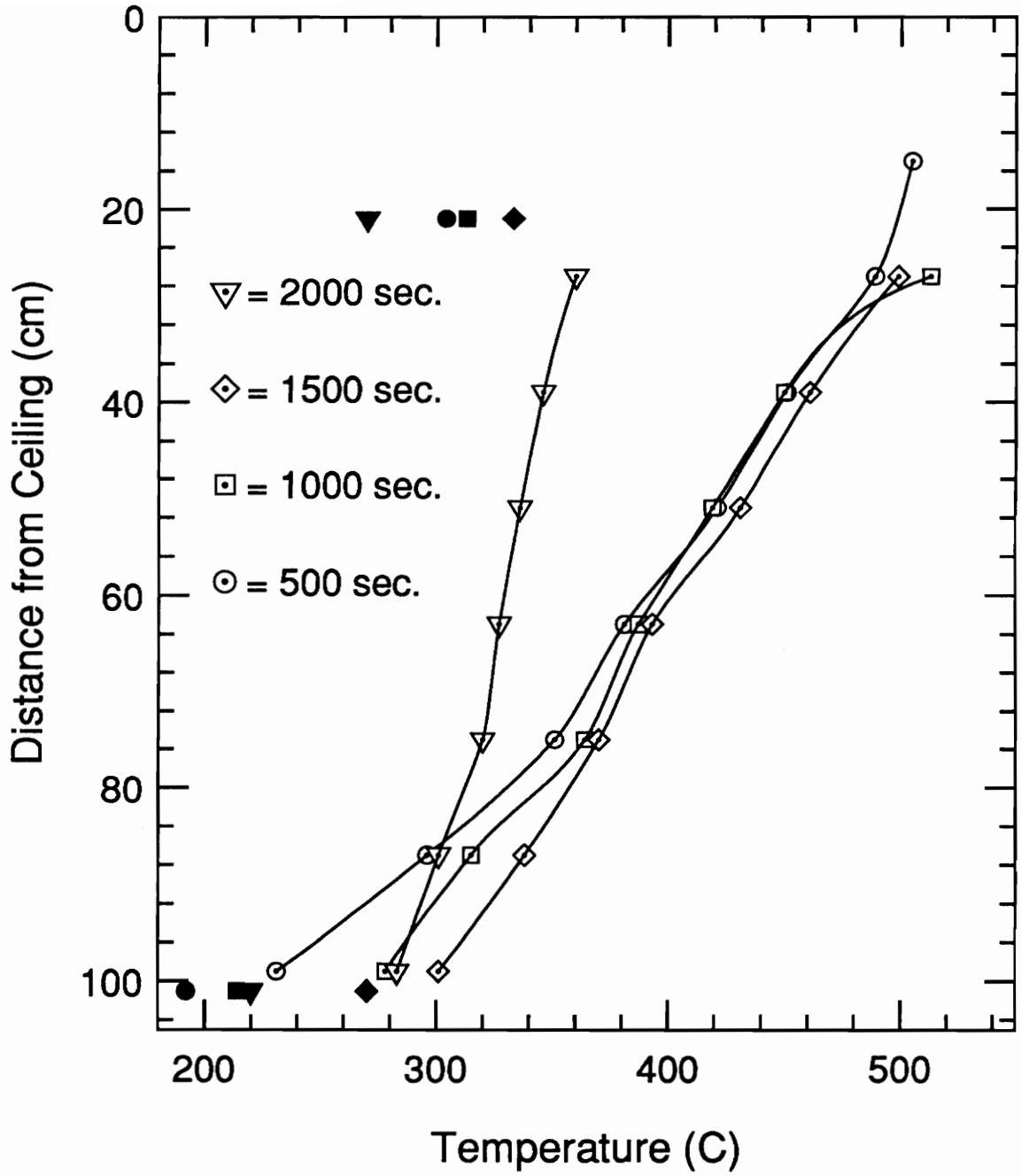

Figure 4.25: Vertical Temperature Profiles for Test #19: Full Scale Pan, Window Removed

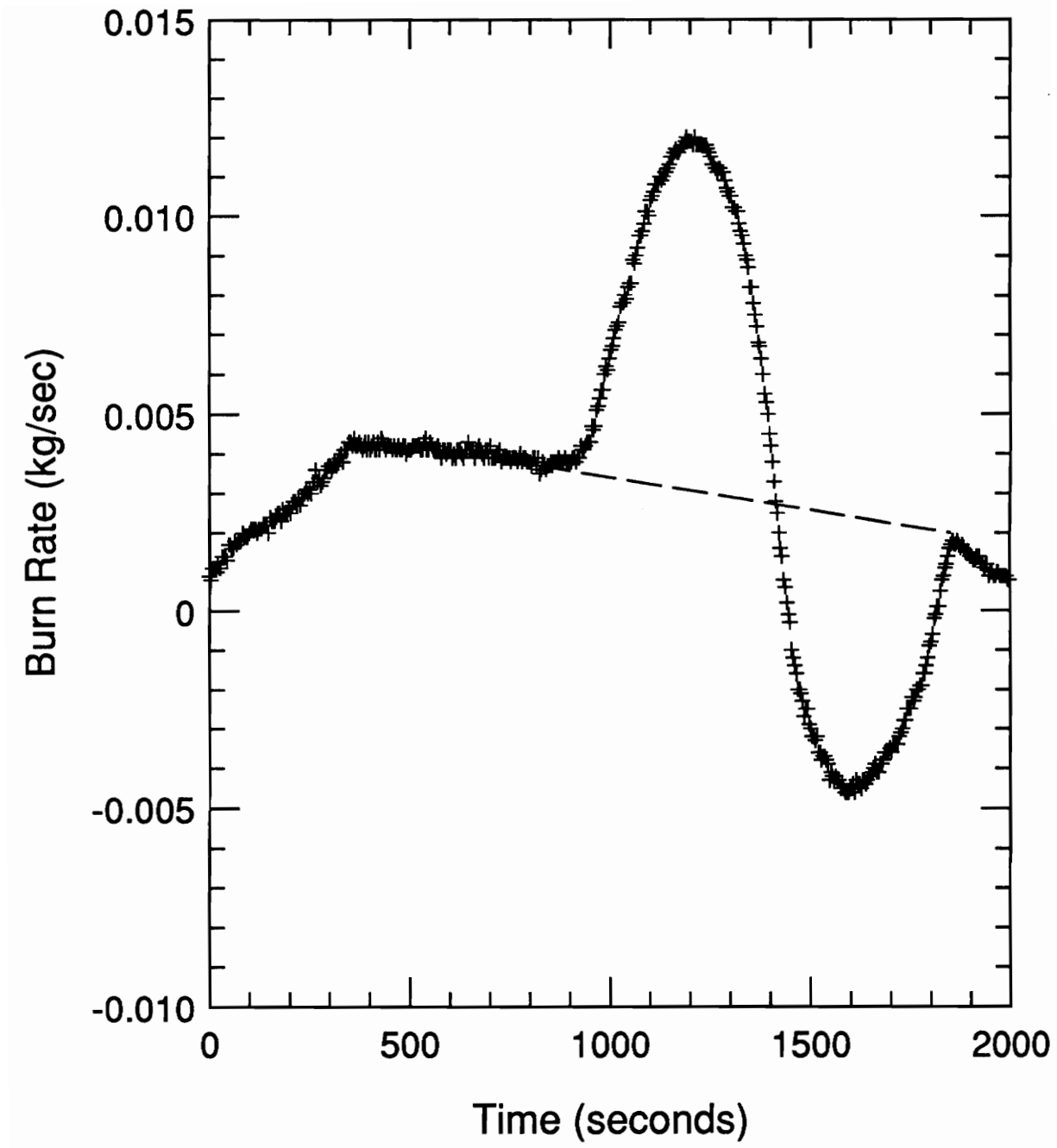

Figure 4.26: Burn Rate-Time History for Test #20: 83.8 cm diameter Pan

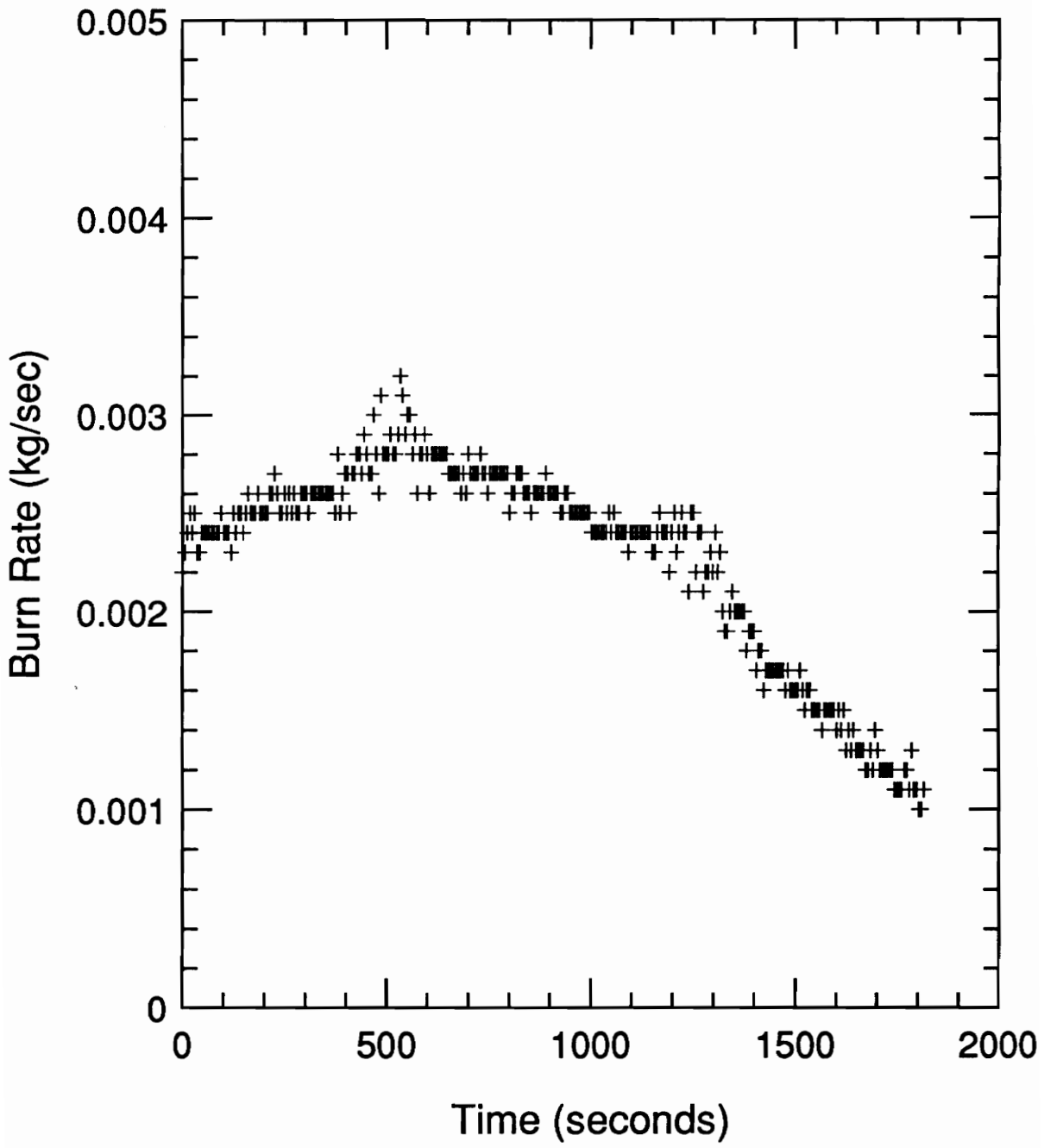

Figure 4.27: Burn Rate-Time History for Test #21: 62.2 cm diameter Pan

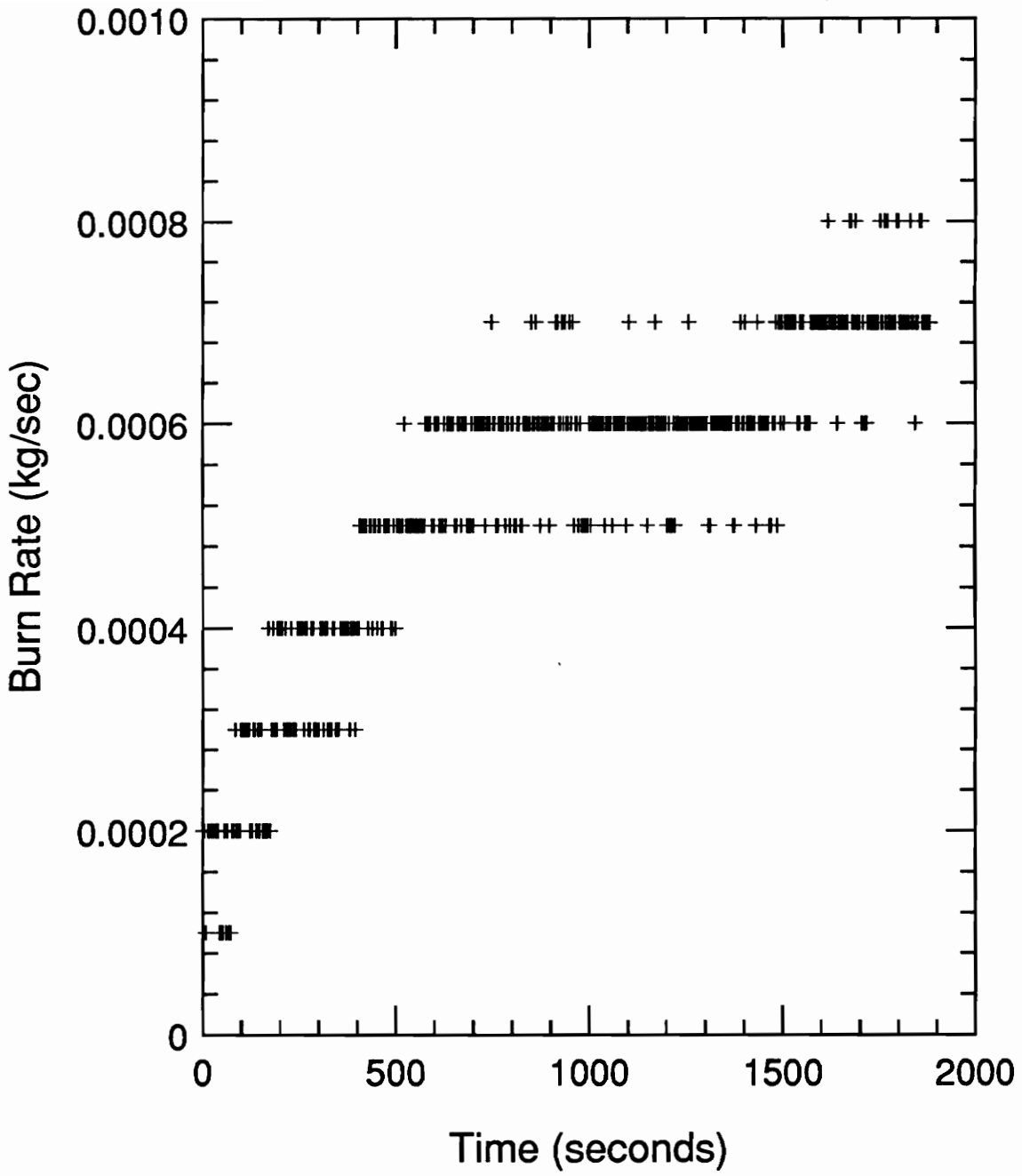

Figure 4.28: Burn Rate-Time History for Test #22: 27.9 cm diameter Pan

represent a more likely behavior. Neglecting this variation, each plot indicates steadier burning rates than those reported earlier for the full scale pan tests with average values of 4.1 ± 0.2, 2.6 ± 0.2, and 0.6 ± 0.08 g/sec characterizing the 83.8, 62.2, and 27.9 cm diameter fuel pans, respectively. Although the burn rates increase with pan diameter, an opposite trend is seen when these values are normalized by the fuel surface area (Figure 4.29).

Analysis of the plume and exhaust equivalence ratios yield some interesting results. In the case of the 83.8 cm diameter fuel pan, both equivalence ratios are roughly the same value (Figure 4.30). A dashed line beginning at 1000 seconds represents the estimated equivalence ratio after the load cell drift occurred. However, as demonstrated in Figures 4.31 and 4.32, the two equivalence ratios do not compare as well for the 62.2 and 27.9 cm diameter tests. In both instances, the exhaust equivalence ratios are about 33% less than the plume equivalence ratios. In further analysis, plume equivalence ratios were used since they were more realistic physically. Average plume equivalence ratios of 0.86 ± 0.2, 0.71 ± 0.03, 0.65 ± 0.05, and 0.12 ± 0.02 were determined for the full scale, 83.8 cm diameter, 62.2 cm diameter and 27.9 cm diameter pans, respectively. Figure 4.33 shows a graphical representation of the increasing plume equivalence ratios observed with increasing pan diameters.

Heat release rates, utilizing the three calculation methods, as a function of time are displayed in Figures 4.34-4.36 for each of these tests. Agreement for the three methods is good in both Figures 4.34 and 4.35 excluding the last 1000 seconds in Figure 4.34 where the dashed line represents where the load cell drifted. In Figure 4.36, poor agreement is observed between the three methods with values based on oxygen depletion as much as 2.5 times those seen for the exhaust gas method.

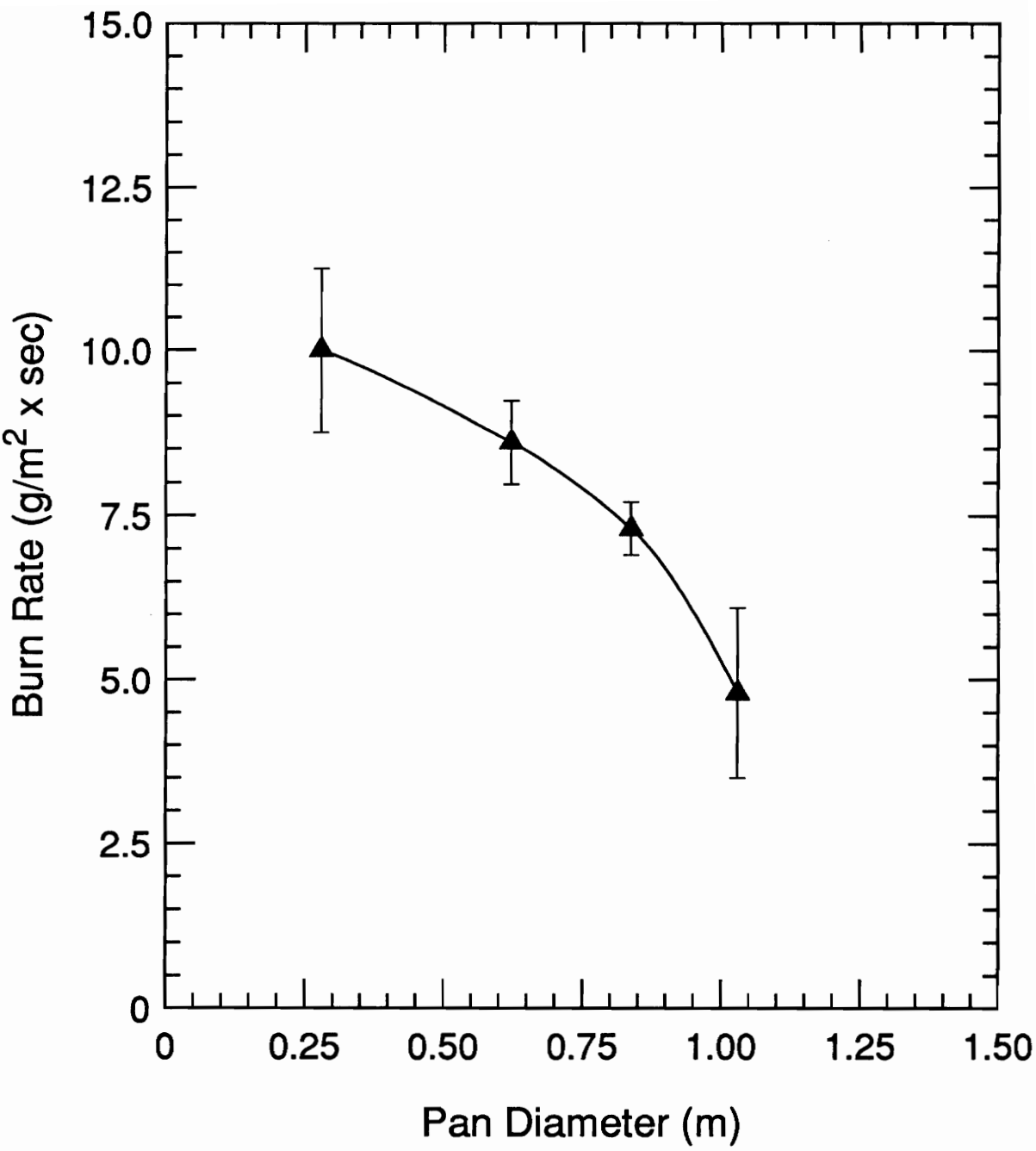

Figure 4.29: Average Enclosed Burn Rate Per Fuel Surface Area vs. Pan Diameter

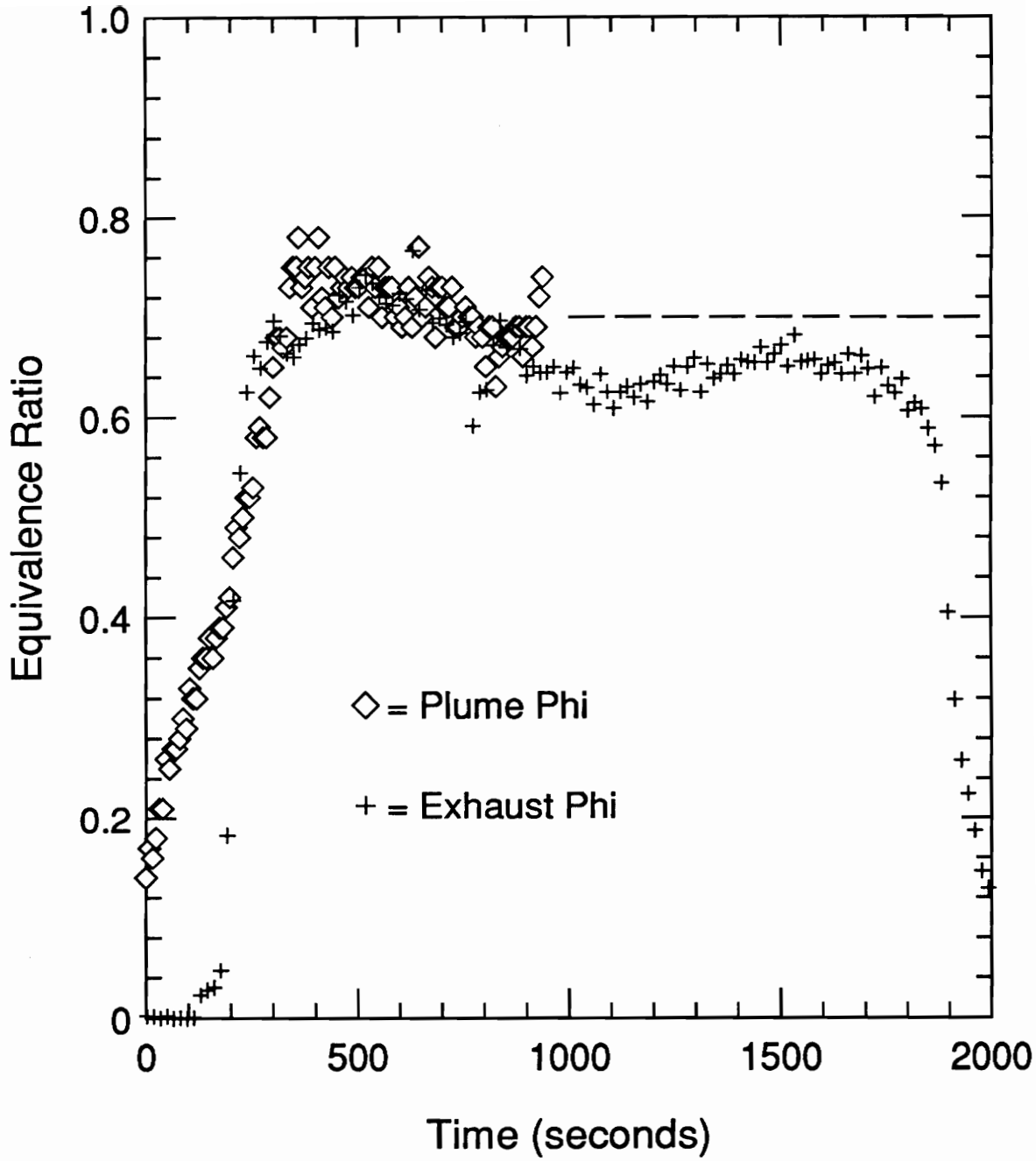

Figure 4.30: Plume and Exhaust Equivalence Ratio-Time Histories for Test #20: 83.8 cm diameter Pan

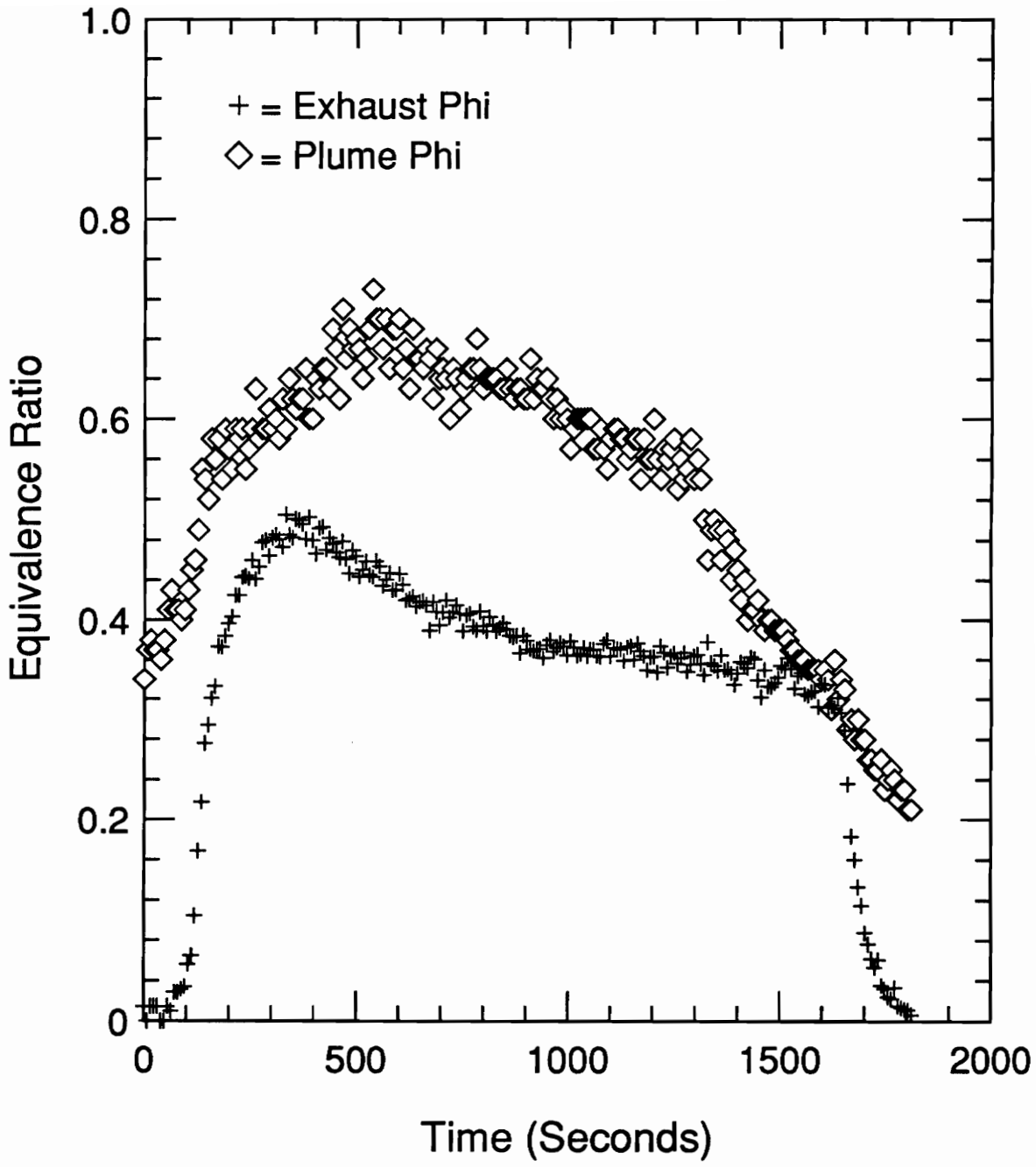

Figure 4.31: Plume and Exhaust Equivalence Ratio-Time Histories for Test #21: 62.2 cm diameter Pan

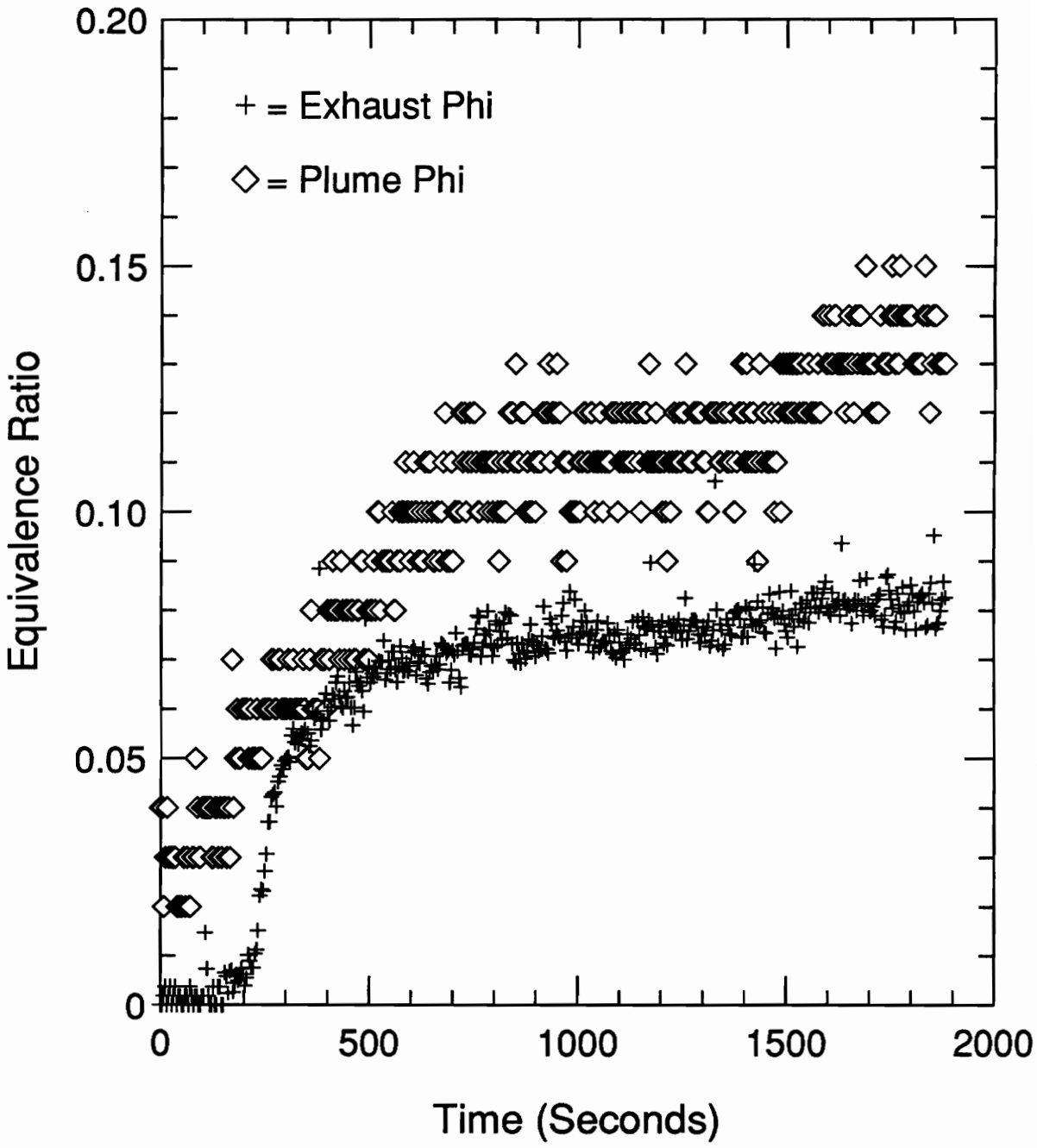

Figure 4.32: Plume and Exhaust Equivalence Ratio-Time Histories for Test #22: 27.9 cm diameter Pan

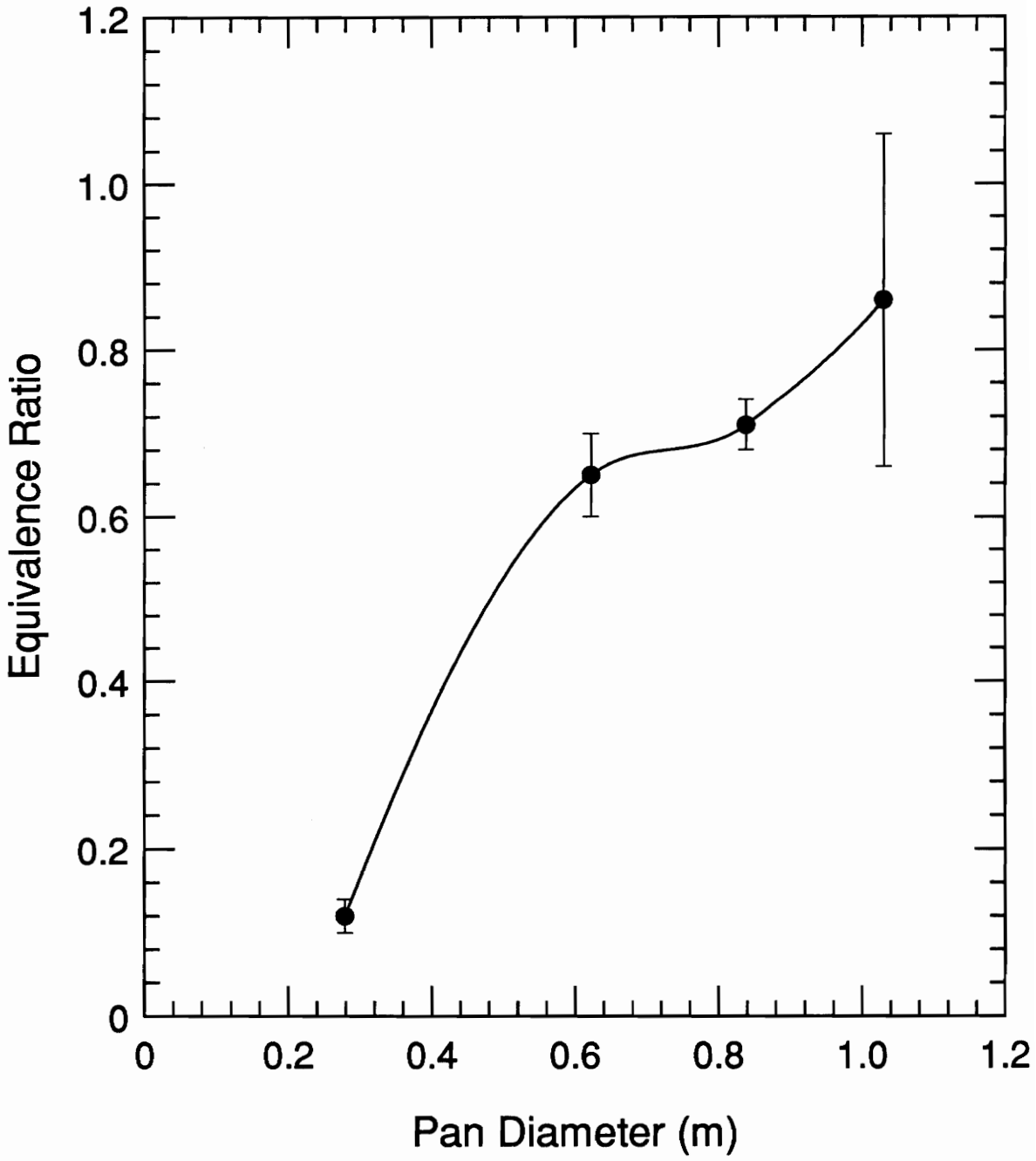

Figure 4.33: Average Plume Equivalence Ratio vs. Pan Diameter

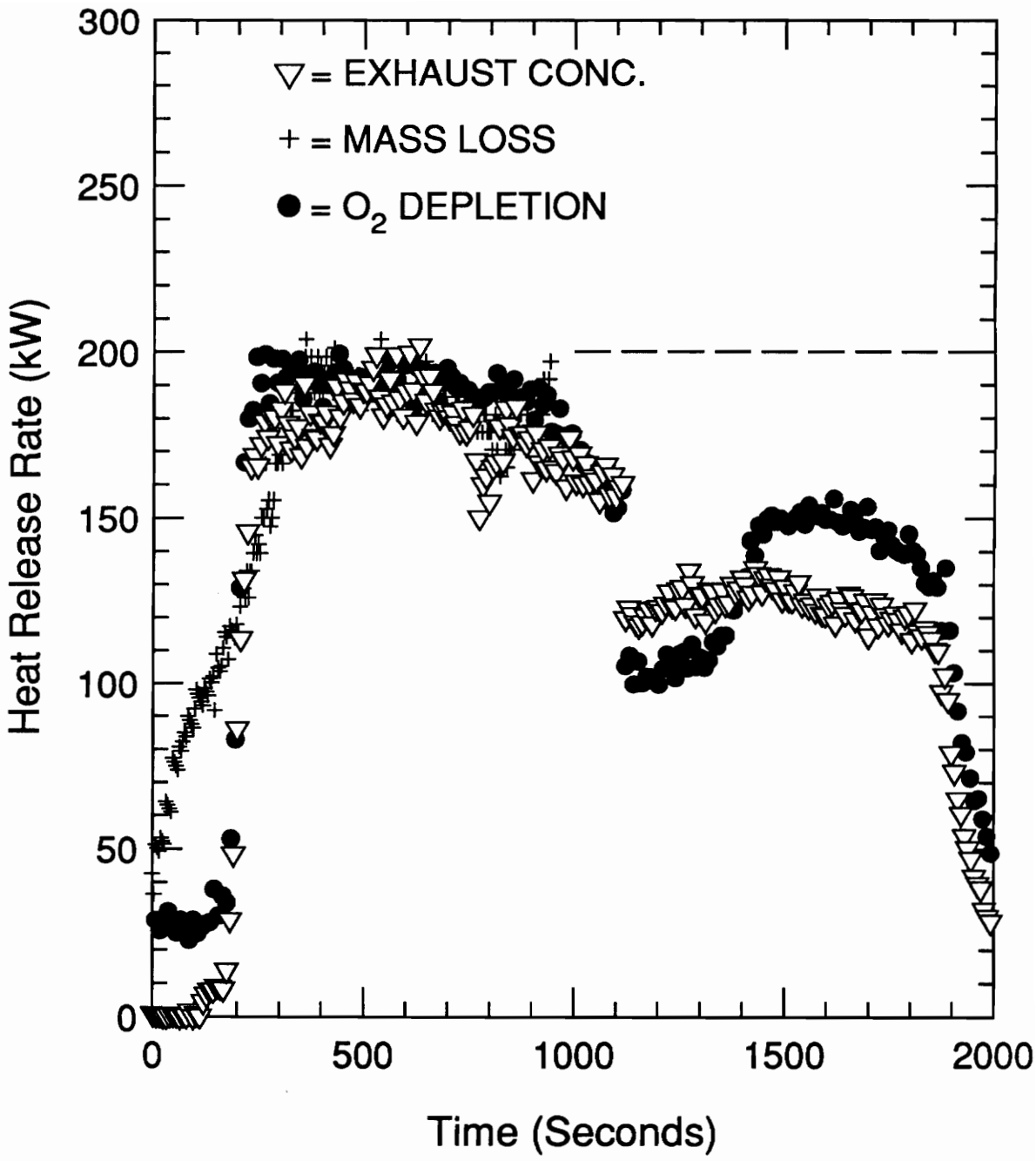

Figure 4.34: Heat Release Rate-Time Histories for Test #20: 83.8 cm diameter Pan

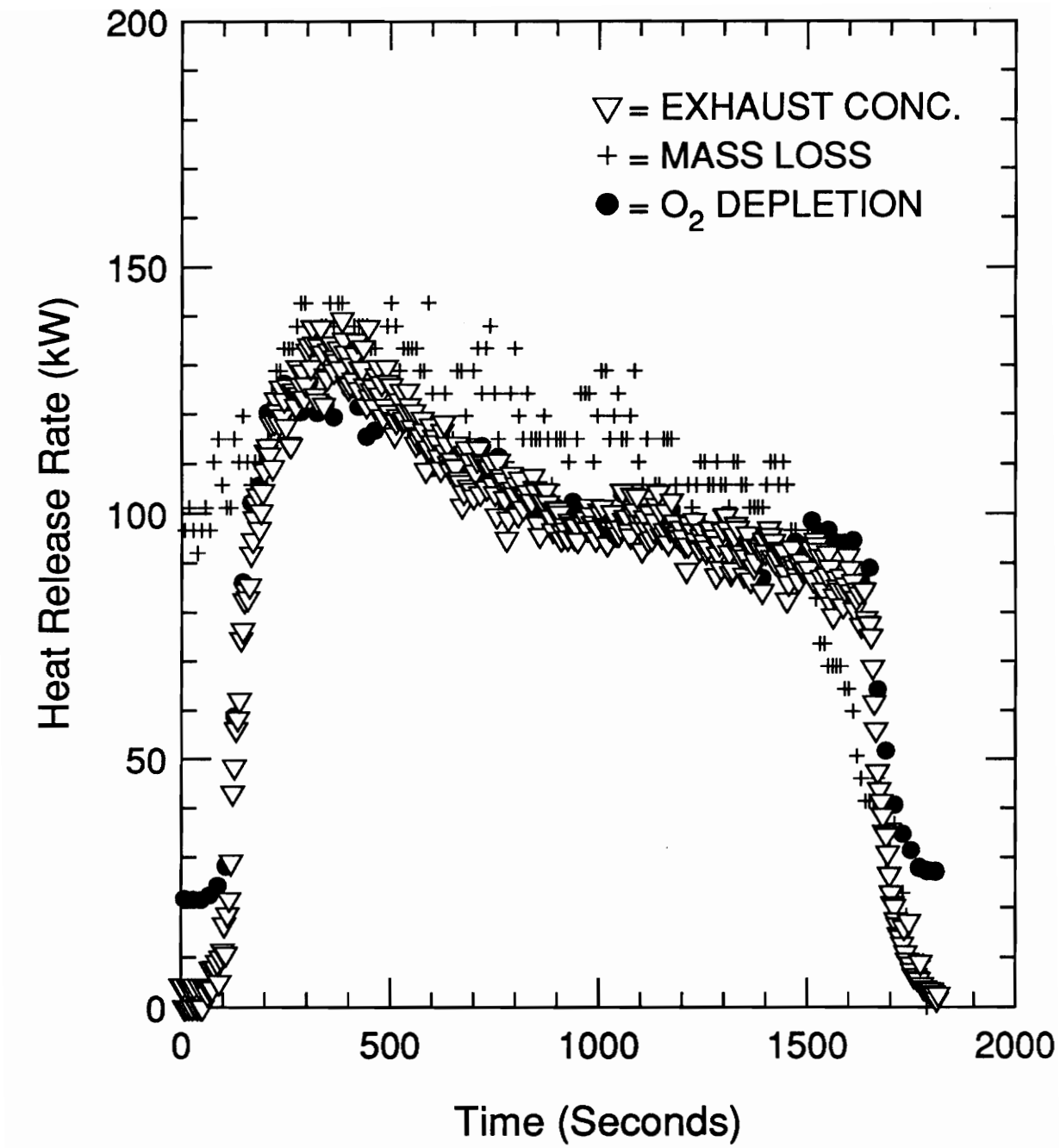

Figure 4.35: Heat Release Rate-Time Histories for Test #21: 62.2 cm diameter Pan

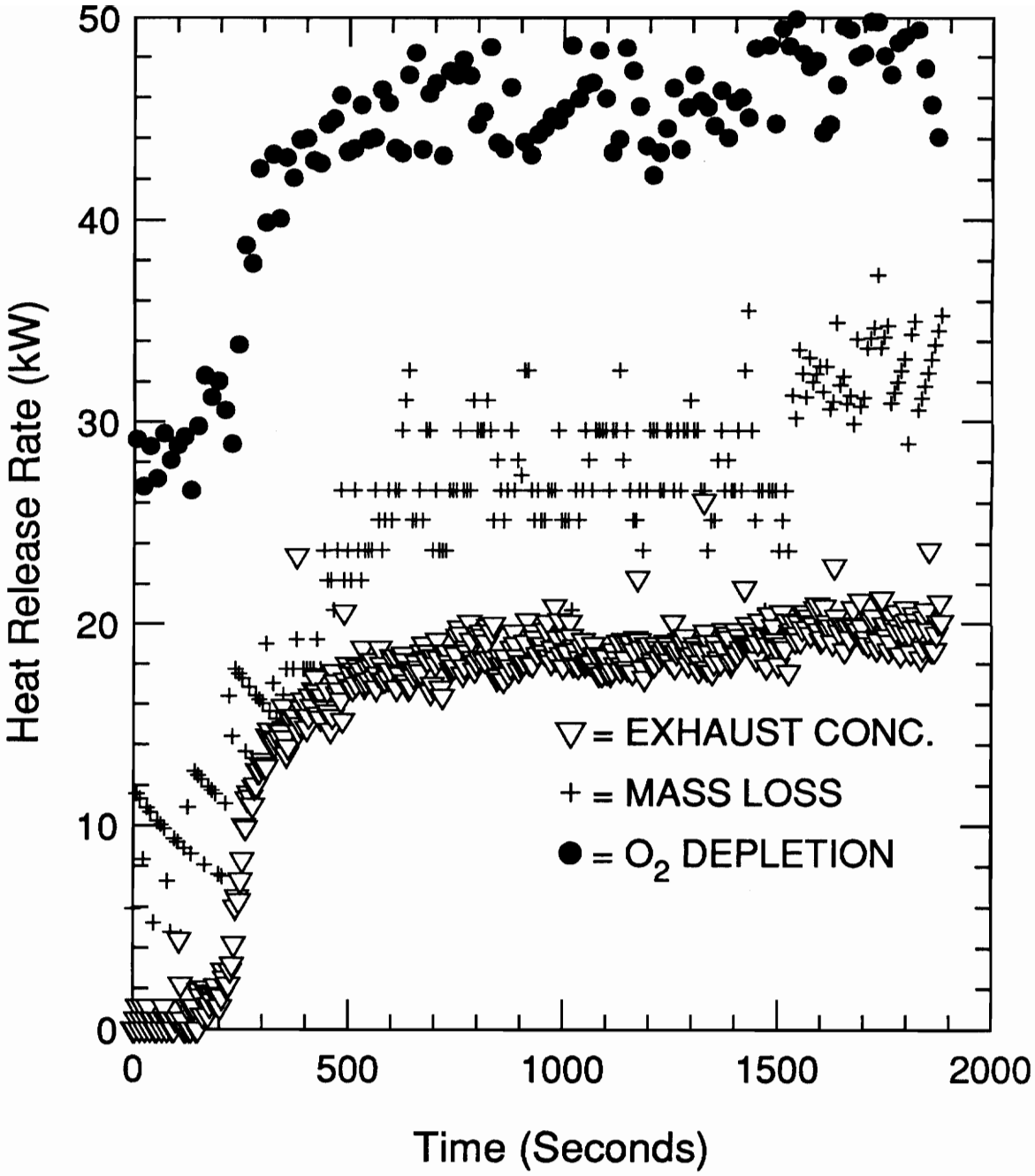

Figure 4.36: Heat Release Rate-Time Histories for Test #22: 27.9 cm diameter Pan

Next, exhaust concentrations of carbon monoxide, carbon dioxide, oxygen, and unburned hydrocarbons are shown. Oxygen and carbon dioxide concentrations as a function of time are shown in Figure 4.37 for Test #20 (83.8 cm diameter pan), where a minimum oxygen concentration of 4% is reported. In addition, carbon monoxide and hydrocarbon concentrations measured in this same test are shown in Figure 4.38 as a function of time. The carbon monoxide rises to a peak concentration of 1.5% 500 seconds into the fire and then declines to an asymptotic 0.8% for the remainder of the fire. Hydrocarbon measurements peak at 11000 ppm at the same time as the carbon monoxide concentration peaks. They then experience a fall to 6250 ppm and increase back to nearly 10000 ppm. At 500 seconds, where the carbon monoxide and hydrocarbons peak, there is no noticeable change in carbon dioxide or oxygen concentrations as would be expected.

During the 62.2 cm diameter pan test, no significant levels of hydrocarbons and a peak value of 0.4% carbon monoxide were measured. (Figure 4.39). In addition, the carbon dioxide is observed to undergo an initial rise followed by a decline to a steady value of 6%. The same behavior, with a minimum of 6.5%, occurs with the oxygen concentration except it is being consumed not produced.

Figure 4.40 shows that in the 27.9 cm diameter test, very little oxygen is consumed. In fact, oxygen concentrations did not fall below 18%. Consequently, zero concentrations of carbon monoxide and hydrocarbons were measured.

A comparison of the peak carbon monoxide concentration and the minimum oxygen concentration as a function of pan diameter are shown in Figures 4.41 and 4.42, respectively. As the pan diameter is increased, carbon monoxide production rises in an exponential fashion while oxygen consumption decreases also in an exponential fashion.

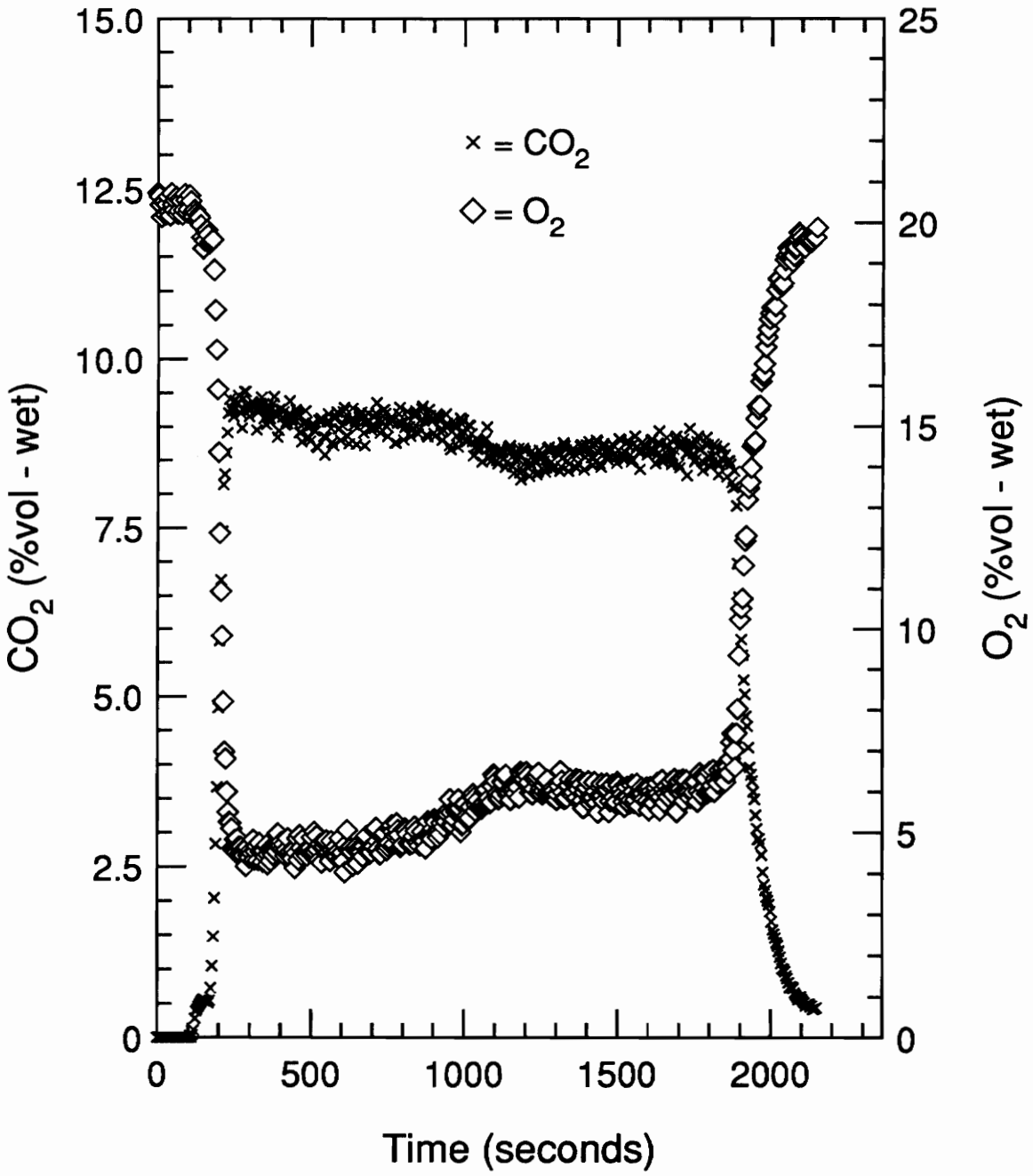

Figure 4.37: Carbon Dioxide and Oxygen Concentration-Time Histories for Test #20: 83.8 cm diameter Pan

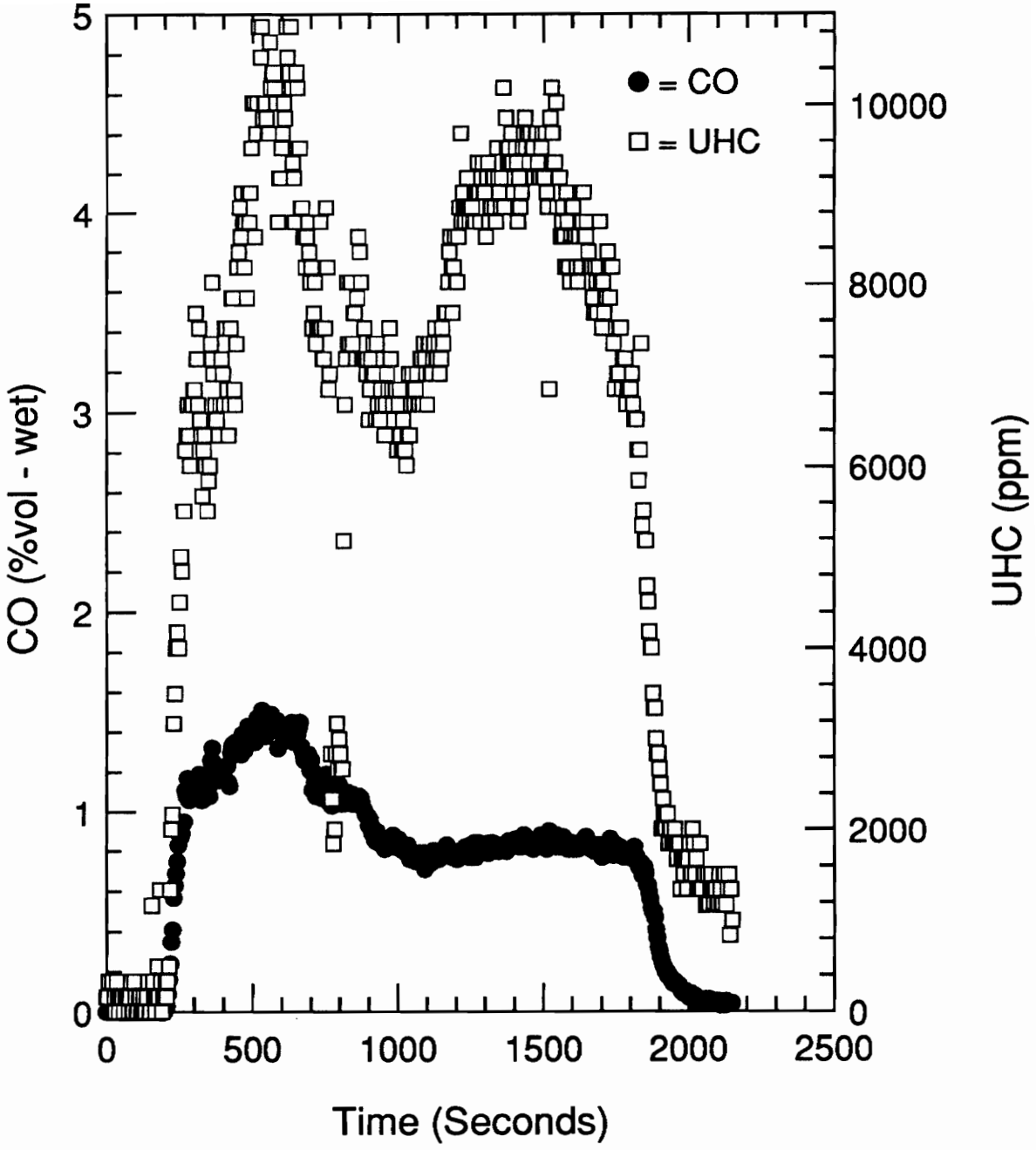

Figure 4.38: Carbon Monoxide and Unburned Hydrocarbon Concentration-Time Histories for Test #20: 83.8 cm diameter Pan

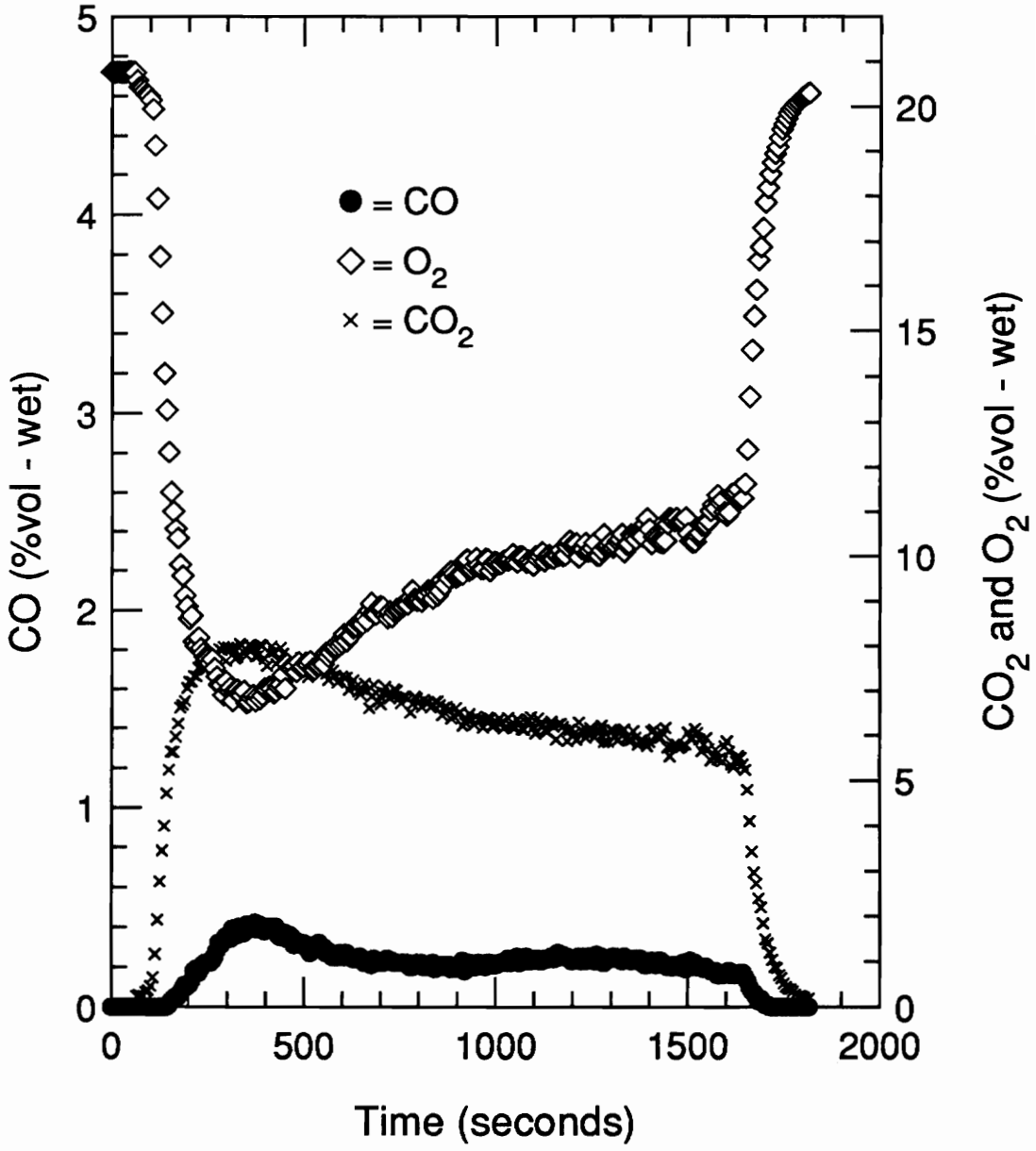

Figure 4.39: Carbon Monoxide, Carbon Dioxide and Oxygen Concentration-Time Histories for Test #21: 62.2 cm diameter Pan

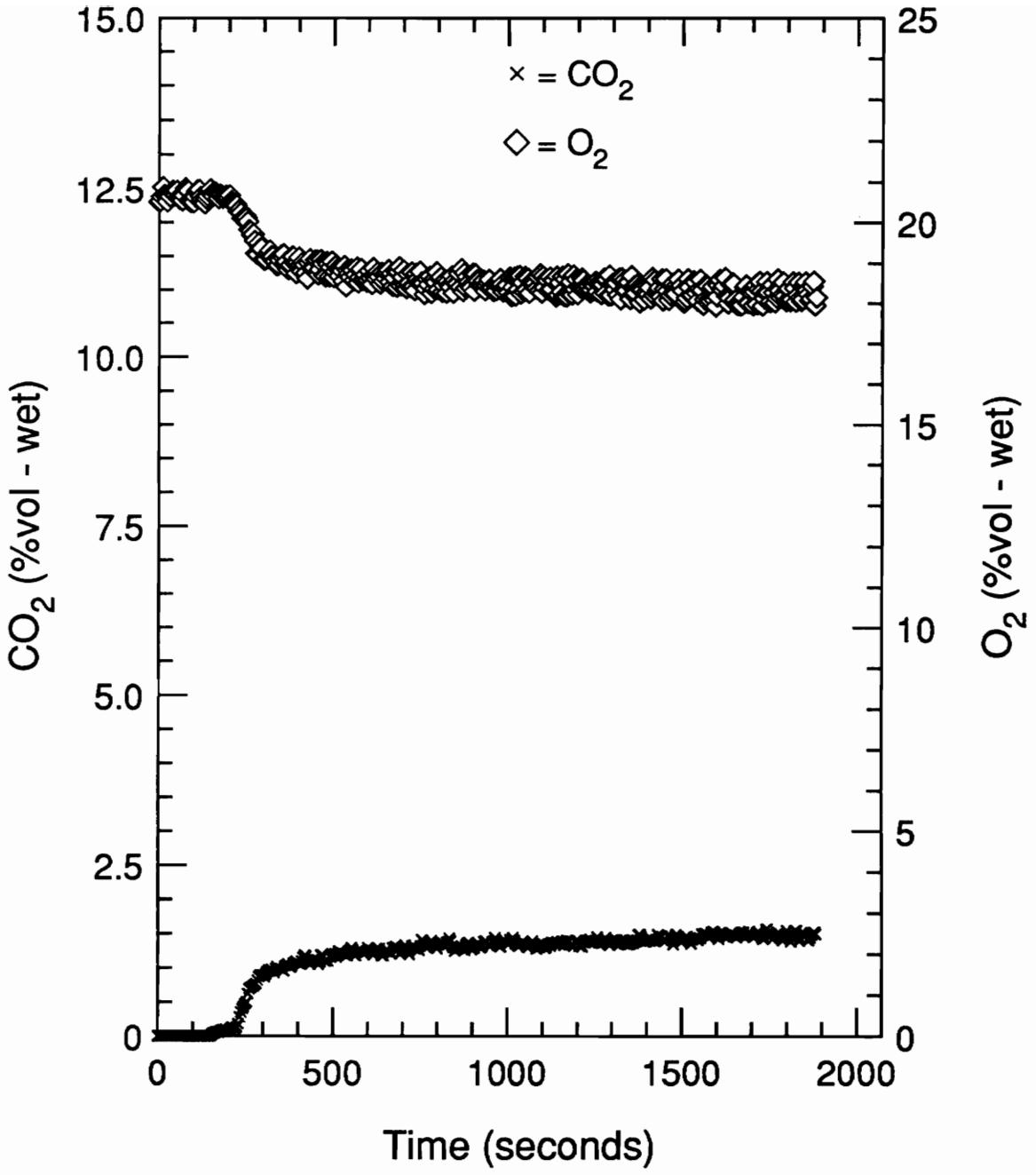

Figure 4.40: Carbon Dioxide and Oxygen Concentration-Time Histories for Test #22: 27.9 cm diameter Pan

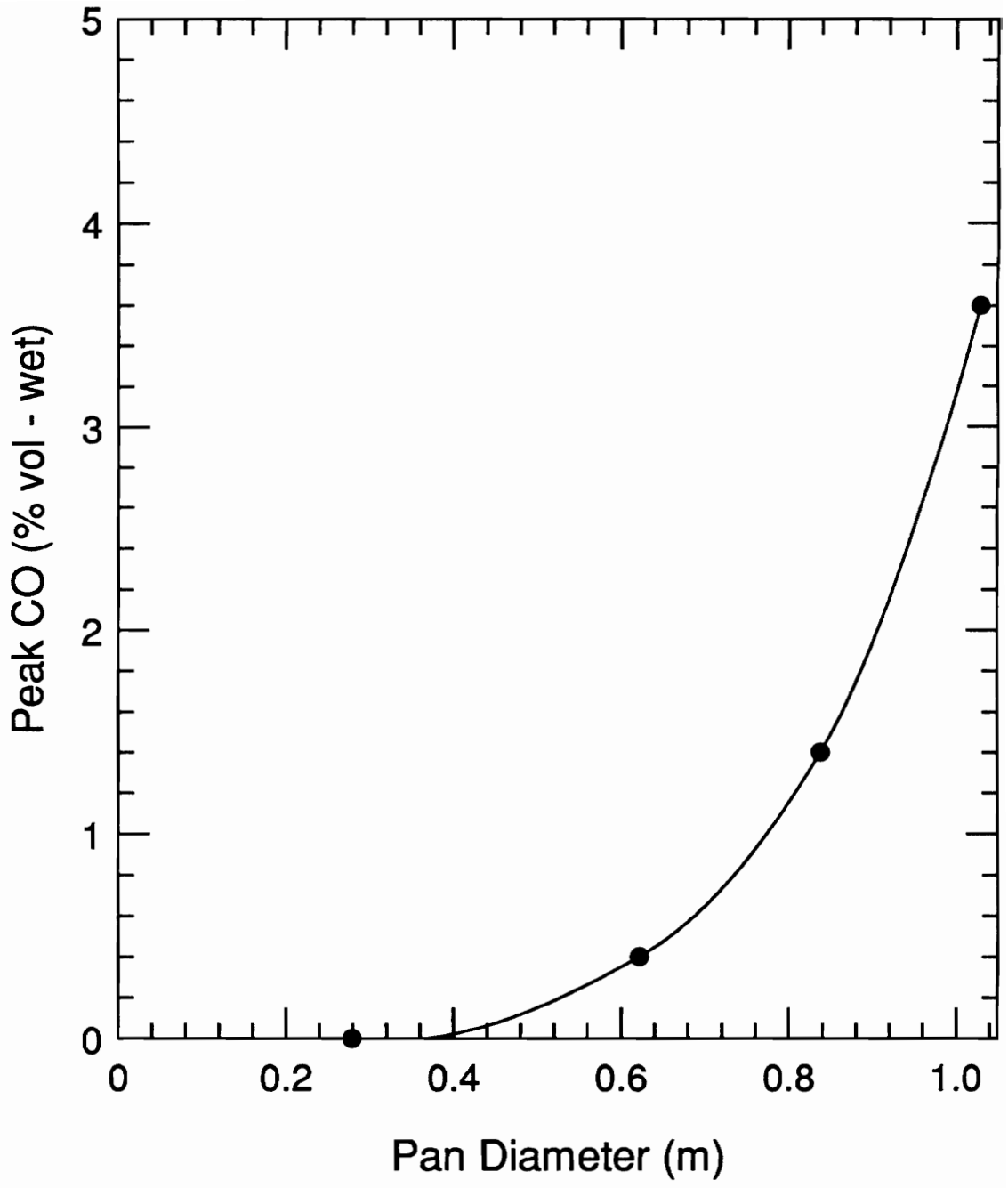

Figure 4.41: Peak Carbon Dioxide Concentration vs. Pan Diameter

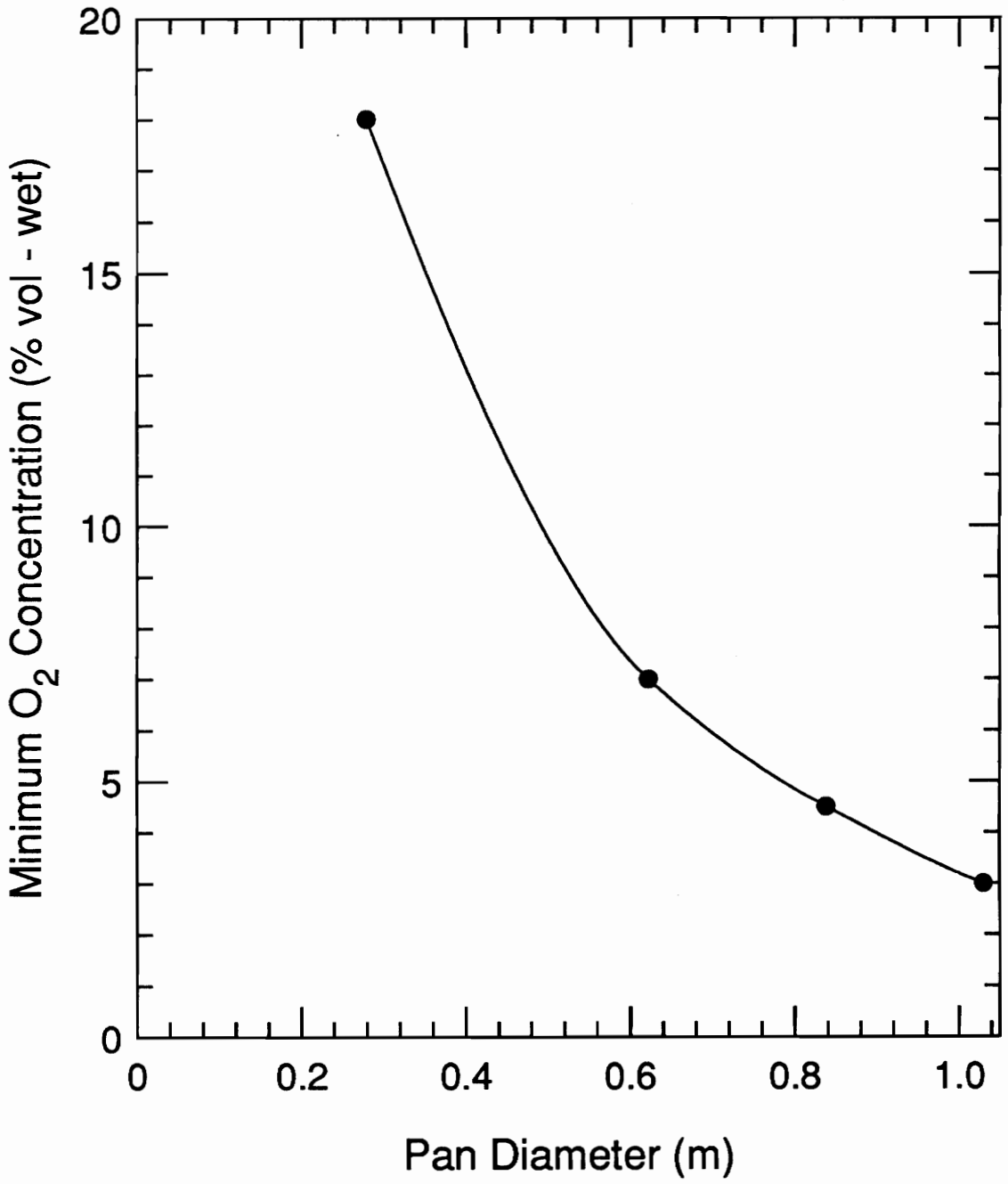

Figure 4.42: Minimum Oxygen Concentration vs. Pan Diameter

This trend observed in carbon monoxide production supports the conclusion that more complete combustion occurs as the pan size is decreased since less carbon monoxide is generated.

Time histories of the thermal environments for each of these three tests are provided in Figures 4.43-4.45. A successive decrease in temperatures is noticed as the pan diameter decreases. A plot of the peak ceiling temperature (estimated as TC1) versus pan diameter is shown in Figure 4.46 where temperatures are observed to increase from 150C in the smallest pan test to 800C in the largest pan test.

Temperature profiles for each of these tests are plotted in Figures 4.47-49. In each case, the profiles are rather linear. However, a slight stratification is seen in Figure 4.49 at 77 cm from the glovebox ceiling. Comparison of the thermocouples by the glovebox exhaust reveals trends consistent with those observed and discussed in the full scale pan test section.

Figures 4.50 and 4.51 represent a comparison of the smoke yields, expressed as grams of smoke produced per grams of fuel burned, and smoke generation rate, expressed as the rate of smoke production per fuel surface area ($g/sec*m^2$), for the three reduced surface area pans, respectively. General trends show that the smoke yield and smoke generation rate increase with decreasing pan size. The higher noise level seen with the 27.9 cm diameter pan yields is a reflection of the unsteady load cell measurements. Steady state yields range from 0.04 for the largest pan to 0.2 for the smallest pan while the generation rates range from 0.2 to 2.2 g/m^2*sec for these same tests.

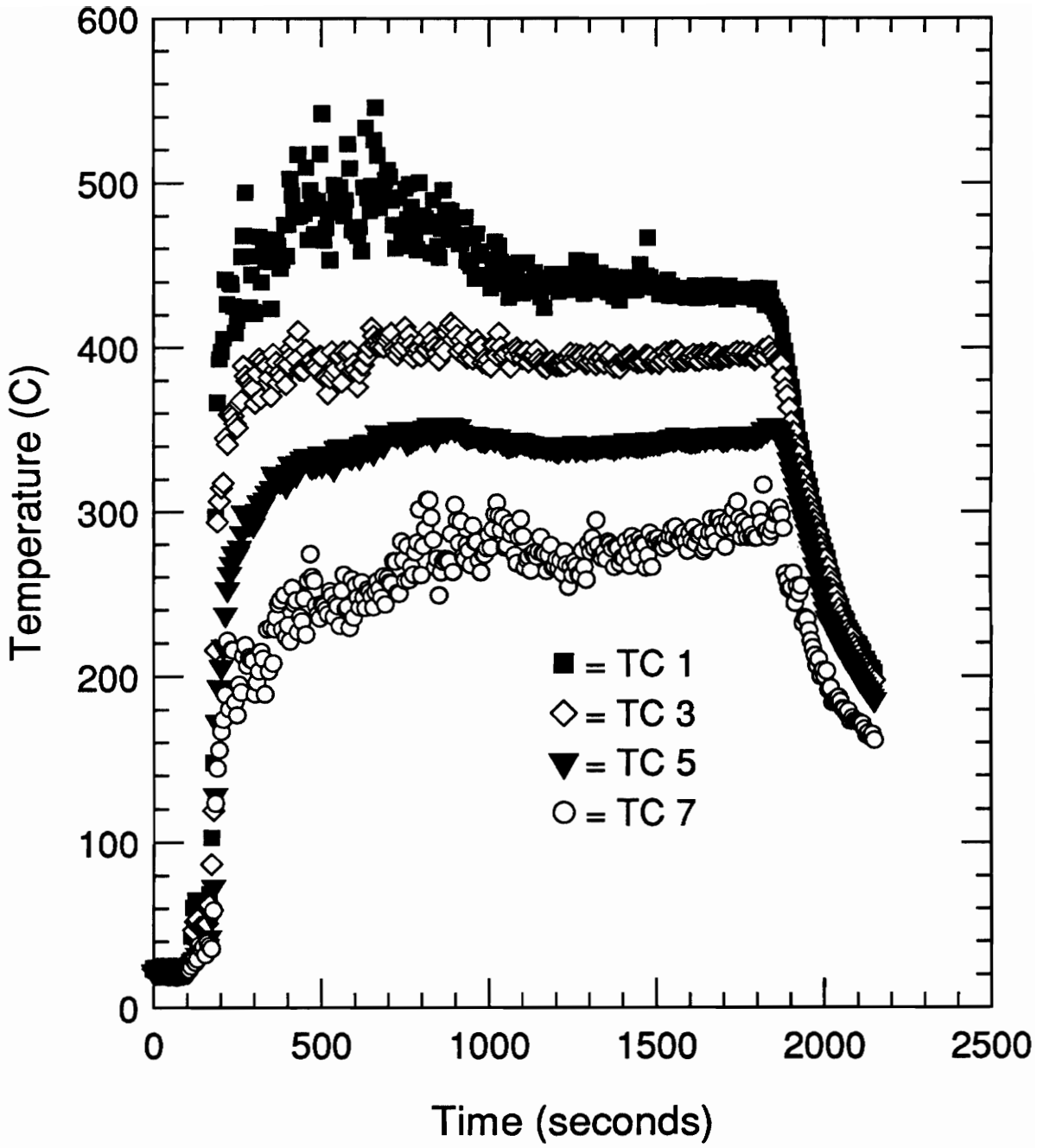

Figure 4.43: Thermocouple Rake Temperature-Time History for Test #20: 83.8 cm diameter Pan

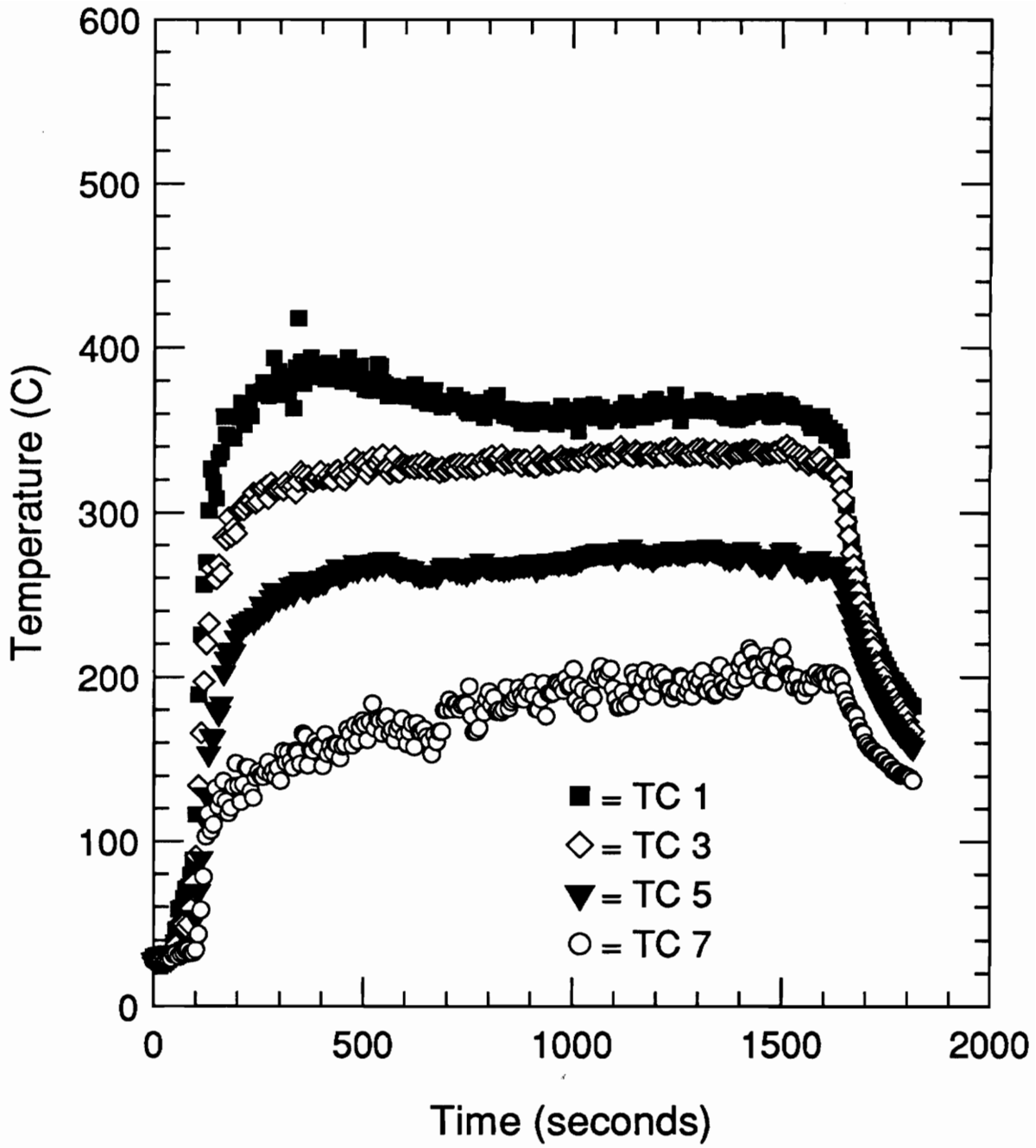

Figure 4.44: Thermocouple Rake Temperature-Time History for Test #21: 62.2 cm diameter Pan

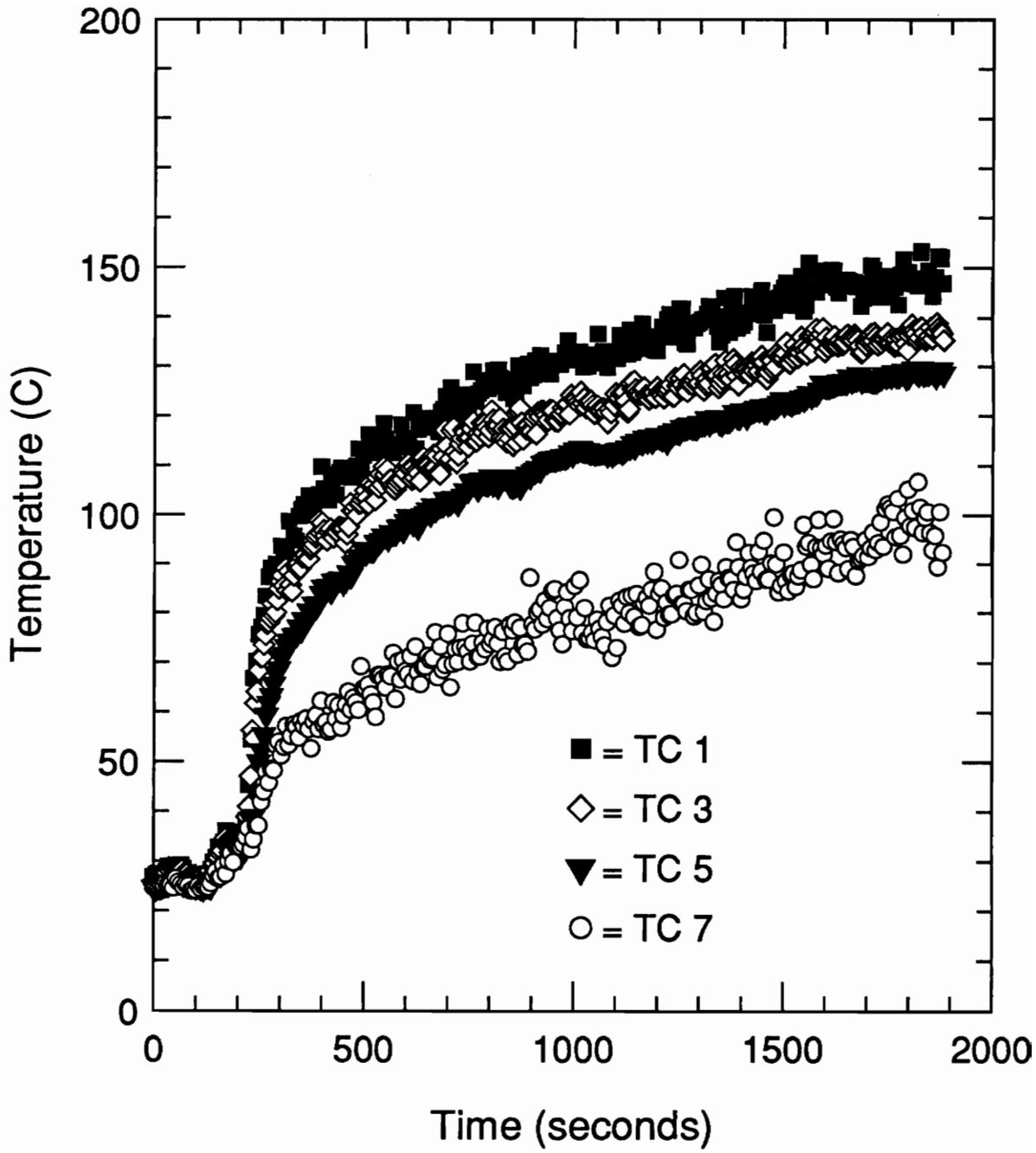

Figure 4.45: Thermocouple Rake Temperature-Time History for Test #22: 27.9 cm diameter Pan

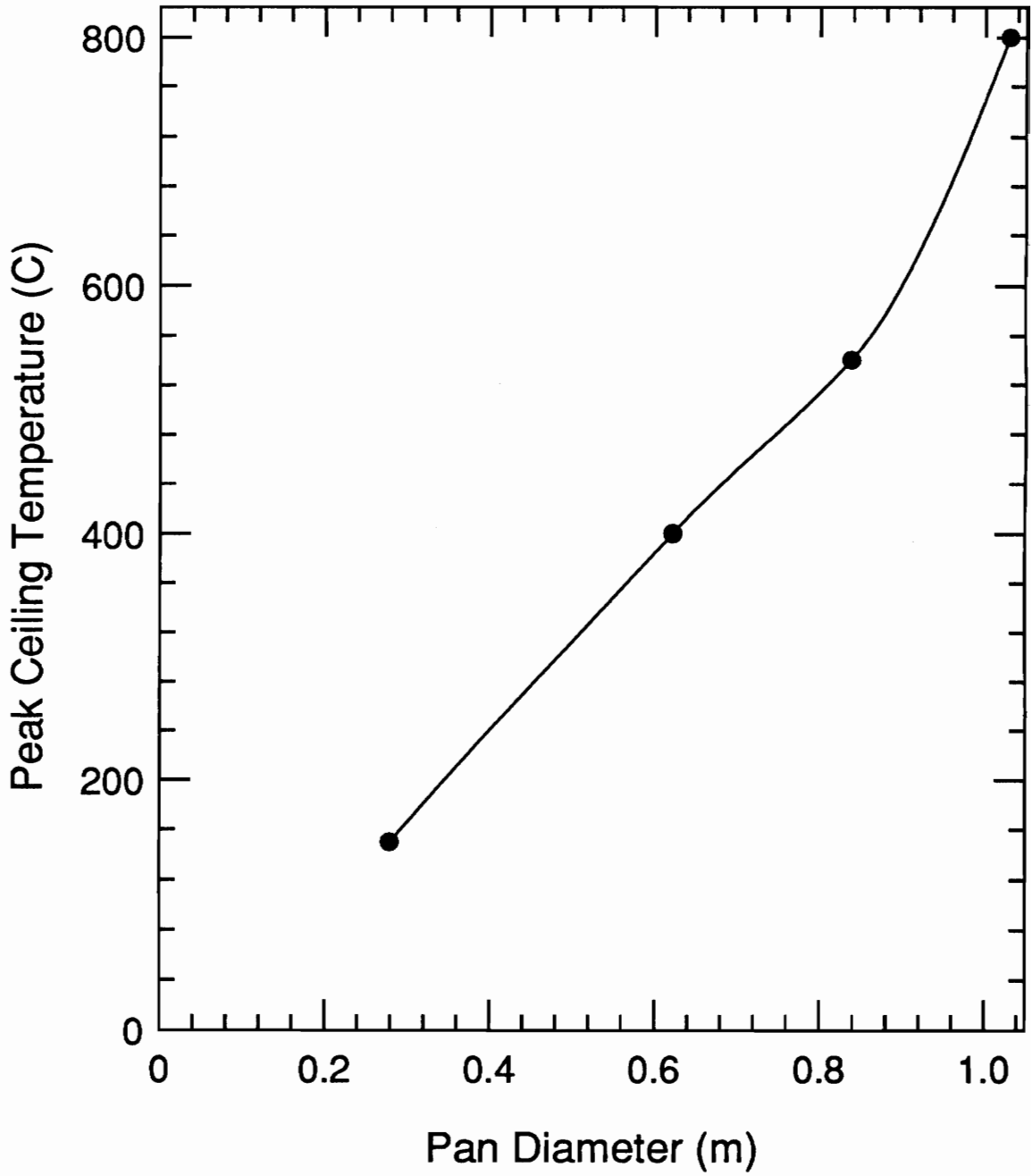

Figure 4.46: Peak Ceiling Temperature vs. Pan Diameter

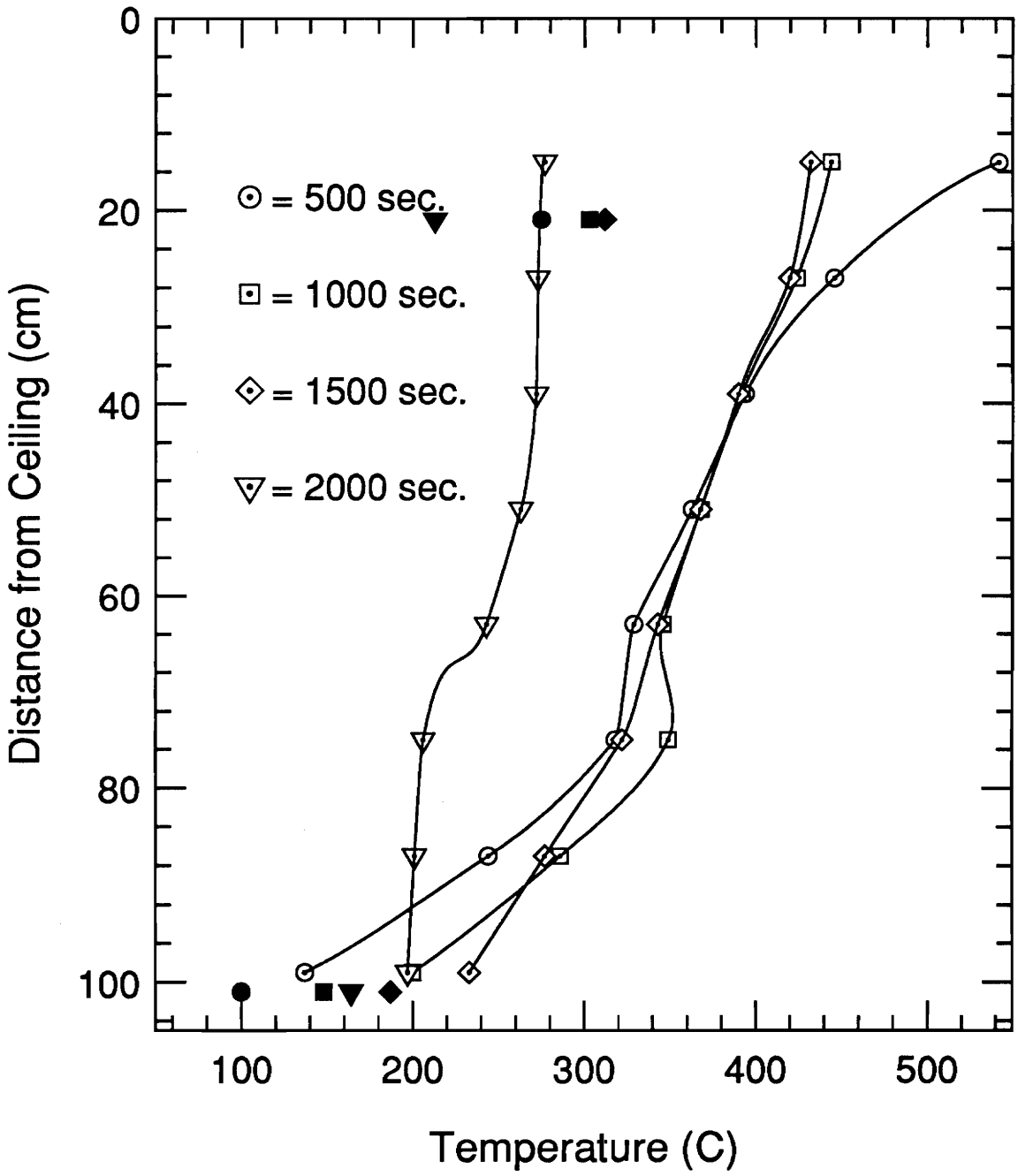

Figure 4.47: Vertical Temperature Profiles for Test #20: 83.8 cm diameter Pan

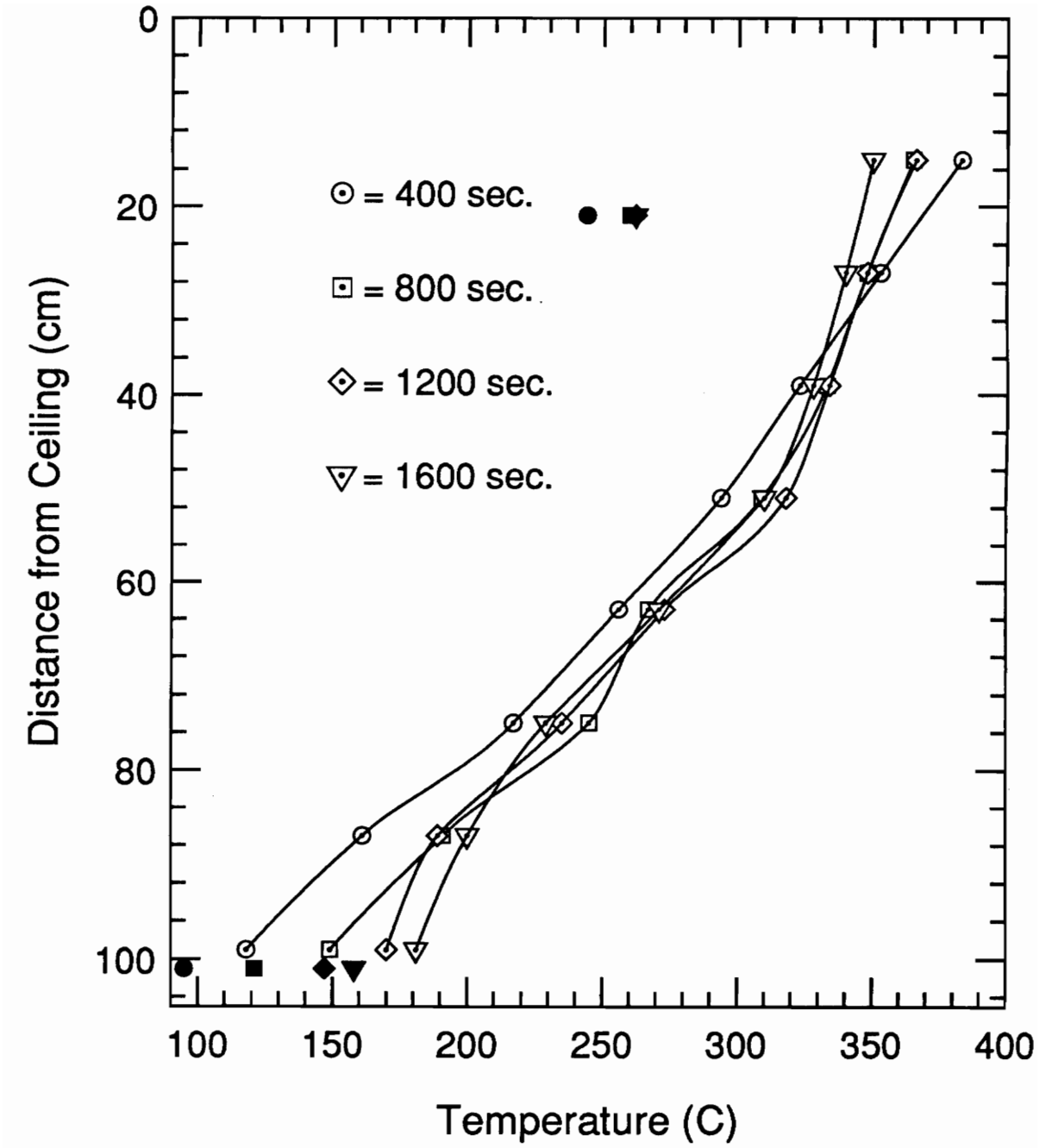

Figure 4.48: Vertical Temperature Profiles for Test #21: 62.2 cm diameter Pan

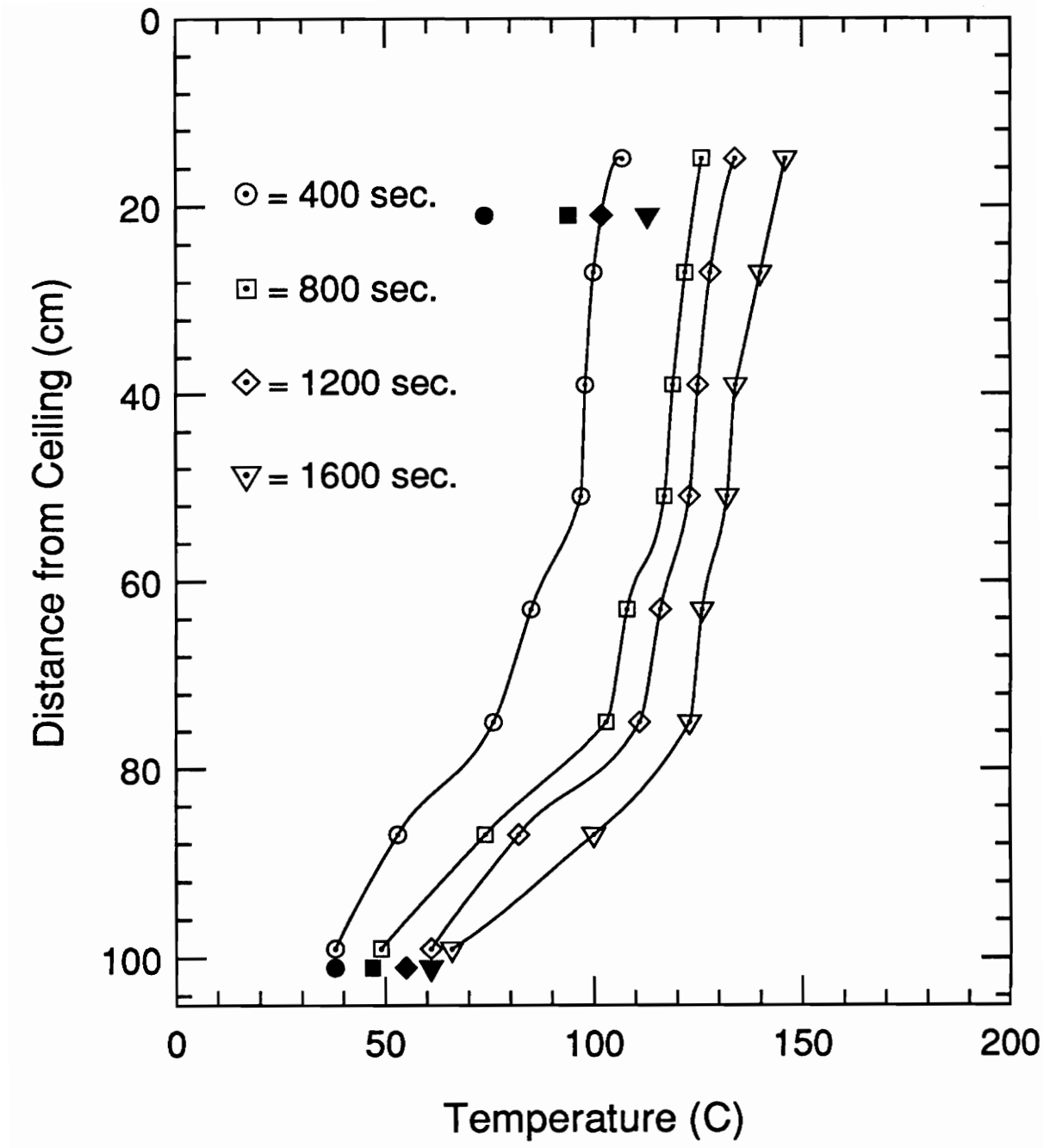

Figure 4.49: Vertical Temperature Profiles for Test #22: 27.9 cm diameter Pan

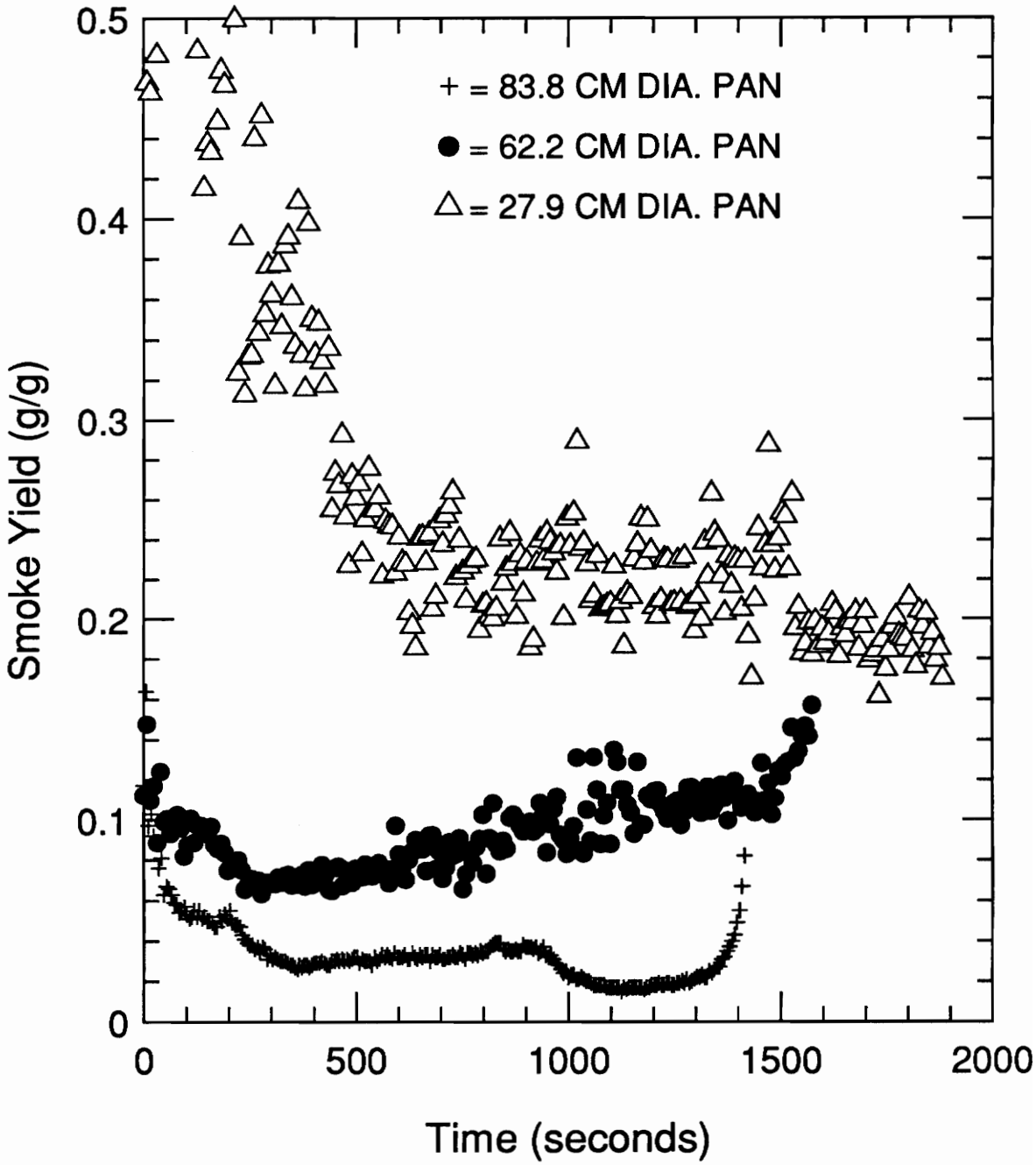

Figure 4.50: Comparison of Smoke Yield-Time Histories for Tests #20-22: 83.8 cm, 62.2 cm and 27.9 cm diameter Pans

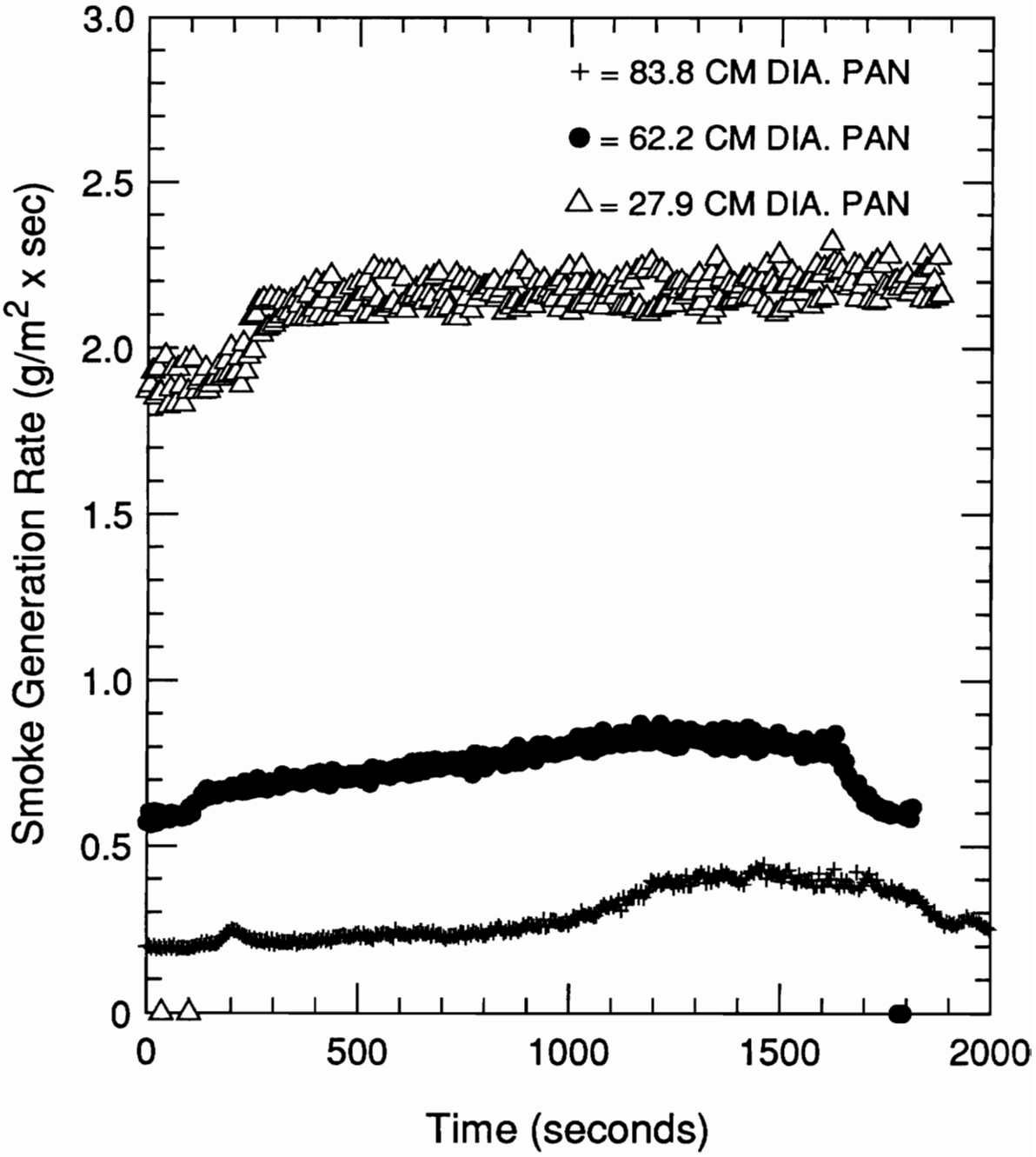

Figure 4.51: Comparison of Smoke Generation Rate-Time Histories for Tests #20-22: 83.8 cm, 62.2 cm and 27.9 cm diameter Pans

5. DISCUSSION

5.1 Introduction

This section summarizes the response of the glovebox to internal fires. Furthermore, as an attempt to provide useful information for fire modelling, the dependence of fuel surface area on fixed ventilation rate fires will be assessed. In addition, the behavior of these tests is compared and contrasted with the conventional compartment fire models: well-stirred reactors and 2-layer systems. To facilitate this discussion, Foote's previous forced ventilation work will be used as a comparison as well as Gottuk's natural ventilation compartment fire experiments.

5.2 Assessment of Glovebox Safety

Overall, the glovebox design proved to be fire safe in situations where the box was sealed. Based on full scale pan results, the possibility of a substantial glovebox fire is not overwhelming as only one of the three fires actually burned until all fuel was consumed. Conditions are so close to the stability limits, (i.e. a self-sustaining flame), that if a fire did occur, it is likely to self-extinguish. Even in the test where the fire continued until the fuel was gone, no significant failure occurred to allow exhaust gases to bypass the exhaust duct.

An explanation of why one of the three normal full scale pan tests was stable enough to continue until the fuel was gone is not known. The exhaust flow rates were approximately the same in each test. However, comparison of the fire environments experienced in Tests #8 & 9 show that a higher burn rate occurred in the non-extinguishing test as well as a hotter thermal environment.

On the other hand, introduction of additional ventilation openings led to containment loss. While allowing up to four open glove holes did not provide enough ventilation to support the fire, sporadic gas outflow did occur while a flame was present. Conversely, losing one of the windows did introduce enough oxygen to support the fire. It was clear that losing a window was the worst case since the outflow of exhaust gases was steady throughout the fire and constituted a larger volume than that which occurred in the tests with gloves missing. It is important to note that a catastrophic failure was not experienced in any of these test situations. While containment was lost in the added ventilation opening tests, the fire was never able to develop to its potential as demonstrated in the open burn tests.

The window design proved to be adequate to maintain glovebox integrity. All windows cracked soon after pan ignition but remained intact. This observation is noteworthy since these windows are edge-protected and, to remain consistent with Skelly's findings, should have failed catastrophically [5]. In both window types though, there was a component which prevented complete failure. In the ceiling, the wire was responsible for preventing window breakage. For the front windows, the composite structure was responsible for the lack of breakage. This conclusion is supported by observation of the glass condition when windows were removed from the gaskets. The laminate melted so that the three layers of glass, each with a different crack pattern, were separated. Also important to the window design were the metal keepers or window guards. In some tests, the gaskets burned considerably even though they were protected from flame impingement. It is believed that windows would have fallen out in the absence of these guards.

Moreover, the use of glove hole covers also proved to be of great value. In some of the longer tests, the gloves began to pyrolyze and holes formed in them. These covers were successful in blocking the majority of the air exchange through these holes.

5.3 Effects of Reduced Fuel Surface Areas

This section provides a comparison of the burning behavior observed in the free burn and enclosed burn scenarios. Furthermore, trends in the fire behavior exhibited for the reduced fuel surface area glovebox experiments will be explained.

5.3.1 Comparison of Open Burn vs. Enclosed Burn Characteristics

Table 5.1 compares the average open burn rates to the average burn rates observed in the glovebox. Normally, open burn rates are at least several times smaller than enclosed burn rates provided that the fuel/air ratio is close to stoichiometric. This behavior is caused by the radiation feedback that occurs in an enclosure [13]. An opposite trend, however, is demonstrated in this table. Figure 5.1 shows the open and enclosed burn rates per fuel area as a function of pan diameter. In all tests, the enclosed burn rate is lower than the open burn rate, reaching a reduction of nearly an order of magnitude for the largest fuel pan. Also of interest is the opposite trend in burn rate per fuel area seen with increasing pan diameters: normalized open burn rates increase with pan diameter while normalized enclosed burn rates decrease with pan diameter. These trends lead to the conclusion that the overhead forced ventilation is inhibiting the burn characteristics.

The vast difference in the resulting heat release rates for these fires is apparent in Figure 5.2. A much sharper rise in heat release rate occurs for the open burn tests than for the enclosed burns. Initially, with the smallest fuel pan, the heat release rates are

Table 5.1: Average Open and Enclosed Burn Rates

Pan Size	Open Burn Rate (g/sec)	Enclosed Burn Rate (g/sec)
.91 m x .91 m	26.7 +/- 3.2	4.0 +/- 0.2
83.8 cm dia	17.1 +/- 0.4	4.1 +/- 0.2
62.2 cm dia	6.1 +/- 0.3	2.6 +/- 0.2
27.9 cm dia	0.9 +/- 0.1	0.6 +/- 0.08

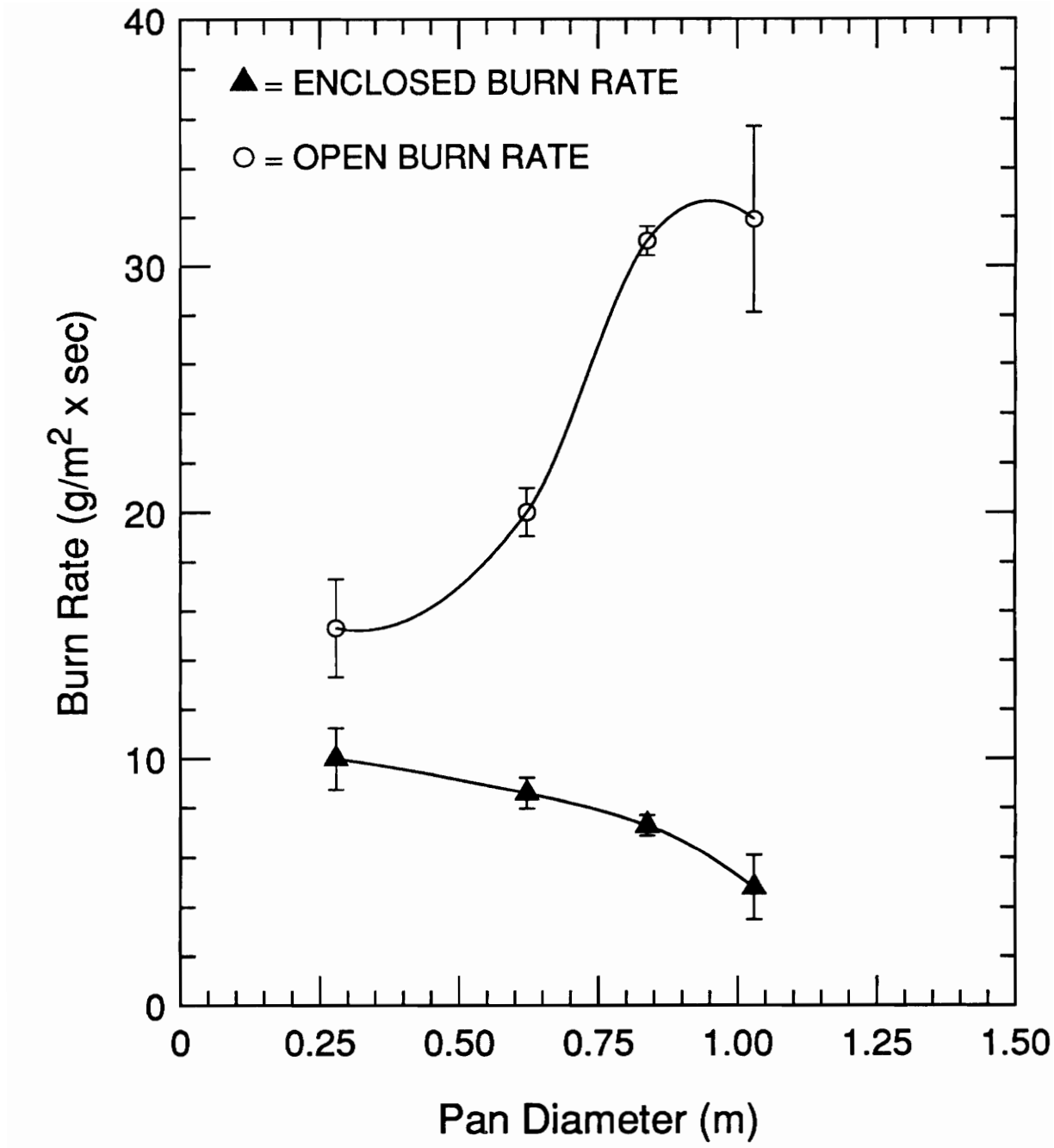

Figure 5.1: Average Open and Enclosed Burn Rates Per Fuel Surface Area vs. Pan Diameter

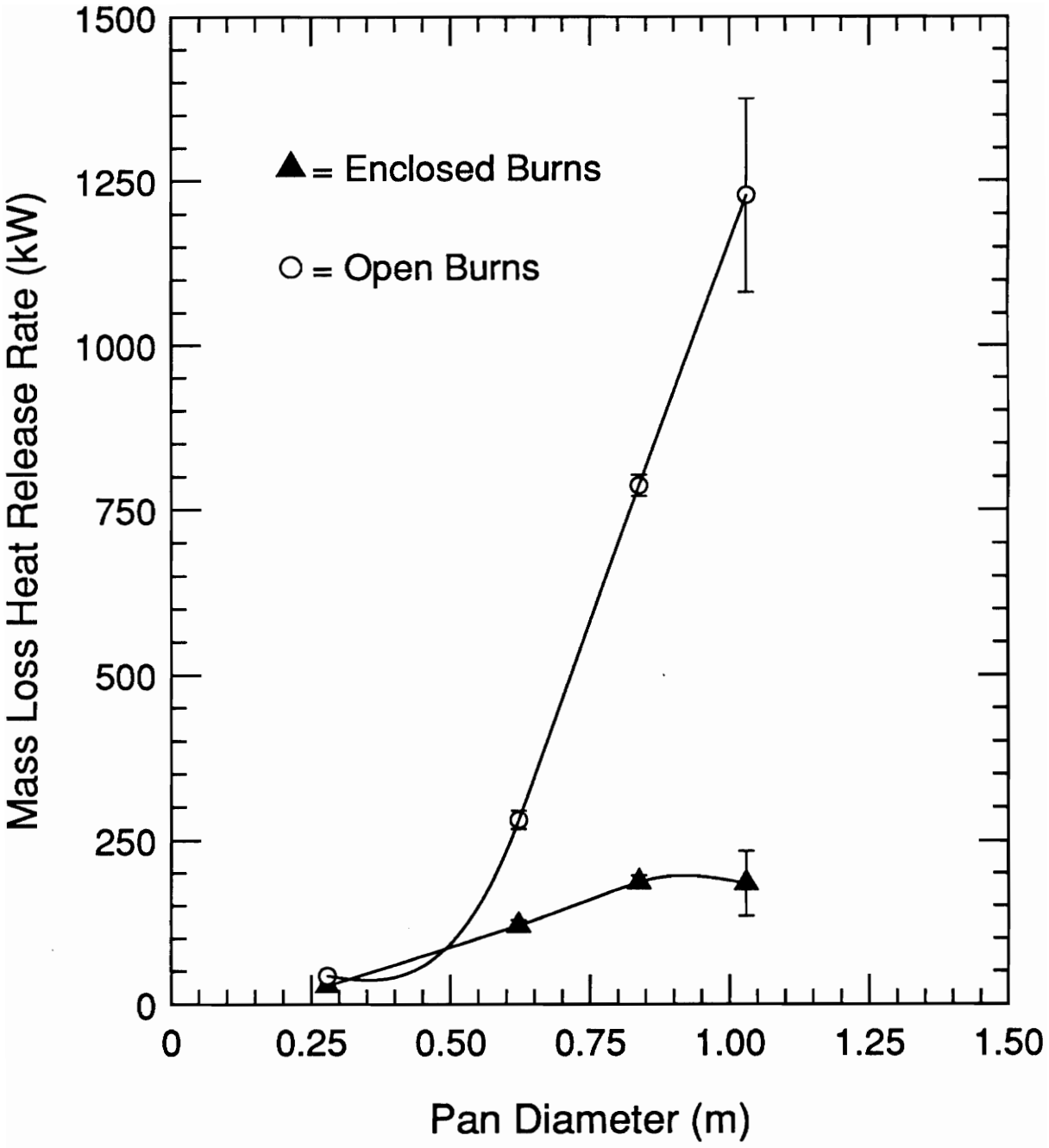

Figure 5.2: Comparison of Mass Loss Heat Release Rates for Open and Enclosed Burn Tests

roughly the same, but as the diameter increases, the heat release rate for free burning conditions can be as much as 7 times that for enclosed burning conditions, as seen with the largest fuel pan.

5.3.2 Comparison of Enclosed Glovebox Tests

Based on the temperature, heat release rate, and exhaust gas data collected, the fires became less intense and less dangerous as the pan size decreased. To begin with, the mass loss heat release rate is reduced from a maximum value of 184 kW for the 83.8 cm diameter pan fire to 28 kW for the 27.9 cm pan fire. This reduction is significant because the flame spread rate corresponding to a 28 kW fire would be significantly lower in an actual building fire.

Glovebox temperatures measured 21 cm from the ceiling also dropped from an average of 800 C to 170C for the full scale pan test and 27.9 cm pan test, respectively. This information is beneficial since flashover occurs at ceiling temperatures of approximately 600C. Flashover is defined as "the transition from a localized fire to the general conflagration within the compartment when all fuel surfaces are burning " [13]. In most cases, once flashover occurs, escape from a compartment is impossible and fire extinguishment becomes much more difficult.

In addition, carbon monoxide generation decreased from lethal levels in the full scale pan test to a point where it was nonexistent in the smallest pan test. Understanding trends for carbon monoxide generation is crucial since most deaths occurring in building fires are due to carbon monoxide poisoning.

A graph illustrating the mass loss heat release rate as a function of equivalence ratio is shown in Figure 5.3. As expected, the heat release rate increases until an

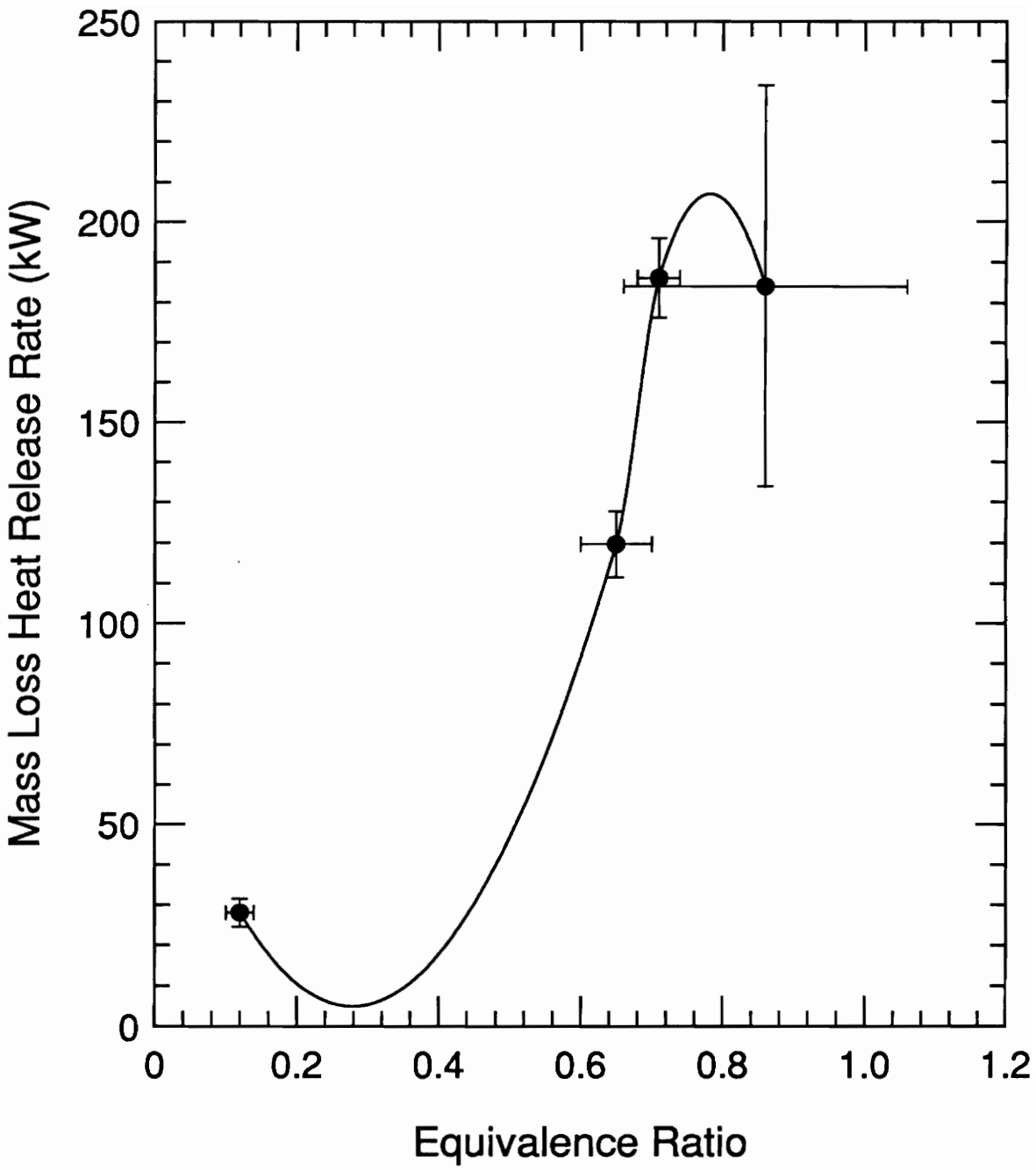

Figure 5.3: Mass Loss Heat Release Rate vs. Equivalence Ratio

equivalence ratio of 0.7. Then, an unusual peak occurs and the heat release rate declines slightly. Perhaps this trend is better characterized by a leveling off after an equivalence ratio of 0.7 rather than a decline as shown.

Smoke calculations show that smoke production per fuel area increases with decreasing diameter and decreasing equivalence ratio. However, the actual smoke volume was much higher in larger pan tests since vision through the windows was only possible in the smallest (27.9 cm) pan test. These trends in smoke yield and smoke generation rate compare with trends seen by Tewarson [28]. However, the magnitude of his measurements differ significantly from the values observed in these tests. He reports a smoke yield of 0.04 typical for hydrocarbon pool fires, whereas smoke yields as high as 0.2 were observed in these tests. Discrepancy between these values may be attributed to the difference in the test conditions. Smoke measurements for compartments fires with overhead forced ventilation have not been documented previously.

5.4 Comparison to Previous Overhead Forced Ventilation Work

Results from these tests show important differences from Foote's overhead forced ventilation tests. Based on oxygen exhaust concentrations and vertical temperature profiles, Foote observed a well-stirred system irrespective of ventilation rate. This set of tests, however, does not follow this pattern. While the vertical temperature profiles are linear and do represent a well-stirred system, the oxygen exhaust concentrations do not fit the model. In some tests, they reached values less than 3%, a value far below the LOI, while the fire was still burning. If a well-stirred model was applied to this test, it would dictate that there was no flame present in the glovebox. Therefore, these fires cannot be modelled as well-stirred reactors.

The modelling that Beyler performed for Foote's tests to predict extinction time cannot be applied to these tests since he assumed that the system was a well-stirred reactor and used the LOI concept. Since exhaust concentrations for oxygen were below the LOI in some cases, this assumption would be invalid for modelling these fires.

An important consideration when analyzing overhead ventilation configurations is the room geometry. Foote's test compartment was 4 m by 6 m by 4.5 m high while the one used in this study was 1.22 m by 3.66 m by 1.22 m high. From a standpoint of aspect ratio, these enclosures are considerably different. This variation can affect the air movement thereby affecting the mixing abilities of the air. The differences in the residence times must also be considered. A residence time of 1 minute was typical for the glovebox experiments while Foote's residence times varied from 0.4 to 0.7 minutes depending on the ventilation rate. Consequently, the gases in the glovebox had a longer time to mix and/or participate in post combustion reactions.

It is also essential to consider the compartment height versus the flame height when comparing these results. A flame which hits the ceiling can change the compartment environment from that observed when the flame does not hit the ceiling. Flames which reach the ceiling are deflected and can cause different exhaust gas circulation patterns. These patterns can enhance vertical mixing which, in turn, creates a well-stirred reactor.

5.5 Comparison to Conventional Two-Layer Systems

Transient exhaust species yields were calculated for Tests #8, 20, 21, and 22 and steady-state values were determined during the same time period as used for the average burn rate. For carbon monoxide and carbon dioxide, these numbers represent the grams

of the compound produced per grams of fuel burned. On the other hand, the oxygen yield is the grams of oxygen consumed per grams of fuel burned.

Transient yields as a function of equivalence ratio are shown in Figures 5.4-5.6 for carbon monoxide, carbon dioxide, and oxygen, respectively. Each figure includes results from Tests #20 and #21 shown on separate plots. In addition to the transient values occurring in that particular test, steady-state values are also represented with an open triangle symbol to provide a comparison. In Figure 5.4, the carbon monoxide yield is observed to increase around an equivalence ratio of 0.5 in both tests. However, the rise is more gradual in Test #21 than in #20 and agreement with the steady-state values is good. Although, carbon monoxide production normally begins around an equivalence ratio of 1, this shift is not unexplained. Kinetic modelling performed by Gottuk has shown that carbon monoxide will "freeze out" at low equivalence ratios if the temperature is below 600C as is the case in these fires [24]. This shift also agrees with results obtained in Beyler's hood experiments [29]. In Figures 5.5 and 5.6, agreement between the transient and steady-state yields is again better for Test #21 than for #20 since the peak yields in Test #20 overshoot the steady-state values.

Steady-state yields for carbon monoxide, carbon dioxide and oxygen as a function of equivalence ratio are provided in Figures 5.7-5.9, respectively. Each figure includes a representation of the steady-state yield as well as the steady-state yield normalized by the maximum yield. On the normalized yield plots, correlations are included which were developed in Gottuk's compartment fire research [24]. These correlations were developed from experiments conducted with hexane, wood, polyurethane, and PMMA as the fuel source. The importance in developing correlations which are robust, i.e.

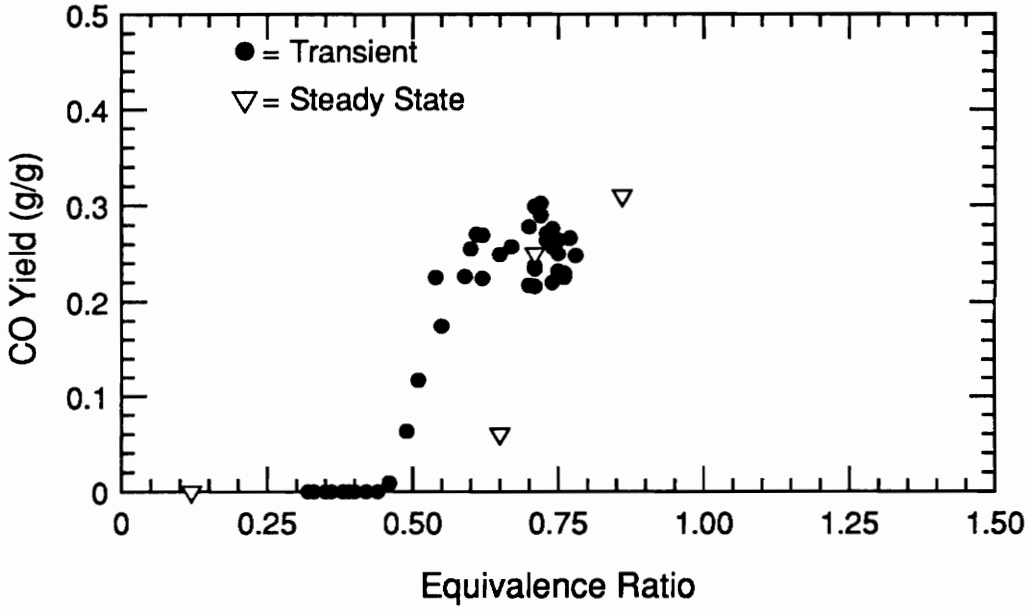

Test #20, 83.8 cm diameter Pan

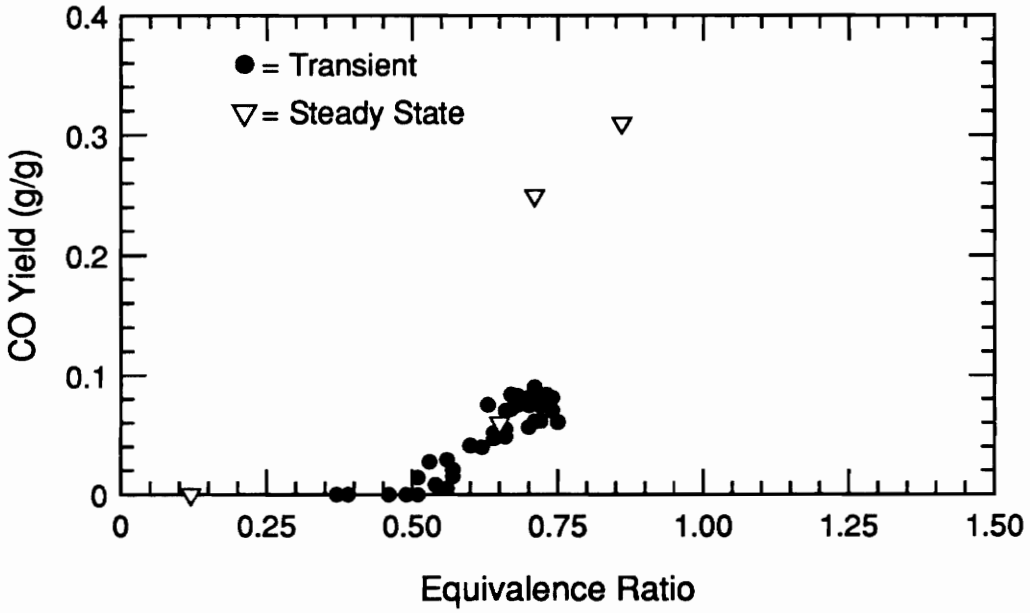

Test #21, 62.2 cm diameter Pan

Figure 5.4: Transient Carbon Monoxide Yields vs. Equivalence Ratio for Test #20 & #21: 83.8 cm diameter and 62.2 cm diameter Pans

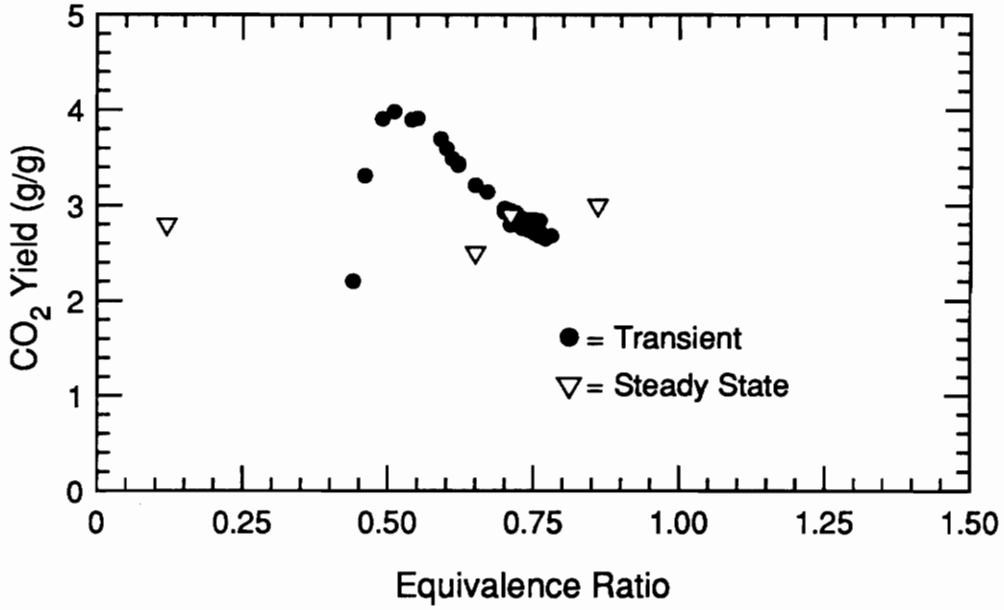

Test #20, 83.8 cm diameter Pan

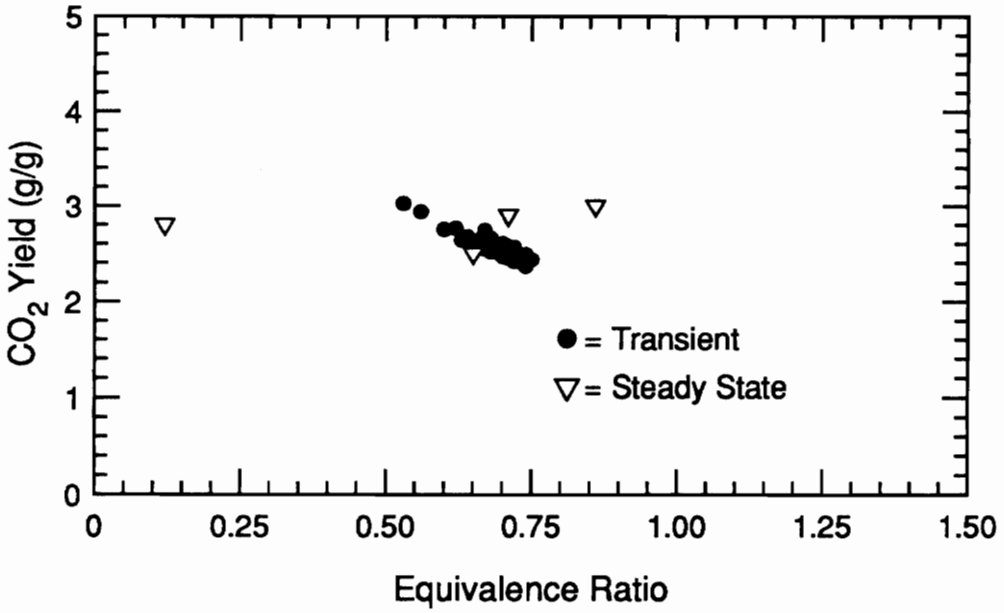

Test #21, 62.2 cm diameter Pan

Figure 5.5: Transient Carbon Dioxide Yields vs. Equivalence Ratio for Test #20 & #21: 83.8 cm diameter and 62.2 cm diameter Pans

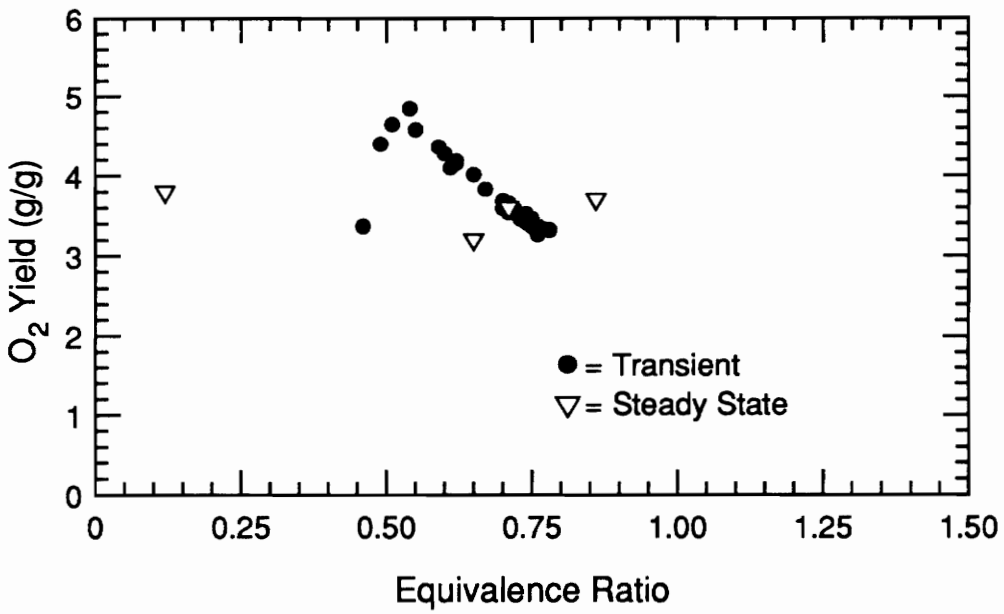

Test #20, 83.8 cm diameter Pan

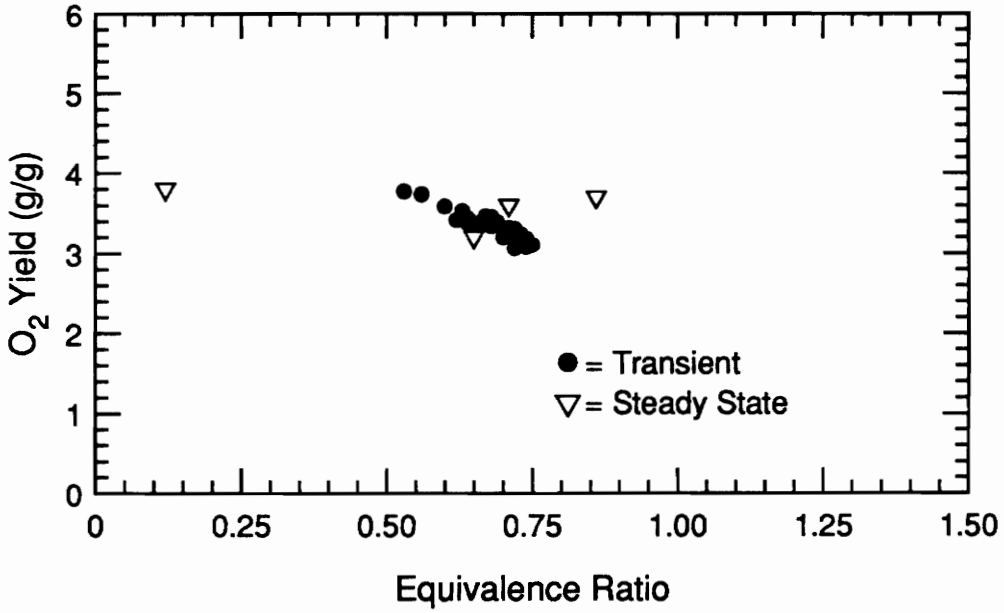

Test #21, 62.2 cm diameter Pan

Figure 5.6: Transient Oxygen Yields vs. Equivalence Ratio for Test #20 & #21: 83.8 cm diameter and 62.2 cm diameter Pans

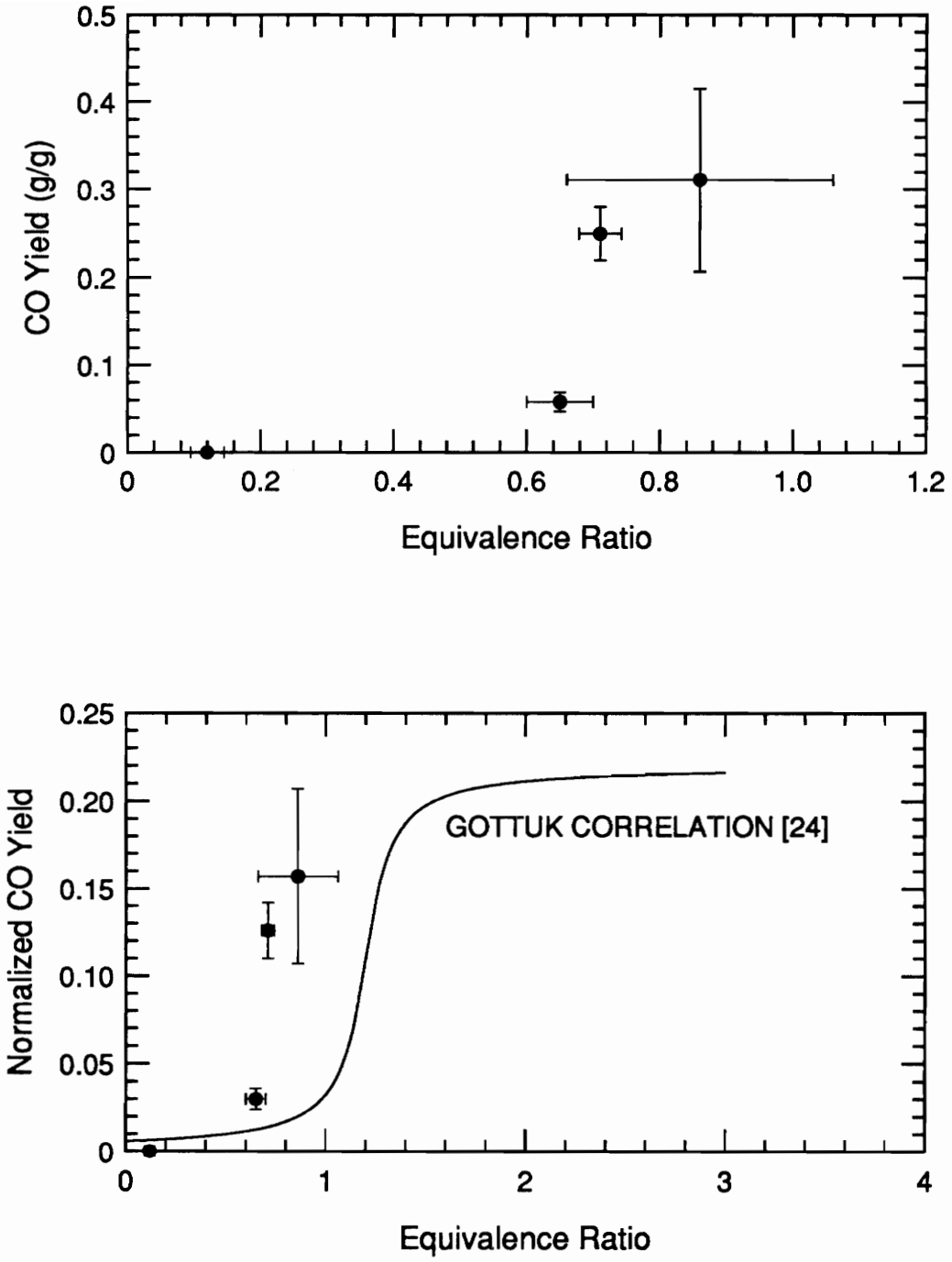

Figure 5.7: Steady-State Carbon Monoxide Yields, Unnormalized and Normalized, vs. Equivalence Ratio

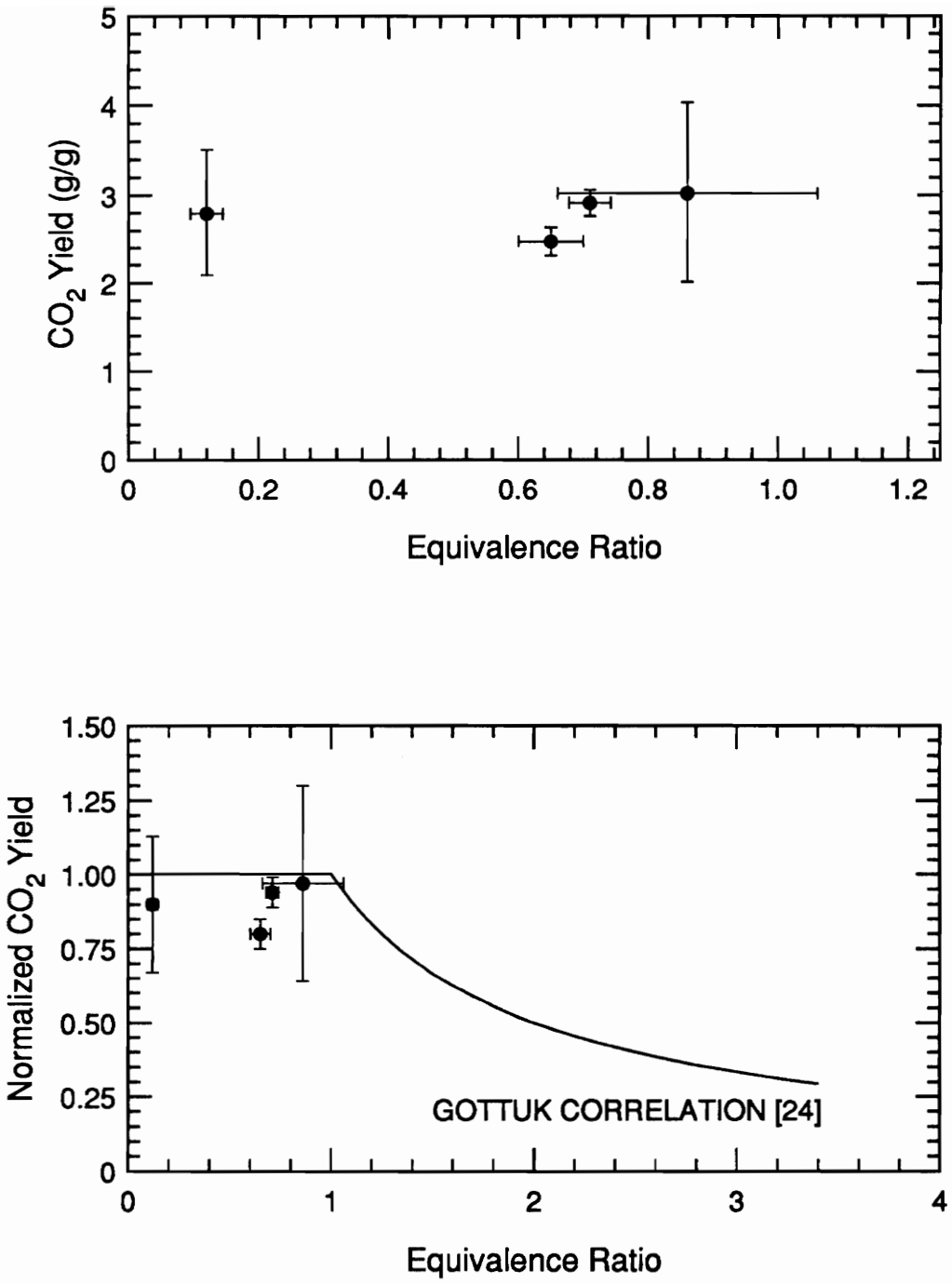

Figure 5.8: Steady-State Carbon Dioxide Yields, Unnormalized and Normalized, vs. Equivalence Ratio

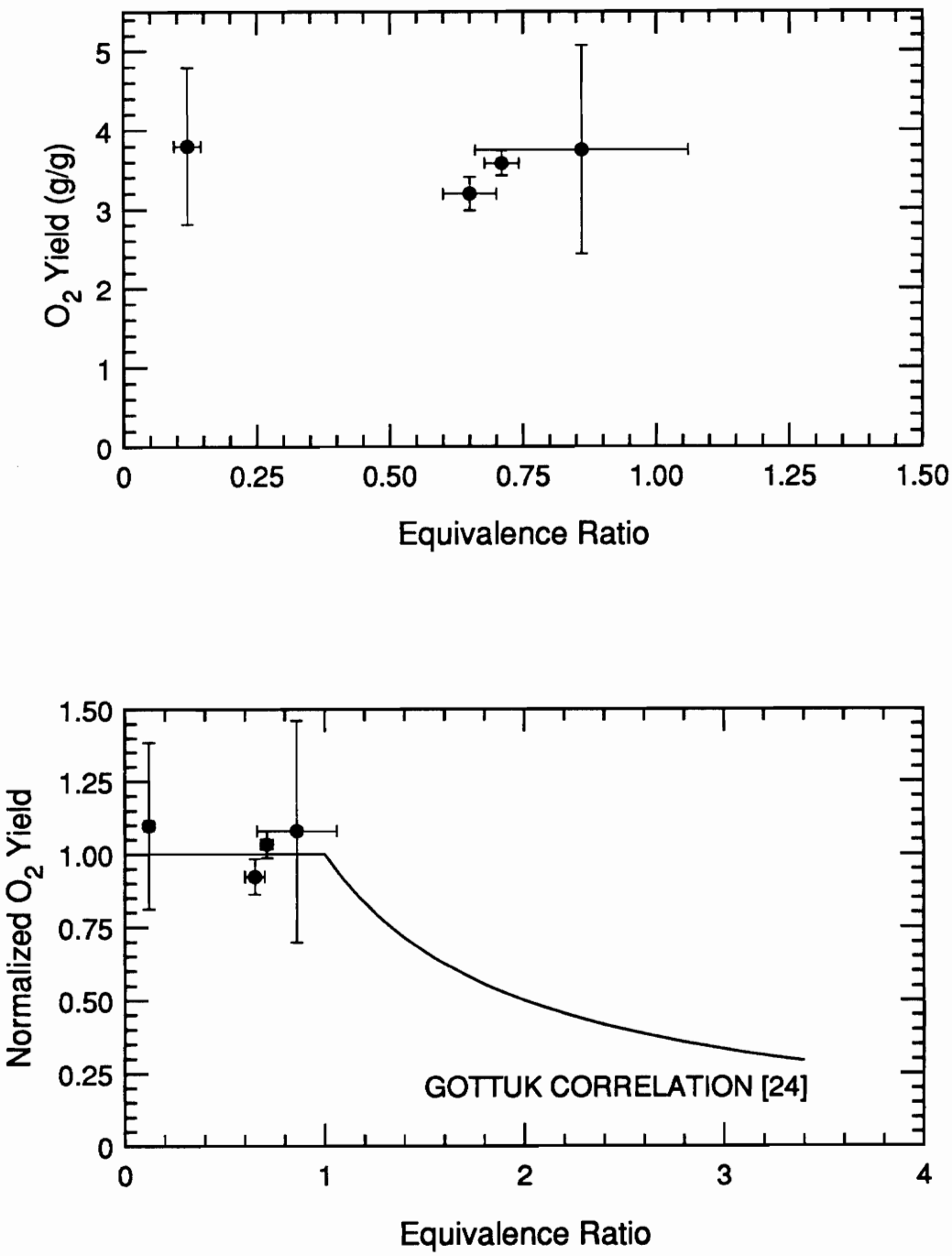

Figure 5.9: Steady-State Oxygen Yields, Unnormalized and Normalized, vs. Equivalence Ratio

independent of the fuel, lies in the fact that actual building fires have multiple fuel sources.

In Figure 5.7, the normalized carbon monoxide yields have the same shape as the correlation but are shifted to the left slightly. As described above, this is believed to be a result of the lower temperatures observed in the glovebox fires. Furthermore, agreement between the normalized carbon dioxide yields and the correlation is also good in Figure 5.8 as is the agreement seen for oxygen yields in Figure 5.9. Theoretically, carbon dioxide and oxygen normalized yields should have a value of 1 until an equivalence ratio of 1. Obviously, several of the points on Figure 5.8 exceed this value but the limits of error place them in a reasonable range.

These results indicate that correlations for exhaust species yields formulated from natural ventilation compartment fires may apply to compartment fires with overhead forced ventilation. Further validation of this thoery could greatly benefit fire modelling.

6. CONCLUSTIONS AND FUTURE RECOMMENDATIONS

6.1 Summary

Under sealed conditions, the glovebox was successful in containing exhaust gases. Full scale mockup tests demonstrated an important potential for a fire. However, fire conditions were near the limits for stable combustion as demonstarted by the fact that only one of the three tests resulted in a fire which fully depleted its fuel. Introducing additional sources of ventilation did not however provide for complete containment. In cases where gloves were removed, the fires could not sustain themselves but prior to extinction, expelled exhaust gases into the atmosphere. Removing a window, however, allowed enough air to support the fire to completion and provided a constant exhaust route for exhaust gases into the atmosphere, which constituted the largest containment loss occurring in these tests. Most importantly, even in tests where the flame was stable enough to consume all fuel, catastrophic failure did not occur and the fires never exhibited burning characteristics as severe as those seen in open burn experiments.

In addition to evaluating glovebox safety, important knowledge was gained about compartment fires with overhead forced ventilation. Contrary to what has been observed in tests conducted in this area previously, the fire environment observed in the current tests does not support a well-stirred reactor model. Furthermore, it does not support a two-zone model, but rather falls somewhere in between. In order to model these fires, a horizontal two-well-stirred reactors model is suggested. This system, explained further in Section 6.2, consists of an initial well-stirred reactor in the air inlet zone and a secondary well-stirred or possibly plug-flow reactor in the post flame zone.

Also, it was determined that fires with a fixed ventilation rate become less dangerous as a reduction in fuel surface area occurs. This conclusion is supported by the trends observed in smaller pan diameter experiments where burn rate, toxic species concentrations, and temperatures decreased with decreasing pan diameters. In contrast to these trends, the smoke yield and generation rate increased with decreasing pan diameters.

6.2 Proposed Zone Model

Neither a well-stirred reactor model nor two-zone system is appropriate for describing the fires observed in this study. Instead, a two-horizontal well-stirred reactor model is proposed for these tests. That is, there are two separate well-stirred reactors present in the box. Initially, air is fed into the compartment where it is immediately entrained into the plume, constituting the first reactor. Then, fuel rich exhaust gases are allowed to mix with the unreacted air and are oxidized thus resulting in a reduced oxygen concentration. Using this model satisfies the criteria imposed by the vertical temperature profiles and low oxygen concentrations.

6.3 Future Recommendations

It is clear that more experimental research needs to be devoted to forced ventilation fires, especially those with overhead forced ventilation. In order to properly assess whether the system is well-stirred or two-layer, vertical gas species concentrations should be measured. In addition, various compartment geometries should be investigated since this characteristic can have a serious impact on the fire behavior. Furthermore, it would be extremely beneficial to build the compartment so that the flame can be monitored.

This modification would allow for visual observations of a layer interface thus validating the existence or nonexistence of a two-layer system. More accurate information on flame stability would also be gained.

REFERENCES

1. Felt, R. E., "Burning and Extinguishing Characteristics of Plutonium Metal Fires," ISO-756, USAEC Report, August 1967.

2. Keski-Rahkonen, Olavi, "Breaking of Window Glass Close to Fire," *Fire and Materials*, **12**, pp. 61-69, 1988.

3. Emmons, H. W., "Window Glass Breakage by Fire," Home Fire Project Technical Report No. 77, Harvard University, 1988.

4. Pagni, P. J., "Fire Physics-Promises, Problems, and Problems," *Proceedings of the Second International Symposium on Fire Safety Science*, pp. 49-66, 1988.

5. Skelly, Michael J., "An Experimental Investigation of Glass Breakage in Compartment Fires," Master of Science Thesis, Virginia Polytechnic Institute and State University, February 1990.

6. Barth, P. K. and Sung, H., "Glass Fracture under Intense Heating," Senior course project, Harvard University, 1977.

7. Patterson, David E., "The Rocky Flats Fire," *Fire Journal*, **15(5)**, January 1970.

8. Williams, A. K., "Recent Improvements in Fire Suppression and Control for Glove-Box Operations At Rocky Flats," *Proceedings of 18th Conference on Remote Systems Technology*, 1970.

9. Erickson, E. D., "Prevention and Control of Glovebox Fires," Dow Chemical Co., Rocky Flats Div., Golden, CO, Report ME-3-69, July 1968

10. Factory Mutual Research Corporation, "Glovebox Fire Safety: A Guide for Safe Practices in Design, Protection and Operations," prepared for USAEC, FMRC Serial No. 17314, 1967.

11. Domning, W. E., "The Fire Test Facility at Rocky Flats - A Status Report," CRDL 950371-6, April 1970.

12. Domning, W. E. and Woodard, R. W., "Glovebox Fire Tests," RFP-1557, USAEC Report in publication, 1970.

13. Drysdale, Dougal, An Introduction to Fire Dynamics, John Wiley and Sons, New York, 1985.

14. Glassman, Irvin, Combustion, Academic Press, Inc., New York, 1987.

15. Beyler, C. L., "Analysis of Compartment Fires with Overhead Forced Ventilation," *Proceedings of the Third International Symposium on Fire Safety Science*, Elsevier Science Publishers, pp. 291-300, 1991.

16. Simmons, R. F., and Wolfhard, H. G., "Some Limiting Oxygen Concentrations for Diffusion Flames in Air Diluted with Nitrogen," *Combustion and Flame*,. **1**, pp. 155-161, 1952.

17. Beyler, C. L., "Flammability Limits of Premixed and Diffusion Flames," SFPE Handbook of Fire Protection Engineering, 1st Ed., Philip DiNenno, Editor-in-Chief, NFPA, Quincy, MA, 1988.

18. National Fire Protection Association, Fire Protection Handbook, Cote, A.E., editor-in-chief, 17th edition, 1991.

19. Alvares, N. J., Foote, K. L. and Pagni, P. J., "Forced Ventilated Enclosure Fires," *Combustion Science and Technology*, 39, pp. 55-81, 1984.

20. Foote, K. L., Pagni, P. J., and Alvares, N. J., "Temperature Correlations for Forced-Ventilated Compartment Fires," *Proceedings of the First International Symposium on Fire Safety Science*, Hemisphere Publishing Corp., New York, pp. 139-148,1985.

21. Backovsky, J., Foote, K. L. and Alvares, N. J., "Temperature Profiles in Forced-Ventilation Enclosure Fires," *Second International Symposium on Fire Safety Science*, Hemisphere Publishing Corp., New York, pp. 315-324, 1989.

22. Deal, S. and Beyler, C., "Correlating Preflashover Room Fire Temperatures," *Journal of Fire Protection Engineering*, 2(2), pp. 33-48, 1990.

23. ASME Research Committee on Fluid Meters, Edited by Howard S. Bean, Fluid Meters: Their Theory and Application, 6th Edition, 1971.

24. Gottuk, D. T., "Generation of Carbon Monoxide in Compartment Fires," Ph.D. dissertation, Virginia Polytechnic Institute and State University, September 1992.

25. Newman, J. S. and Croce, P. A., "A Simple Aspirated Thermocouple for Use in Fires," *Journal of Fire and Flammability*, **10**, pp. 326-336, October 1979.

26. Santoro, R. J., Semerjian, H. G., and Dobbins, R. A., "Interpretation of Optical Measurements of Soot in Flames," *AIAA 18th Thermophysics Conference*, AIAA-83-1516, 1983.

27. Eckbreth, Alan C., Laser Diagnostics for Combustion Temperature and Species, Abacus Press, Cambridge, MA, 1988.

28. Tewarson, A., "Generation of Heat and Chemical Compounds in Fires," SFPE Handbook of Fire Protection Engineering, 1st Ed., Philip DiNenno, Editor-in-Chief, NFPA, Quincy, MA, 1988.

29. Beyler, C. L., "Major Species Production by Diffusion Flames in a Two-layer Compartment Fire Environment," *Fire Safety Journal*, **10**, pp. 47-56, 1986.

APPENDIX A

This appendix provides the shop drawings detailing glovebox panel construction.

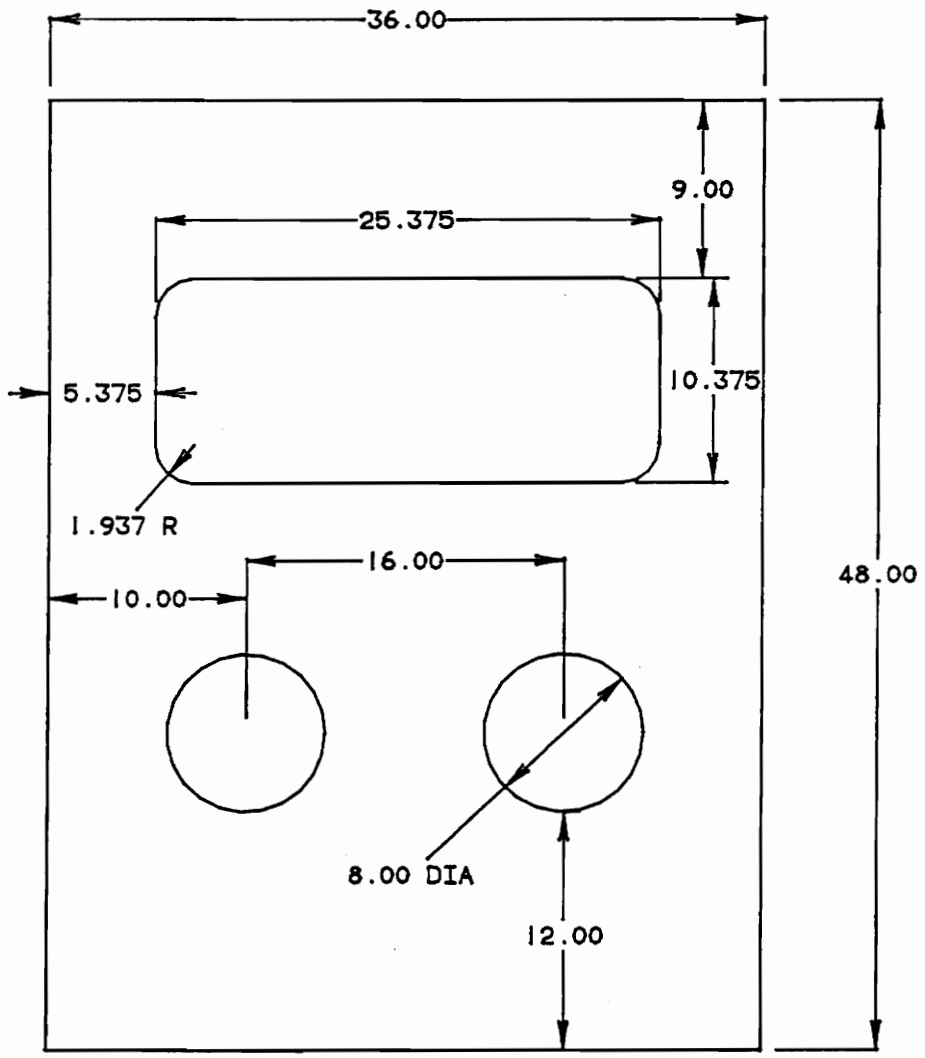

FRONT GLOVEBOX PANELS

DIMENSIONS IN INCHES WITH 1/8" TOLERANCE
MATERIAL: 1/8" STEEL

Figure A.1: Shop Drawing of Front Glovebox Panel

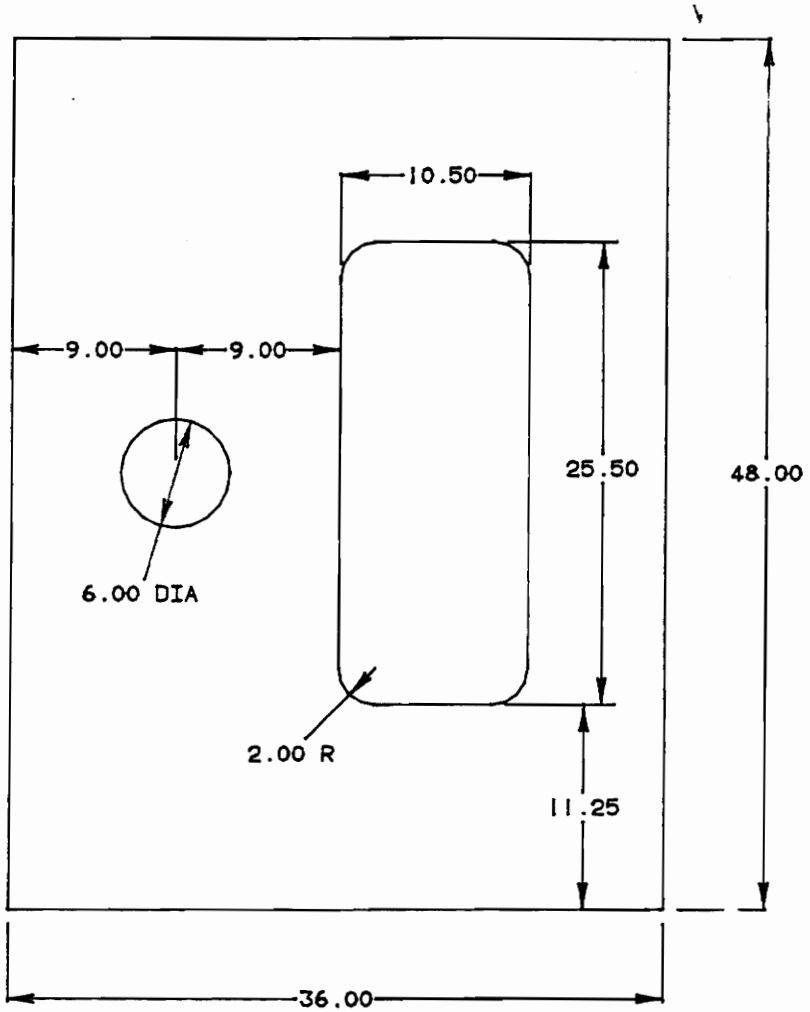

GLOVE BOX OUTSIDE CEILING PANELS

MATERIAL: 1/8" STEEL

DIMENSIONS IN INCHES WITH 1/8" TOLERANCE

Figure A.2: Shop Drawing of Outer Ceiling Glovebox Panel

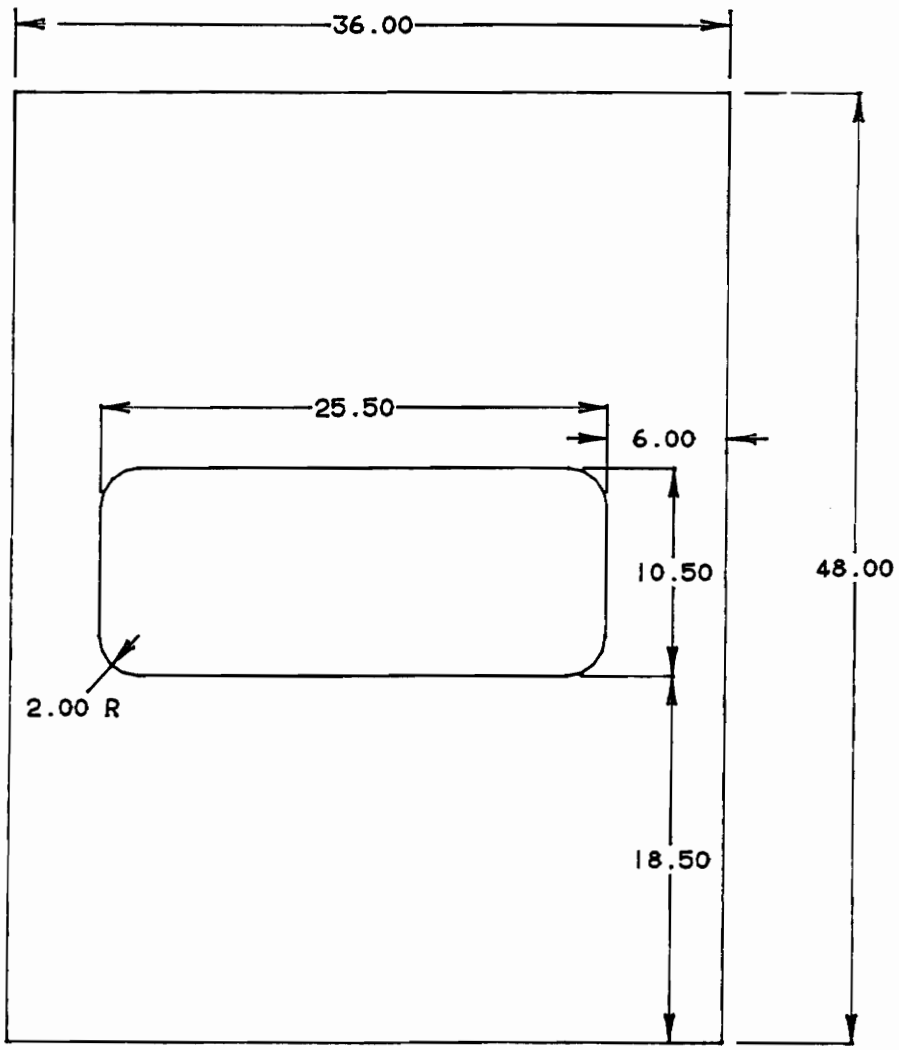

Figure A.3: Shop Drawing of Inner Ceiling Glovebox Panel

APPENDIX B

This appendix includes drawings from Rocky Flats for window gaskets.

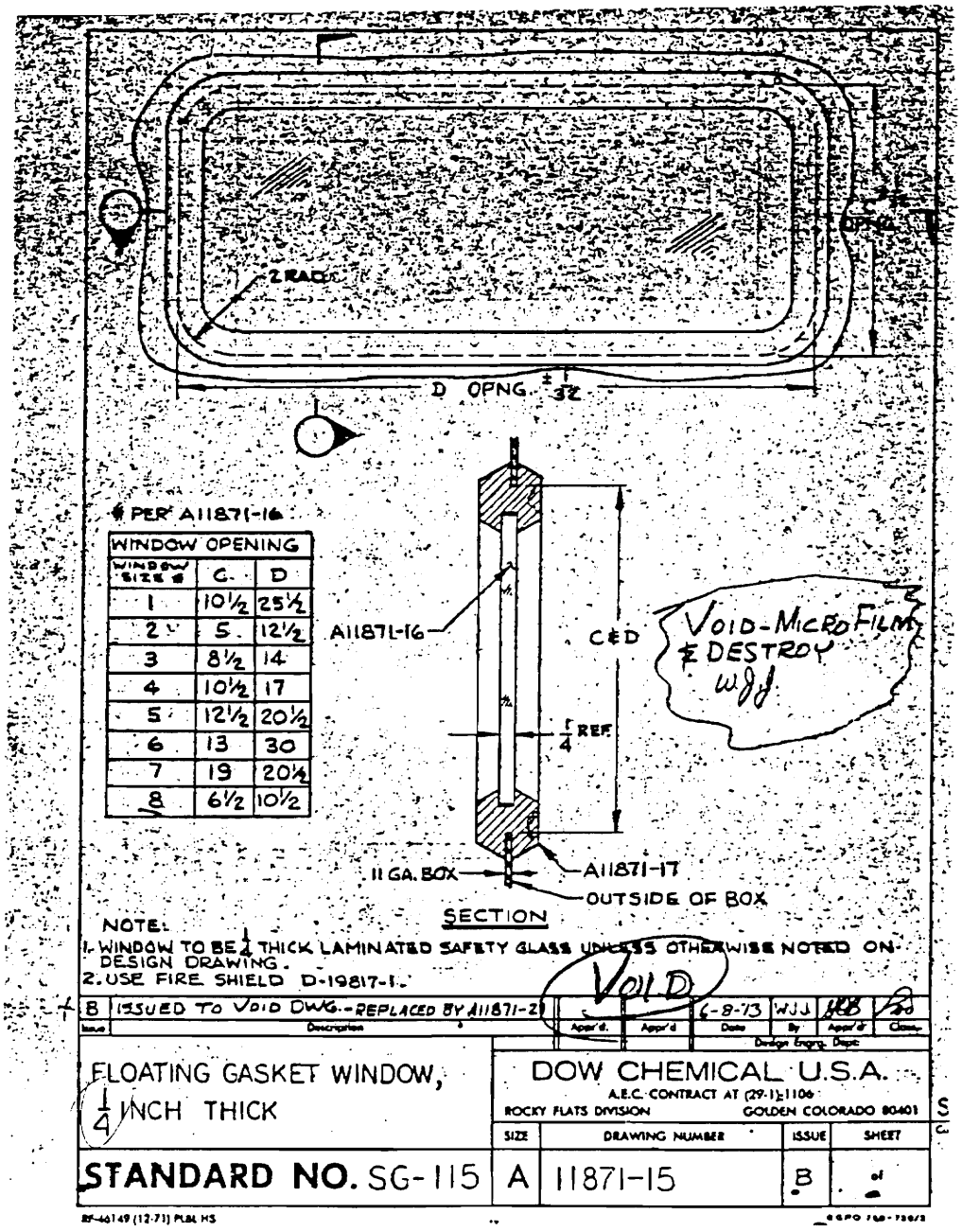

Figure B.1: Ceiling Panel Window Gasket Specifications

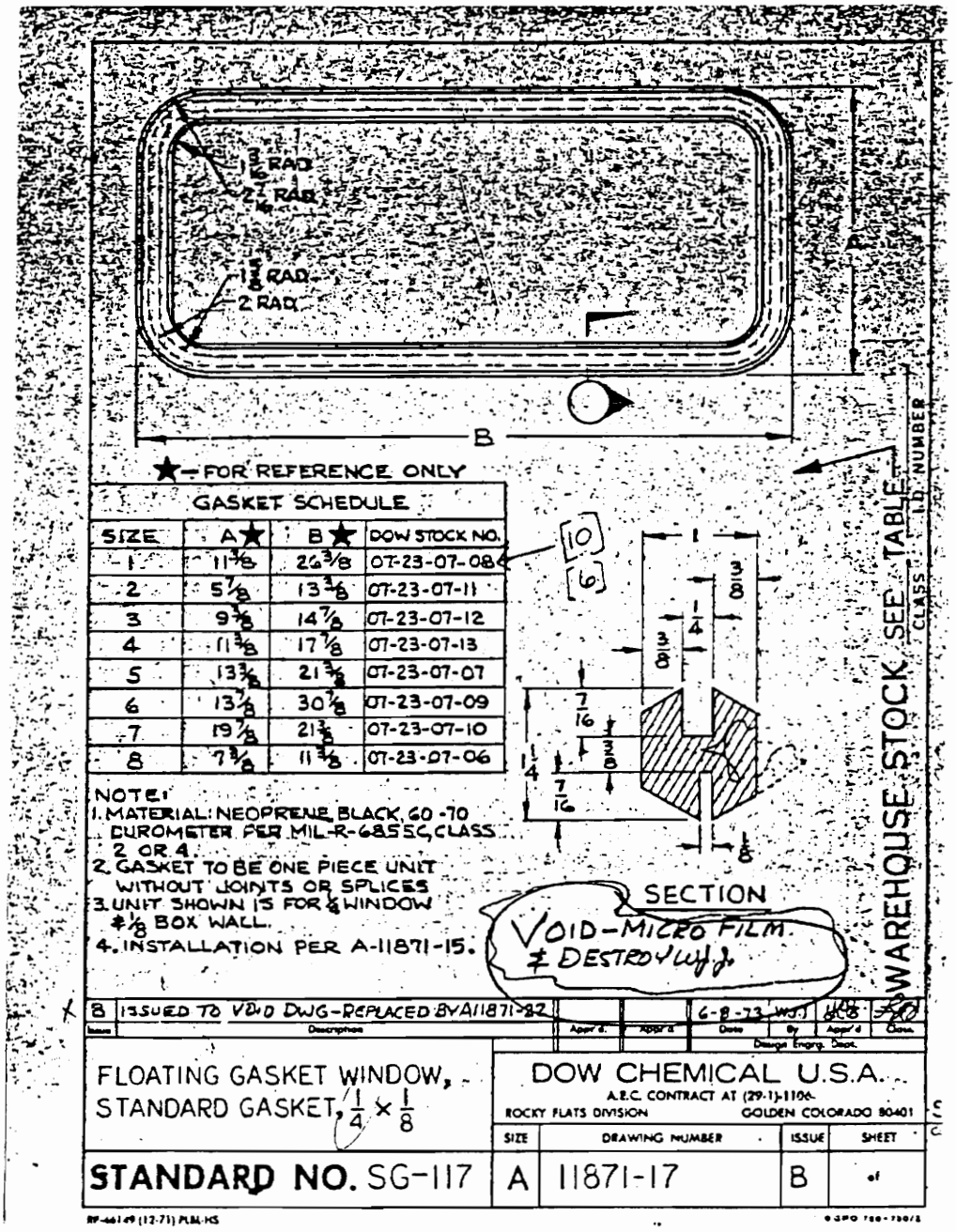

Figure B.2: Ceiling Panel Window Gasket Specifications

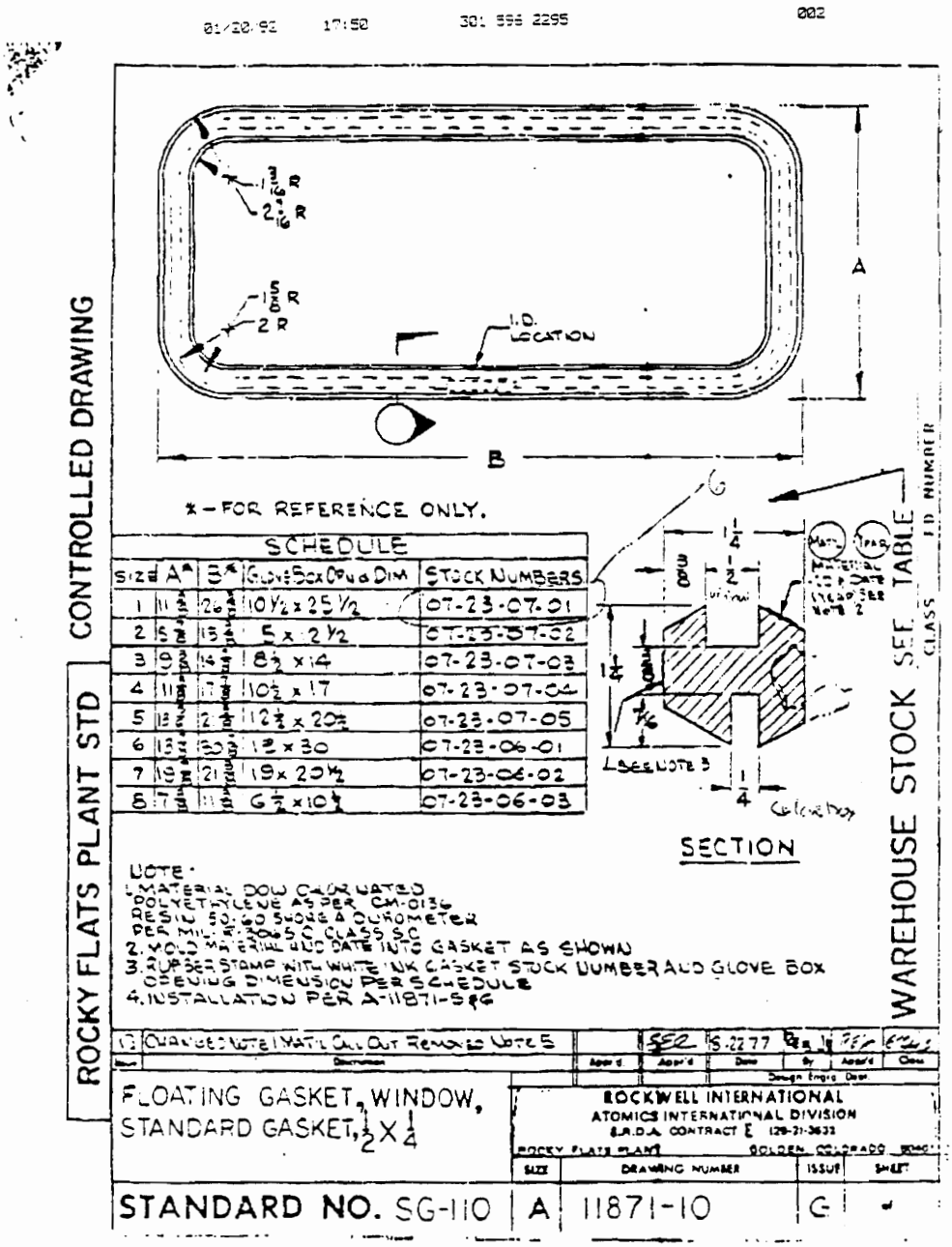

Figure B.3: Front Panel Window Gasket Specifications

APPENDIX C

This appendix includes the blower curve specifications for the Dayton High Pressure, Direct-Drive Blower.

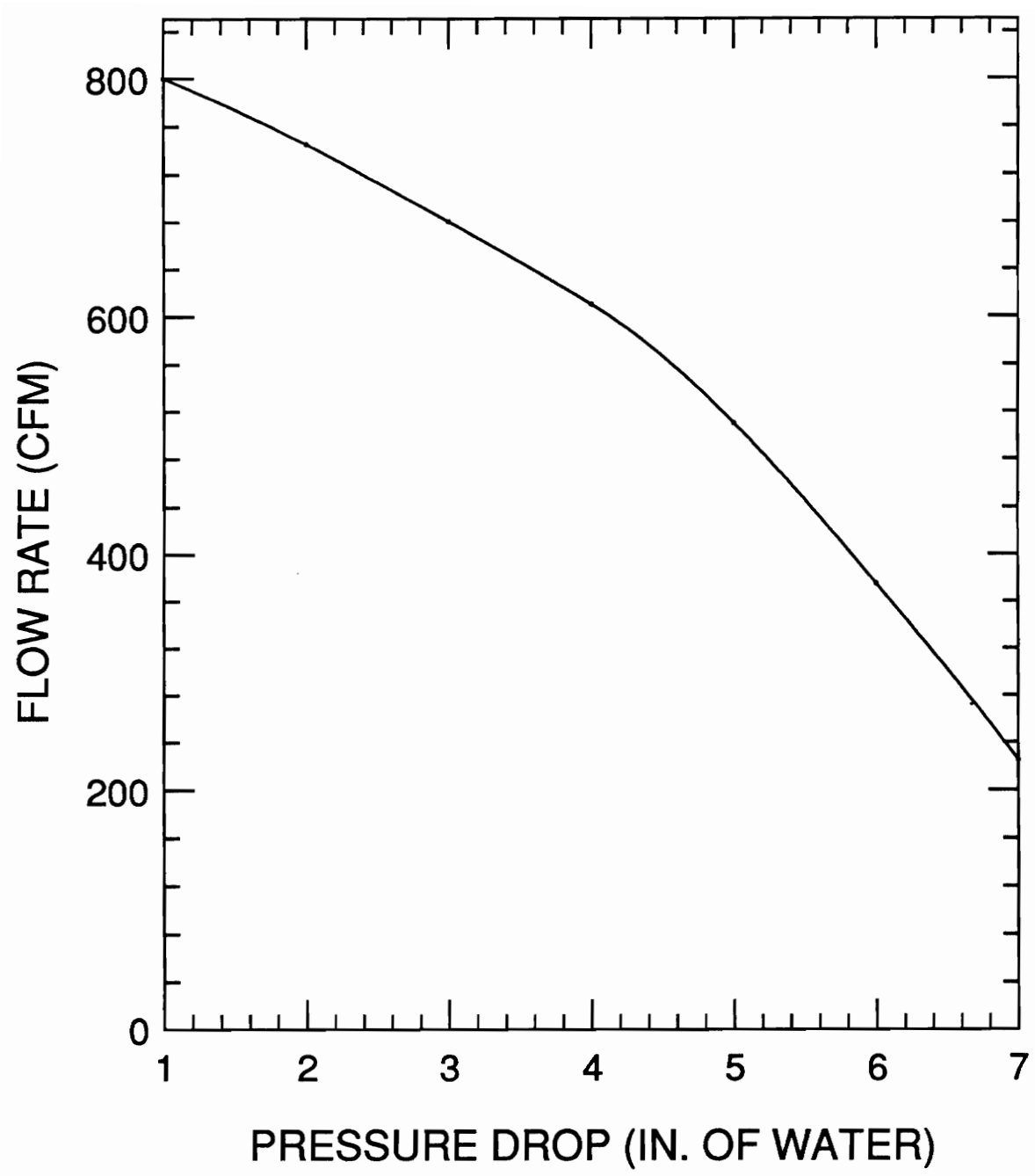

Figure C.1: Performance Curve for Dayton High Pressure, Direct Drive Blower

APPENDIX D

This appendix includes a sample calibration curve for a Medtherm heat flux transducer.

Figure D.1: Calibration Curve for Medtherm Heat Flux Transducer

APPENDIX E

This appendix includes a sample listing of the data acquisition program used.

```
1 DECLARE FUNCTION MEASURE.VOLTS% CDECL (BYVAL CHANNEL%, SEG VOLTS!)
2 DECLARE FUNCTION VOLTS.TO.DEGREES% CDECL (BYVAL TC.TYPE%, SEG VOLTS!,
      SEG DEGREES.C!)
3 DECLARE FUNCTION SELECT.BOARD% CDECL (BYVAL BOARD%)
4 DECLARE FUNCTION ADC.VALUE CDECL (BYVAL CHANNEL%, BYVAL GAIN%, SEG
      ANALOG%)
6 DECLARE FUNCTION ANALOG.TO.VOLTS% CDECL (BYVAL ANALOG%, BYVAL GAIN%,
      SEG VOLTS!)
7 DECLARE FUNCTION MEASURE.THERMOCOUPLE% CDECL (BYVAL TC.TYPE%,
      BYVAL CHANNEL%, SEG DEGREES.C!)
10 DIM DATARRAY(41)
11 CLS
12 PRINT
13 PRINT "GLOVE BOX DATA ACQUISITION PROGRAM UPDATED AS OF 5/5/92."
14 PRINT
15 INPUT "ENTER FILE NAME: ",FILE$
16 INPUT "PRESS ENTER TO BEGIN DATA ACQUISITION.",DUMMY$
17 CLS
18 PRINT "FILE NAME: ";FILE$
19 PRINT "    BOARD 1                    BOARD 2        BOARD 3          BOARD 4"
90 CHANNEL%=0:STATUS%=0:VOLTS!=0:DEGREES.C!=15.1:TC.TYPE%=75
95 ANALOG%=0:GAIN%=0
100 DELTIME!=0:TIME!=0:TIME1!=0:N=0
101 OPEN FILE$ FOR APPEND AS #1
104 X$=INKEY$
106 IF X$="S" THEN GOTO 800
108 IF X$="s" THEN GOTO 800
109 TIME!=TIME!+DELTIME!
110 PRINT "  "
111 PRINT "TIME = ";TIME!
120 TIME1!=TIMER
130 DATARRAY(1)=TIME!
140 BOARD%=1
```

```
141 STATUS%=SELECT.BOARD%(BOARD%)
142 GAIN% = 2
150 FOR CHANNEL%=0 TO 4
155 STATUS%=ADC.VALUE(CHANNEL%,GAIN%,ANALOG%)
156 STATUS%=ANALOG.TO.VOLTS(ANALOG%,GAIN%,VOLTS!)
158 VOLTS!=VOLTS!/2
160 DATARRAY(CHANNEL%+2)=VOLTS!
165 LOCATE 5+CHANNEL%,5
170 PRINT USING "##";CHANNEL%;:PRINT " ";:PRINT USING "##.###";VOLTS!
175 NEXT
220 FOR CHANNEL%=5 TO 7
225 STATUS%=MEASURE.VOLTS%(CHANNEL%,VOLTS!)
233 VOLTS!=VOLTS!*1000
235 DATARRAY(CHANNEL%+2)=VOLTS!
240 LOCATE 5+CHANNEL%,5
245 PRINT USING "##";CHANNEL%;:PRINT " ";:PRINT USING "##.###";VOLTS!
250 NEXT
255 BOARD%=2
260 STATUS%=SELECT.BOARD%(BOARD%)
269 FOR CHANNEL%=0 TO 15
270 STATUS%=MEASURE.VOLTS%(CHANNEL%,VOLTS!)
275 VOLTS!=VOLTS!/100
300 STATUS%=VOLTS.TO.DEGREES%(TC.TYPE%,VOLTS!,DEGREES.C!)
303 VOLTS!=VOLTS!/2
305 DATARRAY(10+CHANNEL%)=DEGREES.C!
310 LOCATE 5+CHANNEL%,20
315 PRINT USING "##";CHANNEL%;:PRINT " ";:PRINT USING "####.##";DEGREES.C!
320 NEXT
340 BOARD%=3
345 STATUS%=SELECT.BOARD%(BOARD%)
350 FOR CHANNEL%=1 TO 7
355 STATUS%=MEASURE.THERMOCOUPLE%(TC.TYPE%,CHANNEL%,DEGREES.C!)
380 DATARRAY(24+CHANNEL%)=DEGREES.C!
390 LOCATE 5+CHANNEL%,37
```

```
400 PRINT USING "##";CHANNEL%;:PRINT " ";:PRINT USING "####.##";DEGREES.C!
405 NEXT
450 BOARD%=4
455 STATUS%=SELECT.BOARD%(BOARD%)
460 CHANNEL%=4
470 STATUS%=MEASURE.THERMOCOUPLE%(TC.TYPE%,CHANNEL%,DEGREES.C!)
475 DATARRAY(28+CHANNEL%)=VOLTS!
480 LOCATE 5+CHANNEL%,57
490 PRINT USING "##";CHANNEL%;:PRINT " ";:PRINT USING "####.##";DEGREES.C!
500 FOR CHANNEL%=5 TO 7
510 STATUS%=MEASURE.VOLTS%(CHANNEL%,VOLTS!)
520 DATARRAY(28+CHANNEL%)=VOLTS!
530 LOCATE 5+CHANNEL%,57
550 PRINT USING "##";CHANNEL%;:PRINT " ";:PRINT USING "####.###";VOLTS!
555 NEXT
625 FOR N=1 TO 35
630 WRITE #1,DATARRAY(N)
635 NEXT N
640 X$=INKEY$
650 IF X$="S" THEN GOTO 800
655 IF X$="s" THEN GOTO 800
660 DELTIME!=TIMER-TIME1!
665 IF DELTIME!>=(1.95#) THEN GOTO 104
670 GOTO 660
675 CLOSE #1
800 PRINT "ELAPSED TIME = ";TIME! "seconds."
810 END
```

APPENDIX F

This appendix includes sample FORTRAN programs used for data reduction.

```
$debug
C    PROGRAM *5EXH.FOR* REDUCES THE EXPERIMENTAL DATA FROM THE FILE
C    CREATED BY PROGRAM -BOX03.EXE-   UPDATED AS OF 7-13-92 MJP
C
C         ***** PROGRAM TO CALCULATE MDOT FUEL FROM WET EXHAUST
C              CONCS. FOR GLOV20 AND GLOV22
C
$LARGE
      IMPLICIT REAL*8(A-H,O-X)
      DIMENSION TIME(1700),DRYCO(1700),DRYCO2(1700),DRYO2(1700)
      DIMENSION FUEL(1700),VFUEL(1700),DELPD(1700)
      DIMENSION FUELRATE(1700),FID(1700),TC(9,1700)
      DIMENSION A(4,4),B(4),X(4)
      CHARACTER*7 FNAME,FANAME
      INTEGER Y,Z
C
C     INPUT RUN PARAMETERS
C
      WRITE(*,*) 'ENTER FILE NAME'
      READ(*,15) FANAME
      WRITE(*,*) 'ENTER OUTPUT FILE NAME (7CHAR)'
      READ(*,15) FNAME
   15 FORMAT(A7)
      WRITE(*,*) 'ENTER PAN WEIGHT'
      READ(*,16) PAN
      WRITE(*,*) 'ENTER NUMBER OF POINTS TO AVERAGE FUELRATE'
      READ(*,17) N
      WRITE(*,*) 'ENTER NUMBER OF POINTS TO SKIP'
      READ(*,17) M
      WRITE(*,*) 'ENTER SPAN CALIBRATION FOR FID'
      READ(*,18) SFID
      WRITE(*,*) 'ENTER ZERO CALIBRATION FOR FID'
      READ(*,18) ZFID
      WRITE(*,*) 'ENTER 1 IF YOU WANT TO APPROX. ORIFICE TEMP'
```

```
      READ(*,14) NTC
   14 FORMAT(I1)
   18 FORMAT(F4.0)
   17 FORMAT(I2)
   16 FORMAT(F5.2)
      WRITE(*,*) 'KICK BACK AND DRINK A BEER'
C     ASSIGN CONSTANTS FOR GAS ANALYZERS---FOR RANGE 3!
      O2CONSTANT=100.0
      O2GAS=.02*4.74

      COCONSTANT=100.
      CORANGE=10.
      COGAS=0.9*CORANGE*.02

      CO2CONSTANT=100.
      CO2RANGE=20.
      CO2GAS=.9*CO2RANGE*.02
C
C     I IS THE NUMBER OF DATA POINTS PER CHANNEL
      I=1
C     J IS THE ARRAY COUNTER
      J=1
C
C     INPUT FILE AND CREATE AN ARRAY FOR EACH CHANNEL
C
      OPEN(5,FILE=FANAME)
   10     READ(5,*,END=11) ATIME
          READ(5,*) ADRYCO
          READ(5,*) ADRCO2
          READ(5,*) ADRYO2
          READ(5,*) AFUEL
          READ(5,*) DUM1
          READ(5,*) AFID
          READ(5,*) ASMKZE
```

```
READ(5,*) ASMOKE
READ(5,*) ATC1
READ(5,*) ATC2
READ(5,*) ATC3
READ(5,*) ATC4
READ(5,*) ATC5
READ(5,*) ATC6
READ(5,*) ATC7
READ(5,*) ATC8
READ(5,*) ATC9
READ(5,*) ATC10
READ(5,*) ATC11
READ(5,*) ATC12
READ(5,*) ATC13
READ(5,*) DUM2
READ(5,*) DUM3
READ(5,*) ATC14
READ(5,*) ARAD3
READ(5,*) ARAD1
READ(5,*) ARAD2
READ(5,*) ADELPD

IF (MOD(I,M).EQ.0) THEN

TIME(J) = ATIME
DRYCO(J) = ADRYCO
DRYCO2(J) = ADRCO2
DRYO2(J) = ADRYO2
VFUEL(J) = AFUEL
FID(J) = AFID
DELPD(J) = ADELPD
TC(9,J) = ATC9
TC(4,J) = ATC4
```

```
                J=J+1
        ENDIF
        I=I+1
        GOTO 10
 11 CONTINUE
   CLOSE (5)

   I=I-1
   J=J-1
C
C  CALCULATE GAS CONC., FUELRATE, HEAT FLUXES
C

 20 FNAME(7:7) = CHAR(80)
   OPEN(UNIT=6, FILE = FNAME, STATUS='NEW')

        DO 23 K=1,J
   DRYCO(K)=DRYCO(K)*CORANGE/5.0
   DRYCO2(K)=DRYCO2(K)*CO2RANGE/5.0
   DRYO2(K)=DRYO2(K)*22./5.08
C  CALCULATE FUELRATE
          FUEL(K) = ((VFUEL(K)-1.)*150./4.)-PAN
 23 CONTINUE

   DO 47 K=2,J
        IF (FUEL(K+1).GT.FUEL(K)) THEN
          FUEL(K) = (FUEL(K+1)+FUEL(K-1))/2.
        ENDIF
 47 CONTINUE
   DO 77 K=1,N
        FUELRATE(K)=(FUEL(1)-FUEL(K+N))/(TIME(K+N)-TIME(1))
 77 CONTINUE

   DO 78 K=J-N+1,J
```

```
        FUELRATE(K)=(FUEL(K-N)-FUEL(J))/(TIME(J)-TIME(K-N))
 78 CONTINUE

    DO 27 K=N+1,J-N
        FUELRATE(K)=(FUEL(K-N)-FUEL(K+N))/(TIME(K+N)-TIME(K-N))
 27 CONTINUE

    DO 24 K=1,J
    Q = FUELRATE(K)*46000.
      IF (NTC.EQ.1) THEN
      DENSITY = (94.657/((TC(9,K)+273.15)*0.287))
      ELSE
      DENSITY = (94.657/((TC(9,K)+273.15)*0.287))
    ENDIF

    AIRRATE= (0.6883*(0.0762**2.)*(DELPD(K)*1333.3)**.5*
   $DENSITY**(-.5))*2118.8
    AIRPHI = AIRRATE/2118.8*DENSITY

    UHC = 47100./(SFID-ZFID) * FID(K)*1000.
    DENOM = 1+(1.08*DRYCO2(K))/100.
    WETCO = DRYCO(K)/DENOM
    WETCO2 = DRYCO2(K)/DENOM
    WETO2 = DRYO2(K)/DENOM

    PHI = (FUELRATE(K)/AIRPHI)*15.
C  INPUT MATRICES

    A(1,1) =    .285*WETCO - 18.
    A(1,2) =    1.-(WETCO/200.)
    A(1,3) =    -WETCO/200.
    A(1,4) =    2.-(.02*WETCO)
    A(2,1) =    .285*WETCO2
    A(2,2) =    -1.-(WETCO2/200.)
```

```
A(2,3) =     -WETCO2/200.
A(2,4) =     -.02*WETCO2
A(3,1) =     .285*WETO2+9.
A(3,2) =     .5-.005*WETO2
A(3,3) =     .5-.005*WETO2
A(3,4) =     -1.-(.02*WETO2)
A(4,1) =     (28.5/1000000.)*UHC
A(4,2) =     -UHC/2000000.
A(4,3) =     -UHC/2000000.
A(4,4) =      -1.-(2.*UHC/1000000.)

B(1)= -1.0434*WETCO
B(2) = -1.0434*WETCO2
B(3) = 27.75-(1.0434*WETO2)
B(4) = -.00010434*UHC

DO 4 Y=1,3
    DO 3 I=Y+1,4
     XMULT=A(I,Y)/A(Y,Y)
      DO 2 J=Y+1,4
      A(I,J)=A(I,J)-XMULT*A(Y,J)
2 CONTINUE
    A(I,Y)=XMULT
 B(I)=B(I)-XMULT*B(Y)
3 CONTINUE
4 CONTINUE
 X(4)=B(4)/A(4,4)
 DO 6 I=3,1,-1
    SUM=B(I)
     DO 5 J=I+1,4
       SUM=SUM-A(I,J)*X(J)
5 CONTINUE
    X(I)=SUM/A(I,I)
6 CONTINUE
```

```
      PHIEX=X(1)

      FDOT = (PHIEX/15.)*AIRPHI
      QEX = FDOT*46000.

C   CREATE OUPUT FILE

      WRITE(6,26)TIME(K),WETCO,WETCO2,WETO2,FID(K),X(1),FDOT,QEX
   26 FORMAT(F7.2,3F7.2,F8.4,2F9.5,F6.1)
   24 CONTINUE
      CLOSE(6)

      STOP
      END
```

```
$debug

C    PROGRAM *5REDCON.FOR* REDUCES THE EXPERIMENTAL DATA FROM THE FILE
C    CREATED BY PROGRAM -BOX03.EXE-   UPDATED AS OF 7-02-92 MJP
C
C          WRITTEN TO USE WITH DATA OBTAINED FROM GLOVE BOX
C             EXPERIMENTS (4th TEST SET).
C
$LARGE
     IMPLICIT REAL*8(A-H,O-Z)
     DIMENSION TIME(1700),DRYCO(1700),DRYCO2(1700),DRYO2(1700)
     DIMENSION FUEL(1700), FID(1700),TC(14,1700)
     DIMENSION RAD1(1700),RAD2(1700),RAD3(1700)
     DIMENSION SMOKE(1700), DELPD(1700), VFUEL(1700)
     DIMENSION SMOKEZ(1700)
     DIMENSION FUELRATE(1700)
     CHARACTER*7 FNAME,FANAME,FBNAME,FCNAME
C
C    INPUT RUN PARAMETERS
C
     WRITE(*,*) 'ENTER FIRST FILE NAME'
     READ(*,15) FANAME
     WRITE(*,*) 'ENTER OUTPUT FILE NAME (7CHAR)'
     READ(*,15) FNAME
   15 FORMAT(A7)
     WRITE(*,*) 'ENTER PAN WEIGHT'
     READ(*,16) PAN
     WRITE(*,*) 'ENTER 1 IF 62 CM PAN, 2 IF 28 CM PAN'
     READ(*,14) NSIZE
     WRITE(*,*) 'ENTER NUMBER OF POINTS TO AVERAGE FUELRATE'
     READ(*,17) N
     WRITE(*,*) 'ENTER NUMBER OF POINTS TO SKIP'
     READ(*,17) M
     WRITE(*,*) 'ENTER SPAN CALIBRATION FOR FID'
```

```
      READ(*,18) SFID
      WRITE(*,*) 'ENTER ZERO CALIBRATION FOR FID'
      READ(*,18) ZFID
      WRITE(*,*) 'ENTER 1 IF ORIFICE TC NEEDS TO BE ESTIMATED'
      READ(*,14) NTC
   14 FORMAT(I1)
   18 FORMAT(F4.0)
   17 FORMAT(I3)
   16 FORMAT(F5.2)
      WRITE(*,*) 'KICK BACK AND DRINK A BEER'

C  ASSIGN CONSTANTS FOR GAS ANALYZERS---FOR RANGE 3!

      O2CONSTANT=100.0
      O2GAS=.02*4.74

      COCONSTANT=100.
      CORANGE=10.
      COGAS=0.9*CORANGE*.02

      CO2CONSTANT=100.
      CO2RANGE=20.
      CO2GAS=.9*CO2RANGE*.02
C
C     I IS THE NUMBER OF DATA POINTS PER CHANNEL
      I=1
C  J IS THE ARRAY COUNTER
      J=1
C
C     INPUT FILE AND CREATE AN ARRAY FOR EACH CHANNEL
C
      OPEN(5,FILE=FANAME)
   10    READ(5,*,END=11) ATIME
         READ(5,*) ADRYCO
```

```
READ(5,*) ADRCO2
READ(5,*) ADRYO2
READ(5,*) AFUEL
READ(5,*) DUM1
READ(5,*) AFID
READ(5,*) ASMKZE
READ(5,*) ASMOKE
READ(5,*) ATC1
READ(5,*) ATC2
READ(5,*) ATC3
READ(5,*) ATC4
READ(5,*) ATC5
READ(5,*) ATC6
READ(5,*) ATC7
READ(5,*) ATC8
READ(5,*) ATC9
READ(5,*) ATC10
READ(5,*) ATC11
READ(5,*) ATC12
READ(5,*) ATC13
READ(5,*) DUM2
READ(5,*) DUM3
READ(5,*) ATC14
READ(5,*) ARAD3
READ(5,*) ARAD1
READ(5,*) ARAD2
READ(5,*) ADELPD

IF (MOD(I,M).EQ.0) THEN

TIME(J) = ATIME
DRYCO(J) = ADRYCO
DRYCO2(J) = ADRCO2
DRYO2(J) = ADRYO2
```

```
        VFUEL(J) = AFUEL
        FID(J) = AFID
        SMOKEZ(J) = ASMKZE
        SMOKE(J) = ASMOKE
        TC(1,J) = ATC1
        TC(2,J) = ATC2
        TC(3,J) = ATC3
        TC(4,J) = ATC4
        TC(5,J) = ATC5
        TC(6,J) = ATC6
        TC(7,J) = ATC7
        TC(8,J) = ATC8
        TC(9,J) = ATC9
        TC(10,J) = ATC10
        TC(11,J) = ATC11
        TC(12,J) = ATC12
        TC(13,J) = ATC13
        TC(14,J) = ATC14
        RAD1(J) = ARAD1
        RAD2(J) = ARAD2
        RAD3(J) = ARAD3
        DELPD(J) = ADELPD
                J=J+1
        ENDIF

        I=I+1
        GOTO 10

 11 CONTINUE
    CLOSE (5)

    I=I-1
    J=J-1
C
```

```
C  CALCULATE GAS CONC., FUELRATE, HEAT FLUXES
C
  20 FNAME(7:7) = CHAR(77)
     OPEN(UNIT=6, FILE = FNAME, STATUS='NEW')

     FNAME(7:7) = CHAR(78)
     OPEN(UNIT=7, FILE = FNAME, STATUS='NEW')

          DO 23 K=1,J
     DRYCO(K)=DRYCO(K)*CORANGE/5.0
     DRYCO2(K)=DRYCO2(K)*CO2RANGE/5.0
     DRYO2(K)=DRYO2(K)*22./5.08

            FUEL(K) = ((VFUEL(K)-1.)*150./4.)-PAN

  23 CONTINUE

C  CALCULATE FUEL RATES
     DO 47 K=2,J
          IF (FUEL(K+1).GT.FUEL(K)) THEN
            FUEL(K) = (FUEL(K+1)+FUEL(K-1))/2.
          ENDIF
  47 CONTINUE

     DO 77 K=1,N
          FUELRATE(K)=(FUEL(1)-FUEL(K+N))/(TIME(K+N)-TIME(1))
  77 CONTINUE

     DO 78 K=J-N+1,J
          FUELRATE(K)=(FUEL(K-N)-FUEL(J))/(TIME(J)-TIME(K-N))
  78 CONTINUE

     DO 27 K=N+1,J-N
          FUELRATE(K)=(FUEL(K-N)-FUEL(K+N))/(TIME(K+N)-TIME(K-N))
```

```
 27 CONTINUE

    DO 24 K=1,J
    Q = FUELRATE(K)*46000.
      IF (NTC.EQ.1) THEN
      DENSITY = (94.657/((TC(4,K)+273.15)*0.287))
      ELSE
      DENSITY = (94.657/((TC(9,K)+273.15)*0.287))
      ENDIF

   AIRRATE= (0.6883*(0.0762**2.)*(DELPD(K)*1333.3)**.5*
  $DENSITY**(-.5))*2118.8
   AIRPHI = AIRRATE/2118.8*DENSITY

        HF1 = RAD1(K)*20.
        HF2 = RAD2(K)*20.
        HF3 = RAD3(K)*20.

   IF (HF3.GT.300) THEN
        HF3 = 0.0
   END IF

   UHC = 47100./(SFID-ZFID) * FID(K)

   DENOM = 1+(1.08*DRYCO2(K))/100.
   WETCO = DRYCO(K)/DENOM
   WETCO2 = DRYCO2(K)/DENOM
   WETO2 = DRYO2(K)/DENOM

   PHI = (FUELRATE(K)/AIRPHI)*15.

C  CALCULATE SMOKE VOLUME FRACTION AND YIELD
    SRATIO = 0.0
   DO 111 I=1,5
```

```
        SRATIO = SRATIO + SMOKEZ(I)
111 CONTINUE
        SRATIO = SRATIO/5.
    WRITE(*,*)SRATIO

   IF (NSIZE.EQ.1) THEN
        AREA = 0.303858
   ELSE IF (NSIZE.EQ.2) THEN
        AREA = 0.061136
   ELSE
     WRITE(*,*)'SOMETHING IS WRONG'
   END IF

        EXTCOEFF = 2.1872*DLOG(SRATIO/SMOKE(K))
        VT = 3.3
        CS = EXTCOEFF/(2.303*4.3596)
        SMOKEYD = (CS*VT)/(FUELRATE(K)*1000.)
        GENSMOK = (CS*VT)/(AREA)
        DMASS = EXTCOEFF*3.3/(2.303*1000*FUELRATE(K))

        SMOKED = 1.3697E-07*EXTCOEFF*1.0E+9
        SMOKEVF = 1.3697E-07*EXTCOEFF*1.0E+9

    QOXY = 3000.*((DRYO2(1)-WETO2)/DRYO2(1))*AIRPHI

    COYIELD=(WETCO*(FUELRATE(K)+AIRPHI)*.009663)/(FUELRATE(K))

   WRITE(6,26)TIME(K),VFUEL(K),FUELRATE(K),AIRPHI,AIRRATE,
  $WETCO,WETCO2,WETO2,PHI
26 FORMAT(F7.2,3F7.4,5F7.2)
   WRITE(7,29)TIME(K),Q,QOXY,UHC,SMOKEYD,GENSMOK,COYIELD,DMASS
29 FORMAT(2F9.2,2F8.1,,F7.4,F7.4,F6.3,F7.3)
24 CONTINUE
   CLOSE(6)
```

```
C ------------------------------------------------------------------------
C    CREATE OUTPUT FILES
C ------------------------------------------------------------------------
     DO 140 K=1,4
          FNAME(7:7) = CHAR(64+K)
       OPEN(UNIT=K, FILE = FNAME, STATUS='NEW')
 140 CONTINUE

     DO 201 K=1,J
     WRITE(1,160)TIME(K),DRYCO(K),DRYCO2(K),DRYO2(K),FUEL(K),
    $                RAD1(K),RAD2(K),RAD3(K),SMOKE(K)
     WRITE(2,180)TIME(K),TC(1,K),TC(2,K),TC(3,K),TC(4,K),TC(5,K),TC(6,
    $K),TC(7,K),TC(8,K),TC(9,K)
     WRITE(3,1000)TIME(K),TC(10,K),TC(11,K),TC(12,K),DELPD(K),FID(K)

 160 FORMAT(F6.1,F6.2,F6.1,F6.2,5F8.4)
 180 FORMAT(F7.1,9F6.1)
1000 FORMAT(4F6.1,F5.3,F8.4)

 201 CONTINUE

     CLOSE (1)
     CLOSE (2)
     CLOSE (3)
     CLOSE (4)

     STOP
     END
```

APPENDIX G

This appendix includes heat flux plots for Tests #8 (Normal Full Scale Pan Test) and #19 (Full Scale Pan Test with Window Removed).

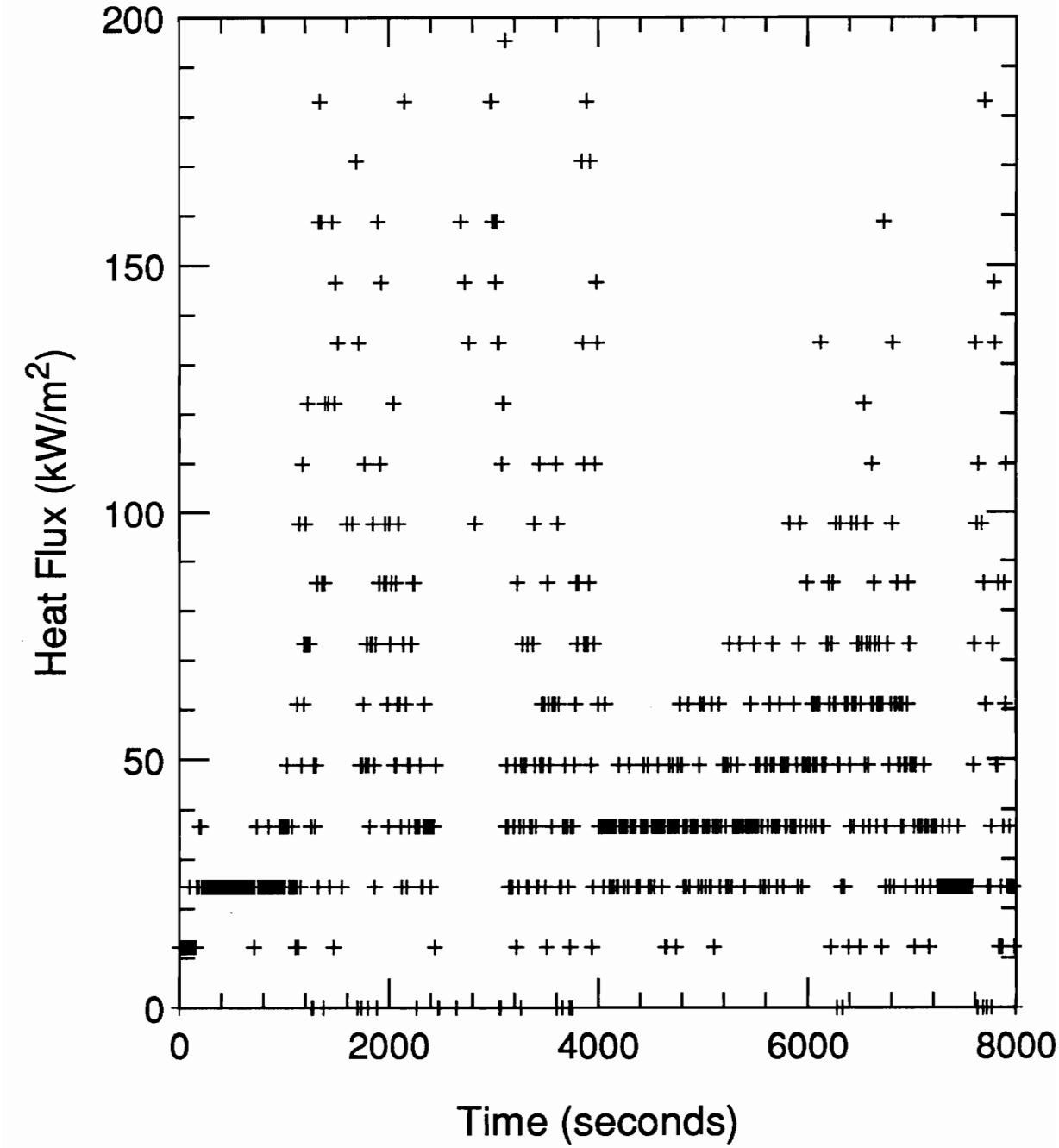

Figure G.1: Heat Flux-Time History for Test #8, Heat Flux Transducer in Floor

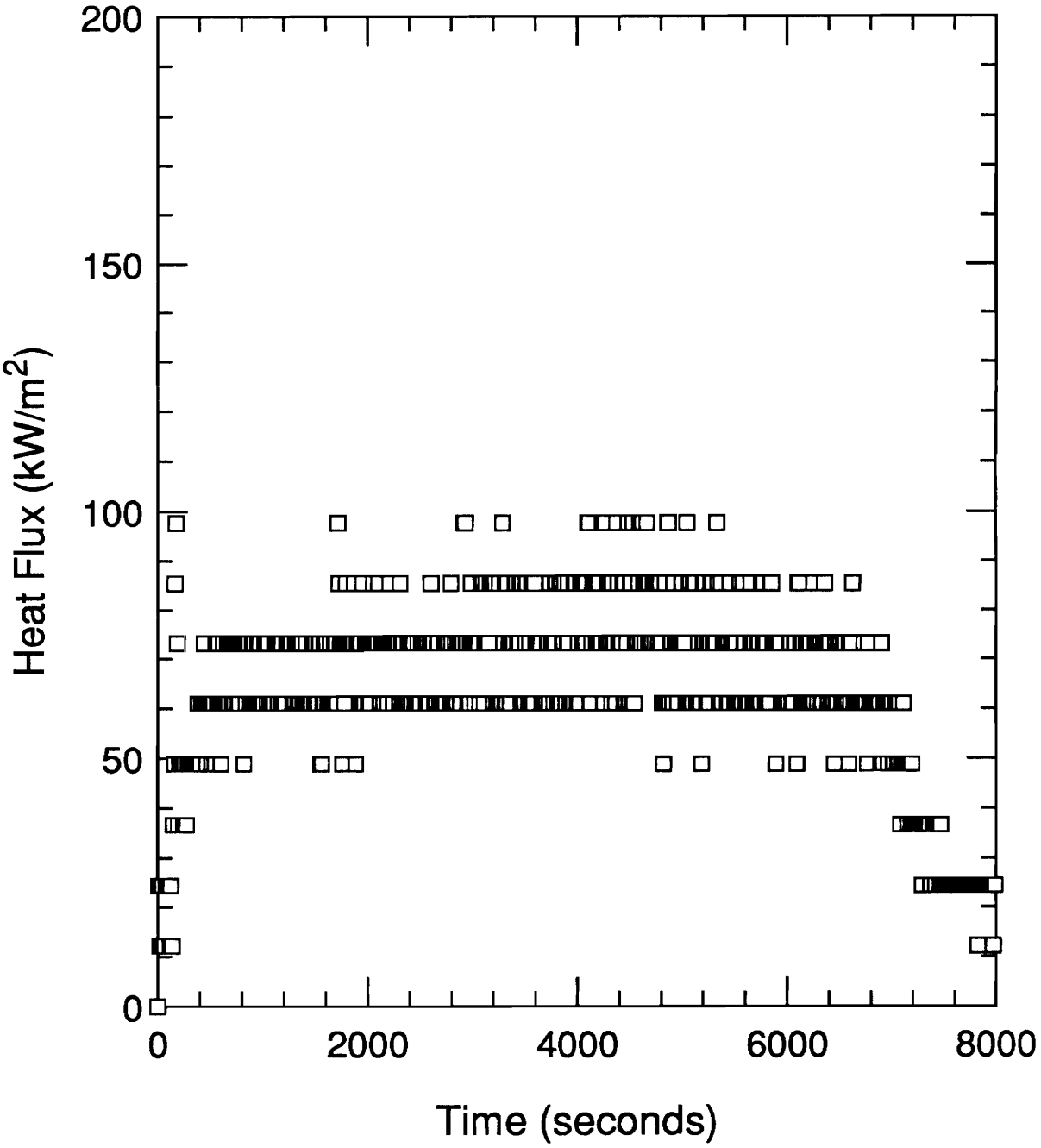

Figure G.2: Heat Flux-Time History for Test #8, Heat Flux Transducer in Side Panel

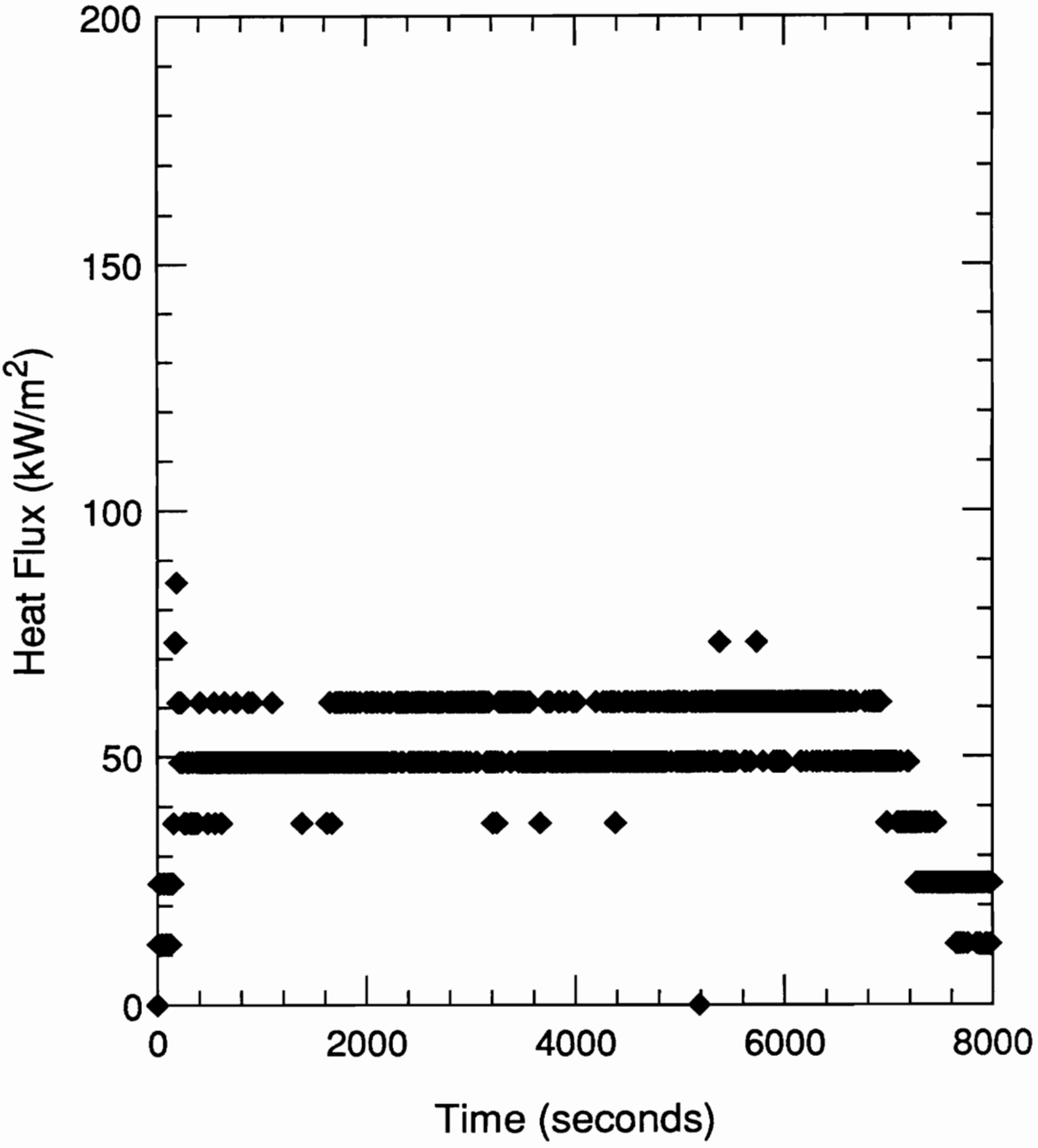

Figure G.3: Heat Flux-Time History for Test #8, Heat Flux Transducer in Ceiling Panel

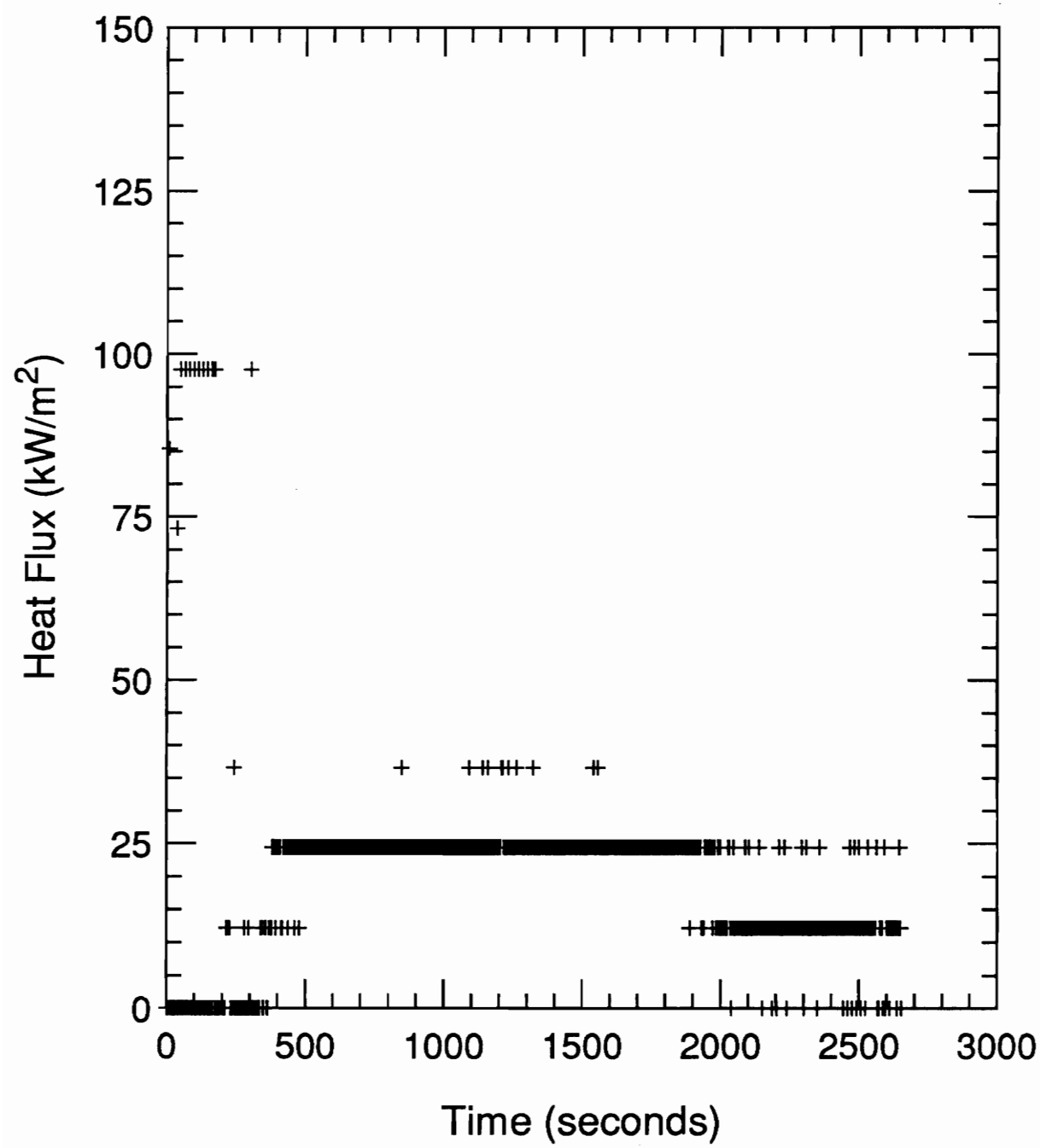

Figure G.4: Heat Flux-Time History for Test #19, Heat Flux Transducer in Floor

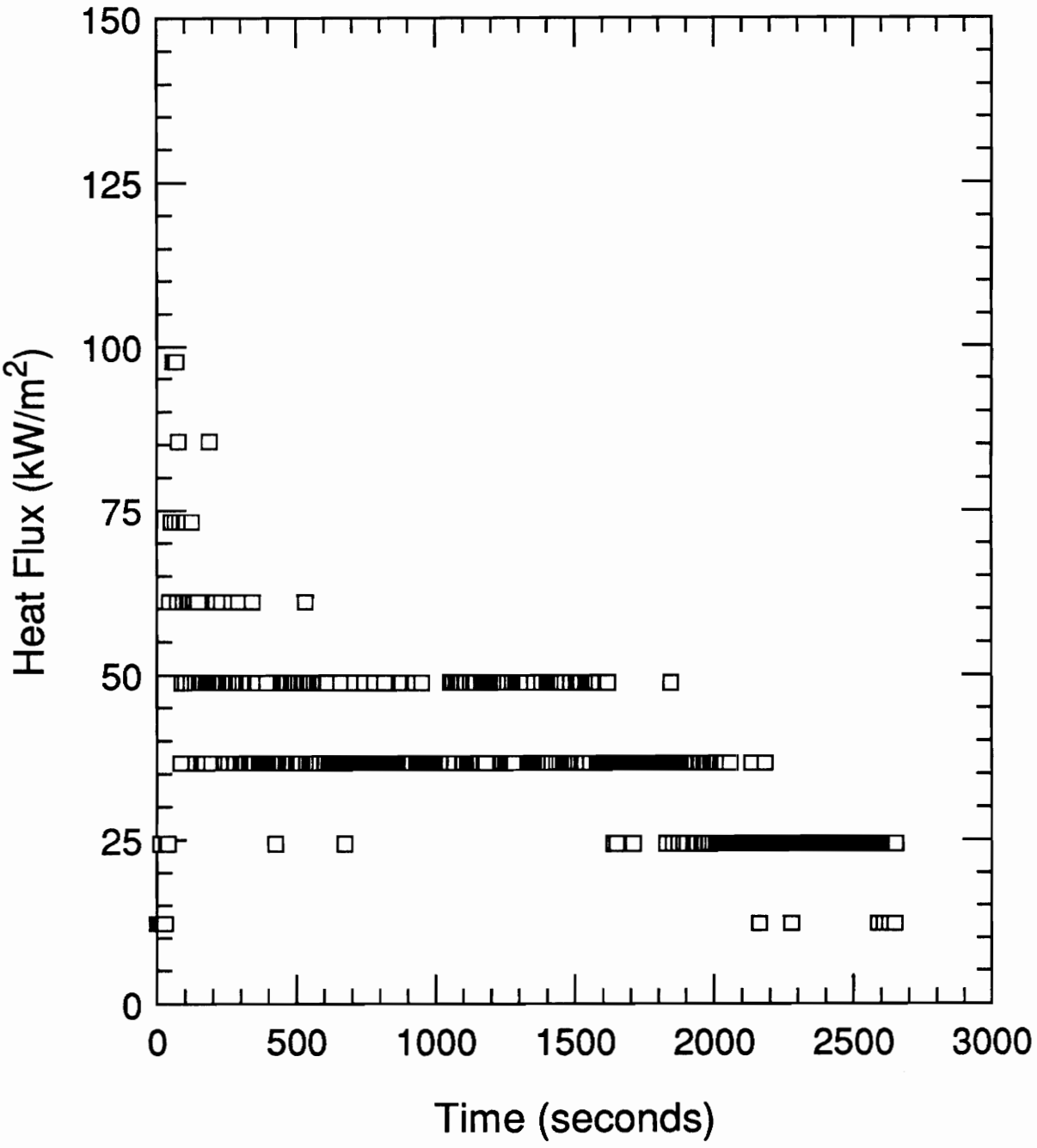

Figure G.5: Heat Flux-Time History for Test #19, Heat Flux Transducer in Side Panel

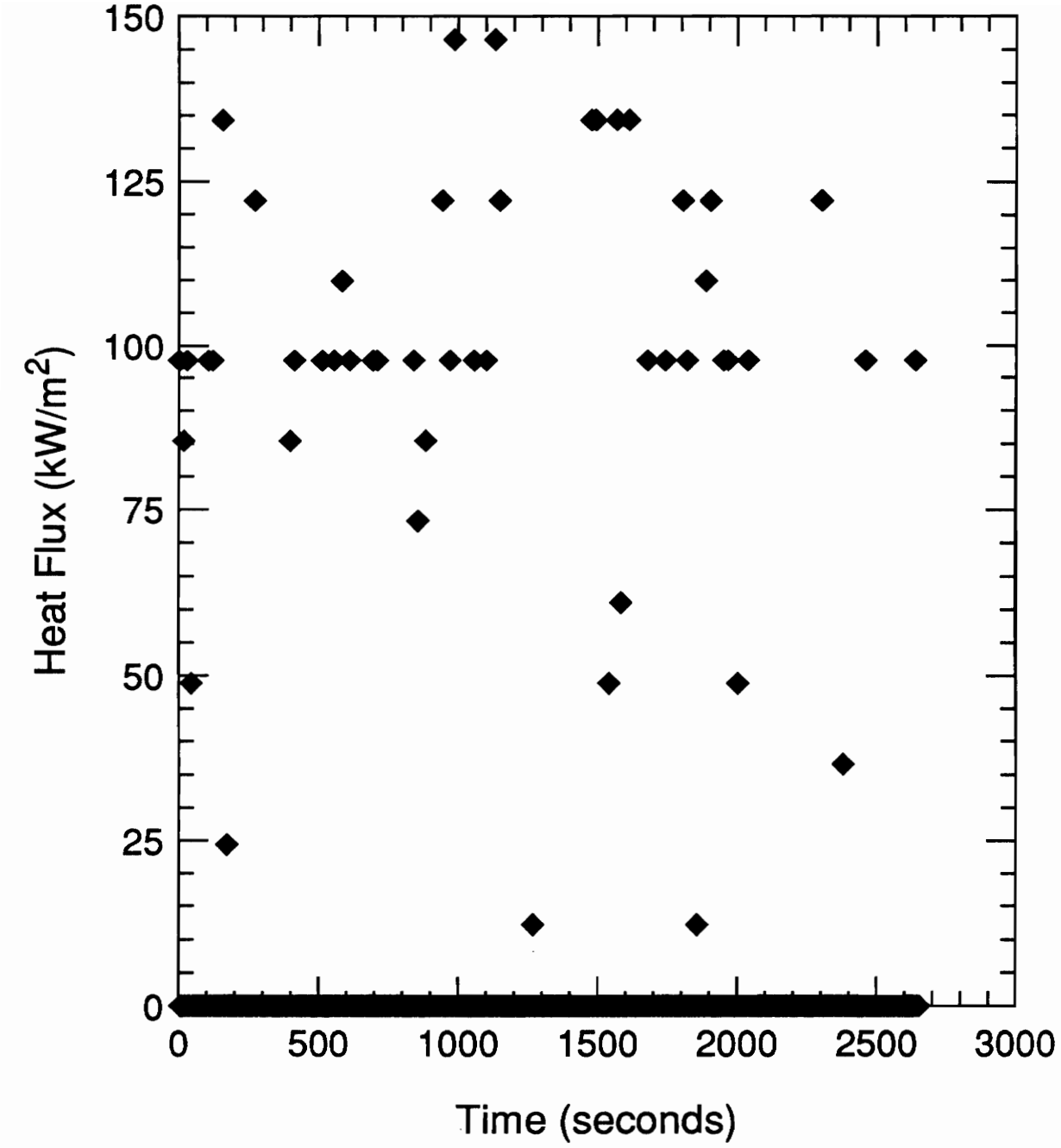

Figure G.6: Heat Flux-Time History for Test #19, Heat Flux Transducer in Ceiling Panel

VITA

Michelle Peatross was born on May 26, 1968 in Fairfax, Virginia. She grew up in Vienna, Virginia and began college at Virginia Tech in the fall of 1986. While in college, she participated in the Cooperative Education Program, working as a utilities co-op at Allied Signal, Fibers Division in Hopewell, Virginia. During her senior year, she conducted undergraduate research under Dr. Roby's supervision. Following the completion of her bachelor's degree in May 1991, she continued this work and began pursuing her master of science degree that fall.

Following graduation, Michelle plans to enter the next phase of her career as a consultant at Hughes Associates, Inc. in Columbia, MD.

Michelle J. Peatross